

# Barunastra ITS for RoboBoat 2025: Nala Ares

Taib Izzat Samawi, M Andi Abdillah, Muhammad Fajri Romadlon, Alifa Hikmawati, Tabitha Natasya Cyntia Dewi, Arundaya Pratama Nurhasan, Jonathan Oktaviano Frizzy, Muhammad Rizki Alfa Thariq, M Farras Rheza Firmansyah, Rumaisha Afrina, Muhammad Fathoni Al Fadh, Rico Dwi Firmansyah, Fergrini Lefranzy Pattinasarany, Iki Adfi Nur Muhammad, Medericus Mundi Miseridityo, Jilan Nabilah Dikairono, Winda Nafiqih Irawan, Farrel Rahmadany Akbar, Athalla Barka Fadhil, Sigmayuriza Senaaji Rasendria, Davin Abhinaya Briet, Dionisius Vito Aubin, Batara Haryo Yudanto, Dipta Mulya Suryono, Rifa Humaira Putri, Nathan Pascalauren Koroy, Terrania Rafva Nareswari, Zahrina Nur Amalina Syamsudin, Sheany Angela Diaz Wijaya, Rudy Dikairono, Muhammad Lukman Hakim

**Abstract**—*Back with Ares, the latest iteration of its ‘Nala’ lineup of autonomous surface vessels (ASV), Barunastra ITS RoboBoat Team is planning to bring innovations in hull and frame design, control systems, software architecture, auxiliary systems, and testing strategies. Ares will champion a significant reduction in weight, software setup/debug times, and electrical systems complexity. Ares will also boast increases in structural integrity, localization accuracy, and wireless communication reliability. Improvements made upon Ares’ design will be rigorously tested to ensure that it fulfills its design criteria—being able to reliably complete all RoboBoat 2025 autonomy challenge tasks.*

## I. OVERVIEW

Barunastra ITS RoboBoat Team (henceforth abbreviated as Barunastra ITS) is a multidisciplinary team of undergraduate students from Institut Teknologi Sepuluh Nopember (ITS). Our passion for becoming the front-runner in student maritime robotics research has provided numerous academic, research, and networking opportunities for team members and broader research communities.

Barunastra’s ‘Nala’ fleet of boats includes vessels used primarily for ASV research and competition purposes. The latest iteration of Nala, called ‘Ares’, is named after the Greek god of courage and war, as its first and primary purpose would be for competing in RoboBoat 2025. Ares, alongside its predecessors Proteus and Theseus will be used for further research and community training after RoboBoat.

This paper discusses the considerations made by Barunastra to maximize Ares’ score in RoboBoat 2025, along with the design strategy and testing scheme implemented to ensure optimal performance throughout the regatta.

## II. COMPETITION APPROACH

Ares should fulfill all RoboBoat 2025 autonomy challenge tasks. Leveraging on experience and legacy systems from previous competitions, which are to be built upon and improved, made us confident in developing an ASV system capable of completing all tasks with high maintainability and manageable on-site troubleshooting complexity.

### A. Regatta Environment

The strong waves and winds of Nathan Benderson Park (NBP) during RoboBoat 2024 proved to be a significant challenge for Proteus 2.0. Ares should be prepared to face similar circumstances, requiring major design changes.



Fig. 1. Proteus 2.0 struggling to operate at NBP

### B. Task Completion

Detailed strategies Ares will use to tackle the tasks are detailed as follows:

**1) Task 1 - Navigation Channel:** Ares must identify the green and red gate buoys to determine whether it is headed in the correct direction, as green buoys are always placed to starboard. Ares should then avoid hitting the gate buoys by:

- Swaying right whenever it is too close to a red gate buoy; or
- Swaying left whenever it is too close to a green gate buoy.

**2) Task 2 – Mapping Migration Patterns:** Ares must identify the closest red and green gate buoys and sail between them. Ares should sail through the largest gap between the obstacle and the nearest gate buoys if it finds any. Ares must also report the number of obstacles after passing ten gate buoy pairs by pivoting.

**3) Task 3 – Treacherous Waters:** Ares should sail through one side of the docking bay arena and check for the following parameters in each bay:

**a) Banner:** Whether it has the correct color/shape.

**b) Occupancy:** Whether it is occupied.

Ares must dock into any unoccupied bay with the correct banner. Otherwise Ares must sail towards the other side of the docking bay arena and check for a) and b).

**4) Task 4 – Race Against Pollution:** Ares must keep track of two things when in holding bay:

- Whether the light panel is red or green; and
- Whether it is inside the holding bay.

Upon green light, it ensure that the mark buoy is both visible and to port. Hence, it should always sway starboard to avoid obstacles. To return to the gates, it should switch to the same approach as for Task 2 but this time assuming the black buoys as obstacles.

**5) Task 5 – Rescue Deliveries:** To complete delivery tasks, Ares should keep a thought process in the back of its mind whenever it is running through any of the other missions.

- If Ares detects either a black triangle or a black plus shape banner and a large object in the same general location, it stops the current process and pivots towards the banner.
- After pointing towards the banner, it must either shoot water on the black triangle banner or launch a racquetball towards the black plus shape banner.

After delivery, Ares must return to its initial heading and continue the task. This parameter can be toggled for specific tasks, such as Task 4, where completion time is crucial. If delivery is separate, Ares will record the delivery boat's position and return after completing the task.

**6) Task 6 – Return to Home:** Using pure visual cues proves to be challenging when completing this task during RoboBoat 2024. As such, Ares must revert to waypoint navigation alongside reactive obstacle avoidance, using its initial position before running Task 1 as the destination waypoint.

**a) Obstacle Avoidance:** Different from Task 4, Ares should now assume all detected objects as an obstacle and move away from them in the direction with least effort (sway right if the obstacle is to its left and vice versa).

**b) Gate Passing:** If it is closer than 5 meters to the start location waypoint, Ares should sail through the middle of the two black gate buoys using a modification of Task 2's algorithm. If at any time only one black buoy is visible, Ares must turn left and right 60° and immediately stop turning whenever it detects two black buoys.

### III. DESIGN CREATIVITY

#### A. Advanced Modular Vessel

A significant reduction in scoring during RoboBoat 2024 Autonomy Challenge unearthed the following design flaws and solutions:

**1) Overdraft:** This occurred due to total component weight exceeding the maximum expected design capacity. This is solved by designing a hull that has a lower draft to secure electrical components on the main deck.

**2) Stern shape:** Proteus' flat stern made reverse movement less stable and in some cases allowed seawater to reach the main deck and damage electrical components. Ares will have a hull that is tapered on both sides to address this issue.

**3) Bow thruster issue:** The lateral proximity between the two bow thrusters proves to be too small, allowing significant turbulence and cavitation. This is resolved by using X-Drive control for holonomic motion.

**4) Overweight Deck Frame:** The main deck frame of Proteus 2.0 was too heavy due to complicated joint parts. Thus, Ares' main deck frame should be lighter yet stronger.

After component arrangement analysis was done, it is found that the payload capacity and service speed resistance of Ares' hull should be at worst similar to Proteus. After thirteen prototype design iterations, a model for Ares' hull was

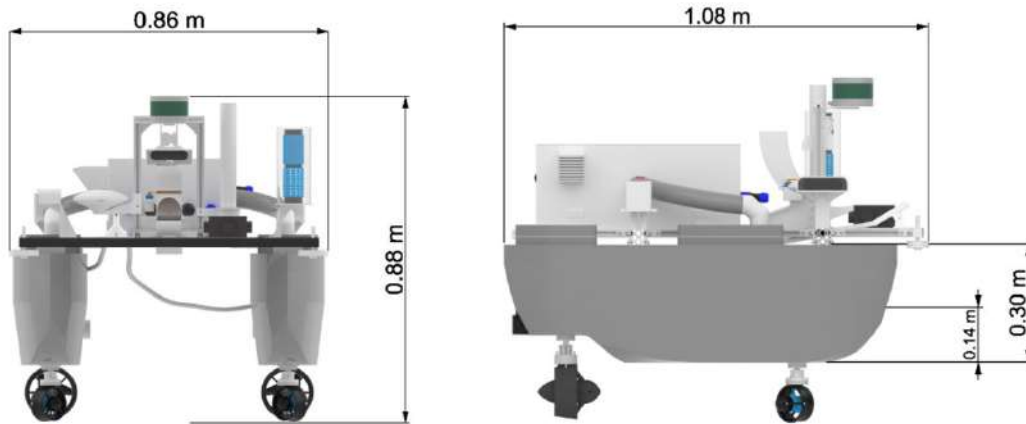


Fig. 2. Ares' render with dimension visualizations

found, boasting higher stability and lower resistance compared to Proteus 2.0. Principal dimension comparison between Proteus 2.0 and Ares can be seen in Table I.

	Proteus 2.0	Ares
Length	0.97 m	0.99 m
Beam	0.84 m	0.86 m
Height Overall	0.90 m	0.88 m
Height	0.30 m	0.30 m
Draft	0.18 m	0.14 m
Block Coeff.	0.54	0.61
Demi-hull	0.64 m	0.60 m
Displacement	37.78 kg	31.77 kg

The main deck frame was redesigned to be simpler yet strong enough to carry the same load as Proteus 2.0. The V-slot aluminum alloy 6063 T5 material is retained due to its sturdiness, but the joints are replaced to double slot angle brackets.

Using this advancement in hull and frame material and design, Ares successfully obtained half the weight of Proteus, which can improve its overall performance in all missions. The tapered stern will allow for efficient reverse motion when executing Task 3. Refer to Appendix B for details on Ares' construction design and production.

### B. Propulsion Configuration

Ares will use two bow thrusters configured in an X-Drive manner and two azimuthal stern thrusters. Like Proteus, Ares will still use

BlueRobotics thrusters due to its efficiency and ease-of-use. We will use either the T200 or T500 thrusters for Ares' propulsion system.

This setup will allow holonomic motion via X-Drive control whilst facilitating greater thrust power for increased thrust scoring and reduced task completion time. We expect to adjust legacy control programs to allow for the T200 and T500 thrusters to work in tandem for X-Drive control if needed. Details regarding the propulsion system and thruster configuration approach can be found in appendix C and C.1.

### C. Object Delivery Mechanism

Past year mechanisms for object delivery [1], [2]; were too heavy since DC motor based systems affected vessel stability and performance. A solenoid-based puncher will instead be used for Ares' object delivery system.

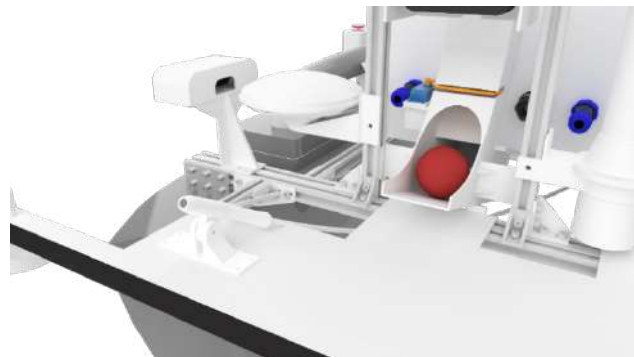


Fig. 3. Water and object delivery apparatus

Ares will use the same mechanism for water delivery as Proteus 2.0 due to its proven efficiency during RoboBoat 2024. The racquetball puncher

system is expected to be lighter and simpler yet powerful enough to launch the racquetballs and hit delivery banners. The launcher can shoot up to three times, reloading via a servo gate. Both the water blaster and racquetball puncher will be fixed at 45° elevation angle for the farthest projectile distance. The detailed approach for object delivery mechanisms can be found in Appendix E.

#### D. Electrical System Compactness

The use of two separate boxes for electrical components in Proteus 2.0 turned out to be too heavy and cumbersome. Ares' electrical system is now simplified into one box, reducing size and component count, by applying modular electrical system principles [3], [4]. The Pixhawk is now the main controller, assisted by the STM32F411CEU6 microcontroller for power monitoring and control over auxiliary devices. The change should reduce the controller and power PCB size by up to 70% whilst maintaining full functionality. Detailed information regarding design and production is available in Appendix G.

#### E. Perception System

1) **Computer Vision:** Ares will be equipped with a primary and a side camera. The side camera is used to observe light panel for Task 4. Both image streams will use YOLOv8-nano for object detection. Ares will also use the ByteTrack framework for object tracking and counting. OpenVINO framework is used to optimize inference speeds on NUC mini-PC environments.

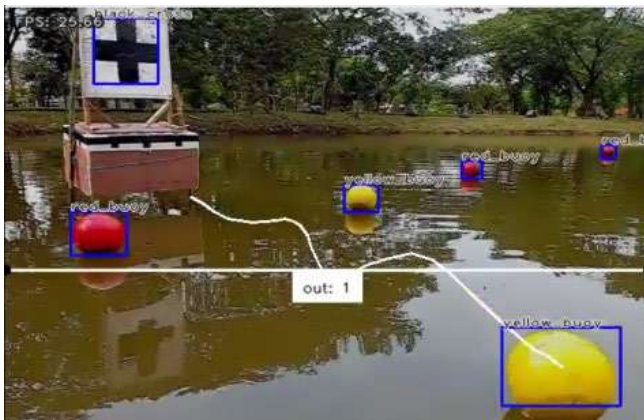


Fig. 4. Object detection, tracking, and counting

2) **Obstacle Avoidance:** LiDAR will be used to implement the principle of the Braitenberg Vehicle [5] for obstacle avoidance, which is especially important for Task 6.

3) **Localization and Mapping:** Alongside using NTRIP for accurate GPS localization, Ares will use Direct LiDAR-Inertial Odometry (DLIO) for localization and mapping. This will be used for optimal docking and rescue delivery performance.

#### F. Software Architecture

We drastically simplified our software architecture. Instead of the bottom-up approach used up until RoboBoat 2024, Ares' autonomy system will use a top-down approach based on a strict sequence of program flow.

There are three active modules: Ares is to receive and process environment information via 'Perception'; decide, think, and strategize via 'Cognition'; then act via 'Behavior'.

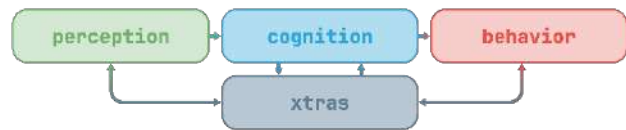


Fig. 5. Simplified software architecture diagram

The passive 'Xtras' module will store all utilities and interfaces and is able to be accessed by all three active modules. Details regarding the new software architecture are available in Appendix F.

### IV. TESTING SCHEME

Performance reduction due to the delayed and rushed preparation for RoboBoat 2024 shifted our attention towards optimizing testing timeline and methods, allowing for more comprehensive analyses of all ASV subsystems. Detailed testing timeline can be found in Appendix H.1.

#### A. Hull and Frame Analysis

1) **Hull Analysis:** We will use *Maxsurf Advanced* to analyze displacement, resistance, stability, and motion of Ares' hull. *Ansys Fluent with Meshing 2024 R2 Software* will also be used to execute *hull drag* analysis. Testing will occur after each hull design iteration and conclude by the 3<sup>rd</sup> week of December, allowing for sufficient time for production and on-water testing.

**2) Main Deck Frame Software Analysis:** We will use *Ansys 2024 R2 Static Structural Mechanical Software* to analyze equivalent stress and total deformation of the main deck frame [6], [7]. We will compare joints using either single-slot or double-slot angle brackets, as well as comparing Proteus 2.0's and Ares' main deck frame designs. Testing will occur after hull analysis, from the 3<sup>rd</sup> week of December until the 2<sup>nd</sup> week of January, allowing up to three weeks for hull production to be done in parallel.

**3) Wave Pool Sea-keeping Analysis:** After the finished product of Ares is completed, wave pool testing will be done to measure its physical response, durability, and structural integrity under wave conditions like those encountered in NBP during RoboBoat 2024. The testing will take place in the wave pool at the National Hydrodynamics Research and Innovation Agency (BRIN) according to BRIN's time allocation, no later than the 3<sup>rd</sup> week of January. Details methods and results can be found in Appendix H.1.

## B. Control System Analysis

**1) Thruster Efficiency:** We will test the following setups for efficiency and speed:

- 4 T500 thrusters;
- 4 T200 thrusters; and
- 2 T200 thrusters at bow, 2 T500 thrusters at stern.

We will swap between the three configurations to test their speed via IMU data and efficiency via battery drain comparison. Testing will be done within a day before any on-water trials are done. Details regarding comparison methods and results are available in Appendix C.1.

**2) Wave Pool Station-keeping Test:** To test whether Ares' control system is prepared for NBP environments, Barunastra ITS will test its station-keeping capabilities on BRIN's wave pool. Testing will be done according to BRIN's time allocation, no later than the 3<sup>rd</sup> week of January. Testing methods and results are available in Appendix H.1.

## C. Computer Vision Testing:

We will test several different YOLO versions to determine the best model in terms of balance

between accuracy and inference speed. Table II details the YOLO models to be compared.

TABLE II LIST OF YOLO MODELS TO TEST

YOLO Version	Model Size
7	tiny
8	nano
9	tiny
10	nano
11	nano

Testing should start after the trial arena is fully installed, a new dataset based on the new arena is considered to result in better comparison between the models. Appendix D.1 details the comparison method and results.

## D. Object Delivery Testing

Comparison analysis will be done towards a sample of different solenoid types to determine which of the options are the most appropriate and efficient for racquetball delivery. Testing is to be done as soon as possible, after sufficient resources to purchase the different solenoid types can be gathered. Details and test results can be found in Appendix E.1.

## E. Software Setup Efficiency Testing

Setup time efficiency of the new software architecture approach will be tested against our legacy architecture. This testing will be done during each on-water trial session from the 3<sup>rd</sup> week of November until the 1<sup>st</sup> week of January. More information regarding testing methods and results is available in Appendix F.1.

## F. Communication and Kill Switch Testing

We plan to test various remote controls by evaluating their operation range to prepare for high-interference environments. We will test the data link reliability of several 5GHz ground control antennas to ensure Ares can reliably relay its status and receive ground commands without relying on remote control interruptions. Several kill switch configurations will be compared to find the one with the lowest delay and highest reliability. Appendix G.1. gives more details regarding communication and kill switch testing.

electrical and autonomy system. These changes

Task Name	Difficulty	Potential Points	Additional Points	Estimated Point	Confidence	Weighted Score	Priority
Navigation Channel	Trivial	250	-	250	100%	2500	1
Mapping Migration Patterns	Easy	650	-	450	100%	2250	2
All Tasks	Hard	1860	2 * total score	3720	24%	875	3
Treacherous Waters	Medium	400	-	400	70%	840	4
Race Against Pollution	Medium	650	-	360	70%	756	5
Return to Home	Easy	100	-	100	80%	400	6
Rescue Deliveries	Hard	950	-	300	60%	180	7

Fig. 6. Task completion priority matrix

### G. On-water Trials

We will install a mock-up arena for RoboBoat 2025 on campus lake. Whilst Ares' hull and frame production is underway, basic ASV functionality will be tested using Theseus and Proteus. Task 1, Task 2, and Task 6 algorithm reliability will be of the highest priority during the first two weeks of on-water trials. X-Drive holonomic motion will also be planned during the first two weeks.

Afterwards, roughly a month of trial will be allocated to focus on fusing IMU and LiDAR (DLIO) to obtain precise localization and mapping. After localization testing, two weeks will be allocated to conduct Task 3, Task 4, and Task 5 trials on the mock up arena.

After the finished product of Ares is completed, Barunastra ITS plans to spend 2 weeks migrating all ASV systems aboard the new hull and frame. Trials for attempting all tasks will be conducted on Ares since. The detailed records and strategy for on-water testing can be found in Appendix H.1.

Fig. 5. visualizes our task priority matrix for RoboBoat 2025. For each task, the weighted score is the product of: the difficulty level (Trivial = 10, Easy = 5, Medium = 3, Hard = 1); the confidence level; and estimated point collection. Weighted scores are then sorted to determine the priority of each mission. Since attempting all tasks results in 2 times the sum of all individual tasks, a dedicated row is added for attempting all tasks.

## V. CONCLUSION

A comprehensive analysis of previous years' implementations has concluded in the design of a new hull and frame, along with changes in

are made based on a systems engineering approach and are rigorously tested via a thorough testing plan. Barunastra ITS dedicates Appendices B–H to detail the test plan and results of each ASV subsystem, as compressing all of them into one appendix might not do justice to the level of depth each analysis has.

Design creativity and testing results have made Barunastra ITS confident that its latest ASV prototype 'Ares' can complete all autonomy challenge tasks during the 2025 RoboBoat season.

## ACKNOWLEDGMENTS

Continued existence and success of Barunastra ITS would not be possible without the support of Institut Teknologi Sepuluh Nopember, alumni, and industry partners. Deepest appreciation and gratitude for support and contributions are given to everyone involved in Appendix I.

## REFERENCES

- [1] F. Januar, R. Ramadhan, R. Permadani, M. Valentia, E. Putra, I. Dananjaya, *et al.*, "RoboBoat 2023: Nala Proteus' technical design report," Institut Teknologi Sepuluh Nopember, Surabaya, Indonesia, 2023.
- [2] M. Abdillah, R. Afrina, M. Arieq, Z. Bahri, S. Christanto, I. Dananjaya, *et al.*, "Technical design report of Nala Proteus 2.0: An autonomous surface vessel by Barunastra ITS RoboBoat Team," Institut Teknologi Sepuluh Nopember, Surabaya, Indonesia, 2024.
- [3] M. A. Roy and G. Abdul-Nour, "Integrating modular design concepts for enhanced efficiency in digital and sustainable

- manufacturing: A literature review,” *Applied Sciences (Switzerland)*, vol. 14, no. 11, Jun. 2024, doi: 10.3390/app14114539.
- [4] Y. Wang, S. Li, X. Wang, and Y. Wang, “Modularization and parametric design of airborne electronic equipment structure,” in *Journal of Physics: Conference Series*, IOP Publishing Ltd, Nov. 2021, doi: 10.1088/1742-6596/2085/1/012007.
- [5] D. Hutabarat, M. Rivai, D. Purwanto, and H. Hutomo, “Lidar-based obstacle avoidance for the autonomous mobile robot,” in Proc. 12th Int. Conf. Information & Communication Technology and System (ICTS), Surabaya, Indonesia, 2019, pp. 197–202, doi: 10.1109/ICTS.2019.8850952.
- [6] M. Acar, M. T. Özlüdemir, O. Akyilmaz, R. N. Celik, and T. Ayan, “Deformation analysis with total least squares,” *Natural Hazards and Earth System Sciences*, vol. 6, no. 4, pp. 663–669, 2006.
- [7] Y. Z. Wang, G. Q. Li, Y. B. Wang, and Y. F. Lyu, “Simplified method to identify full von Mises stress-strain curve of structural metals,” *Journal of Constructional Steel Research*, vol. 181, p. 106624, 2021.

# Appendix A: Component List

Tabitha Natasya Cyntia Dewi, Muhammad Rizki Alfa Thariq, Winda Nafiqih Irawan, Batara Haryo Yudanto

Component	Vendor	Model/ Type	Specs	Custom/ Purchased	Cost	Year	
ASV Hull	Barunastra ITS	Catamaran Hull	Carbon Fiber with LOA: 99 cm, Breadth (Hull only): 20 cm Height (Hull only): 30 cm Draft: 14 cm, Displacement: 31.77 Kg	Custom	\$1532.00	2025	
Platform	Barunastra ITS	V Slot Extrusion	Aluminum Profile 20 x 20 1,52m, 20x40 2,38m V slot silver	Custom	\$76.00	2025	
3D Print	Creality	CR 10 MAX	<a href="#">creality-cr-10-max.pdf</a>	Purchased	Donated	2021	
	eSUN	PLA+	Amount: 10 Rolls Diameter Size: 1.75mm Net Weight: 1Kg/spool	Purchased	\$150.00	2025	
Camera	Logitech	Webcam Brio 4K	<a href="#">Brio-Datasheet.pdf</a>	Purchased	\$129.00	2023	
	Dynamixel	MX-28	<a href="#">MX-28T/R/AT/AR</a>	Purchased	Donated	2024	
	U2D2	Power Hub Board	<a href="#">U2D2 Power Hub</a>	<a href="#">Robotis Shop   All- in-one Smart Actuator</a>	Purchased	\$19.00	2023
	U2D2	Communi- cation Converter	<a href="#">U2D2</a>	<a href="#">Robotis Shop   All- in-one Smart Actuator</a>	Purchased	\$32.10	2023
	Ubiquiti	airMAX Omni Antenna AMO- 5G10	<a href="#">airMAX Omni Antennas Datasheet</a>	<a href="#">Ubiquiti Store</a>	Purchased	\$125.00	2025
Communication	Ubiquiti	Power Beam 5AC Gen2 PBE-5AC	<a href="#">PowerBeam 5AC Gen 2 Datasheet</a>	<a href="#">Ubiquiti Store</a>	Purchased	\$120.00	2025
	Ubiquiti	rocket 5AC PRISM	<a href="#">Rocket Prism 5AC Gen 2 Datasheet</a>	<a href="#">Ubiquiti Store</a>	Purchased	\$250.00	2023
Cooling System	DELTA	Brushless Fan 7x7 cm	<a href="https://www.mouser.co.id/datasheet/2/632/AFC0612DE_AF00-3433575.pdf">https://www.mouser.co.id/datasheet/2/632/AFC0612DE_AF00-3433575.pdf</a>	<a href="#">Products - Industrial Automation</a>	Purchased	\$30.00	2024
CPU	ASUS	NUC Pro 12 i5	<a href="https://www.asus.com/Websites/be-nl/products/plvfwcc56r5rbe7f/pdf/xpo3szp1z9q7noaf.pdf">https://www.asus.com/Websites/be-nl/products/plvfwcc56r5rbe7f/pdf/xpo3szp1z9q7noaf.pdf</a>	Purchased	Donated	2025	



<b>GPS</b>	Sparkfun	GNSS Multi-Band L1/L2	<a href="https://cdn.sparkfun.com/assets/b/4/6/d/e/TOP106_GNSS_Antenna.pdf">https://cdn.sparkfun.com/assets/b/4/6/d/e/TOP106_GNSS_Antenna.pdf</a>	Purchased		
	Sparkfun	ZED F9P	<a href="#">ZED-F9P-02B Data sheet</a>	Purchased	\$133.95	2024
<b>LED Matrix</b>	-	WS2812B 16x16 cm	Power Supply : DC 5V, SMD 5050, IC WS2812, Non Waterproof IP20, Dobel tip : Yes	Purchased	\$12,50	2024
	Velodyne	Puck	<a href="https://hexagondownloads.blob.core.windows.net/public/AutonomousStuff/wp-content/uploads/2019/05/Puck_Datasheet_whitelabel.pdf">https://hexagondownloads.blob.core.windows.net/public/AutonomousStuff/wp-content/uploads/2019/05/Puck_Datasheet_whitelabel.pdf</a>	Purchased	Vendored	2023
<b>LoRa System</b>	SEMTECH	Module LoRa SX1278	<a href="#">SX1276/77/78/79</a>	Purchased	\$5.50	2024
<b>Microcontroller</b>	STM32	STM32F411CEU6	<a href="#">DATASHEET STM32F411CE</a>	Purchased		
	Arduino	Nano	<a href="#">Nano   Arduino Documentation</a>	Purchased	\$7.00	2025
<b>Motor Controls</b>	CUAV	Pixhawk V6X	<a href="#">CUAV Pixhawk V6X Controller</a>	Purchased		
	OVONIC (Spare)	Lithium-Ion Polymer	4S2P 8200mAh 80C 14.8V	Purchased	\$330.00	2024
<b>Power System</b>	HOOVO (Spare)	Lithium-Ion Polymer	6S 6000mAh 60C 22.2V	Purchased	\$75.00	2022
	ONBO (Main)	Lithium-Ion Polymer	4S 7200mAh 50C 14.8V	Purchased	\$80.00	2022
	TATTU (Main)	Lithium-Ion Polymer	3S 2300mAh 45C 11.1V	Purchased	\$70.00	2023
	TATTU (Main)	Lithium-Ion Polymer	6S 10000mAh 25C 22.2V	Purchased	\$23.00	2023
	Spectrum (Spare)	Lithium-Ion Polymer	3S 22000mAh 50C 11.1V	Purchased	\$159.00	2023
	Zeee (Spare)	Lithium-Ion Polymer	6S 9000mAh 100C 22.2V	Purchased	\$35.00	2024

<b>Propulsion</b>	Blue Robotics	T500	<a href="https://bluerobotics.com/store/thrusters/t100-t200-thrusters/t500-thruster/">https://bluerobotics.com/store/thrusters/t100-t200-thrusters/t500-thruster/</a>	Purchased	\$690.00	2024
	Blue Robotics	T200	<a href="https://bluerobotics.com/store/thrusters/t100-t200-thrusters/t200-thruster-r2-rp/">https://bluerobotics.com/store/thrusters/t100-t200-thrusters/t200-thruster-r2-rp/</a>	Purchased	\$200.00	2024
	Flipsky	Mini FSESC4.20 50A	<a href="https://www.amazon.com/FLIPSKY-Electric-Speed-Controller-for-Skateboard-Mini-FSESC4.20-50A-Base-on-ESC-4.12-with-Aluminum-Anodized-Heat-Sink-12s-esc-SB2290SG-Monster-Torque-Brushless-Servo-Black-Edition-11sec-972.1oz-8.4v/dp/B078888888">Amazon.com: FLIPSKY Electric Speed Controller for Skateboard Mini FSESC4.20 50A Base on ESC@ 4.12 with Aluminum Anodized Heat Sink 12s esc SB2290SG - Monster Torque Brushless Servo, Black Edition .11sec / 972.1oz @ 8.4v</a>	Purchased	\$73.00	2024
	Savox	SB-2290SG	<a href="https://www.servotronics.com/products/sb2290sg-monster-torque-brushless-servo-black-edition-11sec-972.1oz-8.4v">SB2290SG - Monster Torque Brushless Servo, Black Edition .11sec / 972.1oz @ 8.4v</a>	Purchased	\$150.00	2024
<b>Launcher System</b>	uxcell	MQ8-ZI5B	Supply Voltage: 12V Bore Size: 1/2 #34 Diameter: 3 cm Primary Force: 10mm = 1000g Ultimate Force: 0mm = 1500g	Purchased	\$10.00	2024
	Savox	SW-0231MG	<a href="https://www.servotronics.com/products/sw0231mg-discontinued-please-see-sw0231mgp-for-replacement">SW0231MG - DISCONTINUED - Please See SW0231MGP for Replacement</a>	Purchased	\$50.00	2024
<b>Teleoperation</b>	Radiomaster	TX16S MKII Mark II	<a href="https://www.servotronics.com/products/tx16s-mark-ii-radio-controller-mode-2-radio-master-rc">TX16S Mark II Radio Controller (Mode 2) – RadioMaster RC</a>	Purchased	\$200.00	2024
	Radiomaster	RP4TD ExpressLRS	<a href="https://www.servotronics.com/products/receiver-radiomaster-rp4td-expresslrs-2.4ghz">Receiver Radiomaster RP4TD EXPRESSLRS 2.4GHz</a>	Purchased	\$25.00	2024
<b>Water Pump</b>	Solar Water Pump	DC 12 V Water Pump 8 watt	Working Voltage: DC 12V Power Rating: 8W Max Water Height: 5m Max Flow: 10 L/min Diameter of Inlet: 15.5 mm Diameter of Outlet: 11 mm High quality solar water pump for DC current	Purchased	\$5.00	2024
<b>Waterproof Connectors</b>	Zeatop Hendar	SP20 Aviation Connector	3P 20mm waterproof aviation Connector	Purchased <a href="https://www.zeatop.com/">zeatop hendar</a>	\$6.00	2024
<b>Algorithms</b>	Barunastra ITS	-	-	Custom	-	2023
<b>Localization and Mapping</b>	Barunastra ITS	-	-	Custom	-	2025
<b>Open-Source Software</b>	ROS2 Humble	-	-	Custom	-	2023
<b>Vision</b>	OpenCV	-	-	Custom	-	-
<b>Autonomy</b>	Barunastra ITS	-	-	Custom	-	2025
<b>Team Size</b>	-	-	29	-	-	-
<b>Testing time: simulation</b>	-	-	Nov 3 <sup>rd</sup> , 2024 – Jan 10 <sup>th</sup> 2025	-	-	-
<b>Testing time: in-water</b>	-	-	Nov 4 <sup>th</sup> , 2024 – Jan 26 <sup>th</sup> 2025	-	-	-
<b>Hardware/Software expertise ratio</b>	-	-	5:4	-	-	-

## Appendix B: Hull and Main Deck Frame

Muhammad Fajri Romadlon, Muhammad Rizki Alfa Thaaariq, M Farras Rheza Firmansyah, Sigmayuriza Senaaji Rasendria, Davin Abhinaya Briet, Dionisius Vito Aubin, Batara Haryo Yudanto, Dipta Mulya Suryono

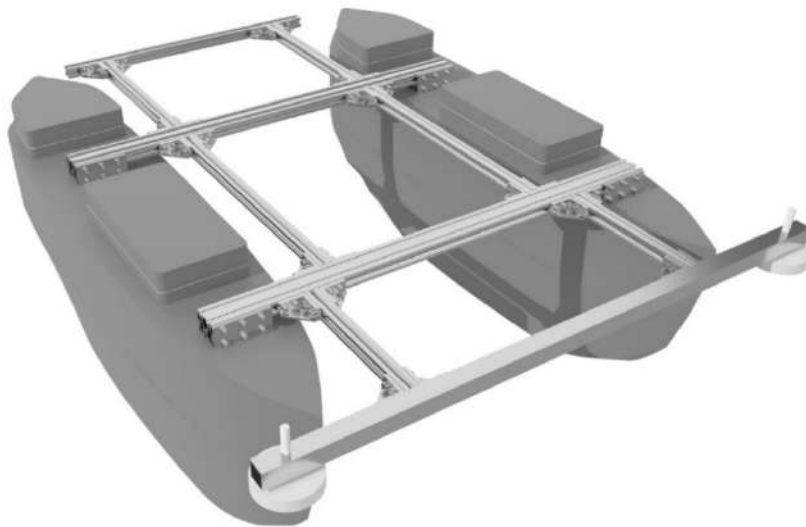


Fig. 1. Ares' hull and frame design

### I. INTRODUCTION

This appendix details Ares' hull and frame design and implementation, accommodating optimal autonomy performance for RoboBoat 2025. All design and production process are explained in-depth to give a clear explanation on how Barunastra achieve a versatile and reliable hull.

### II. HULL DESIGN

#### A. Retrospective Payload Calculation

Proteus has a total *displacement* ( $\Delta$ ) of 37.76 kg, which was considered enough to carry the calculated load on board based on its *Dead Weight Tonnage* (DWT) calculated using (1).

$$DWT = \Delta - LWT \quad (1)$$

While LWT, which only consists of the hull, is found to be six kilogram per hull after production process. Since the ship is catamaran hull which consists of two hulls, overall LWT is 12 kg.

$$\begin{aligned} DWT &= 37.76 \text{ kg} - 12 \text{ kg} \\ DWT &= 25.76 \text{ kg} \end{aligned} \quad (2)$$

Using the acquired DWT from (2), the amount of allowable load to be carried on board (*payload*) can be calculated using (3):

$$Payload = DWT - rt \quad (3)$$

While *rt* is its *provision weight* (weight that is assumed to gradually decrease over time). In a real-sized ship, this will be the weight of fuel, logistics supply, crew provision, etc. As an ASV, Proteus virtually had no decrease in weight during the entire operation. Thus, *rt* could be neglected. Therefore, the *payload* or allowable load to be carried on board Proteus is 25.76 kg.

Considerations with the Electro-programming Division concluded that the total *payload* weight for Ares is planned to be not much different from that of Proteus. Table I details the list of components considered for total *payload* mass calculation.

TABLE I PAYLOAD MASS CALCULATION

Item	Qty.	Mass (kg)	
		Per Item	Total
Electrical Box	1	7	7
T500 Thruster	2	1.7	3.4
T200 Thruster	2	0.5	1
Battery S	2	1.3	2.7
Battery L	4	0.6	2.5
Frame	1	3	3
Water gun	1	0.2	0.2
Water pump	2	0.2	0.4
Lidar	1	0.8	0.8
Bumper	1	0.2	0.2
Omni Antenna	1	0.2	0.2
Radar	1	0.2	0.2
Camera	1	0.2	0.2
Ball Launcher	1	1	1
Camera frame	1	0.2	0.2
Lidar frame	1	0.1	0.1
<b>Total Load</b>			23.1

Aside from principal dimension, Proteus' hull was analyzed using *Maxsurf Resistance*. The result shows that at the targeted service speed of 1.5433 m/s, proteus' resistance value via *slender body calculation* method is 26.23 N. Ares' hull should optimally have either a significantly lower resistance or at worst have the same resistance value compared to Proteus'.

### B. Design Approach

In designing the hull that could meet the team's objectives, Barunastra carried out iterations over time until all determined criteria were fulfilled. All results had been compared to each other in terms of resistance using *Maxsurf Resistance Software*. Of thirteen prototype iterations, only four of them met the criteria. Among those four, eleventh and thirteenth were debated since they both excel in all criteria. The difference between these two

prototypes lies only in the shape of their decks. Prototype 11<sup>th</sup> has a wider deck shape which makes it easier for propulsion maintenance due to the larger hatch holes whilst prototype 13<sup>th</sup> has a slim deck shape. However, after various considerations, the decision came to prototype 13<sup>th</sup> since prototype 11<sup>th</sup> has extreme curvature at the end of its stern that would make it difficult to be produced. The principal dimension of Ares hull is shown in Table II.

TABLE II ARES' HULL PRINCIPAL DIMENSION

Properties	Value
Length	0.99 m
Beam	0.2 m
Height	0.3 m
Draft	0.14 m
Block Coeff.	0.611
Displacement	31.77 kg

Besides having a smaller displacement in its scantling draft, the hull of Ares can obtain a bigger displacement when simulated using *Maxsurf Modeller* at the same draft compared to the Proteus' shown in Table III.

TABLE III DISPLACEMENT COMPARISON

	Proteus	Ares
Length	0.97 m	0.99 m
Beam (1 hull)	0.2 m	0.2 m
Height	0.3 m	0.3 m
Draft	0.18 m	0.18 m
Block Coeff.	0.544	0.620
Displacement	37.78 kg	44.20 kg

### C. Resistance Analysis

After the hull model for Ares had been decided, its resistance was analyzed using *ANSYS Fluent software* to determine the resistance that will be experienced by the hull when it is exposed to water and air current. Unlike *Maxsurf Resistance* which employs the formula of *slender body*, *ANSYS Fluent* was used since it yields a greater precision and accuracy. The result was then compared with Proteus' which is shown in Table IV.

TABLE IV ARES' HULL DRAG ANALYSIS

	Proteus	Ares
Speed	1.5433 m/s	1.5433 m/s
Hull Resistance	31.9745 N	14.3367 N
Air Resistance	2.0358 m	2.1879 m
Volume Friction	0.615356	0.607347
Max Wave Height	0.06631 m	0.09807 m

(Detailed comparison of wave pattern can be seen in Appendix B.1)

The result shows that Ares has less total resistance, indicating better hull performance in terms of minimizing drag.

#### D. Stability Analysis

The goal of this analysis is to determine the ideal component placement on board and predict the behavior of the ship when exposed to waves. Two software were used: *Maxsurf Stability* to analyze the stability under the load, and *Maxsurf Motions* which predict the ship movement when exposed to waves. In *Maxsurf Stability*, three methods called hydrostatic, equilibrium, and large angle stability were used. Prior executing analysis, load case, which will be used as input data, was calculated and shown in Table V.

TABLE V ARES' TOTAL LOAD CASE CALCULATION

	Qty.	Unit Mass (kg)	Total Mass (kg)	Long. Arm (cm)	Trans. Arm (cm)	Vert. Arm (cm)
Lightship	2	3.5	7	49.8	0	17
Electrical box	1	7	7	39	0	40
Thruster T500	2	1.7	3.4	18	0	-12
Thruster T200	2	0.5	1	75	0	-3
Battery S	2	1.3	2.7	68	0	3
Battery L	4	0.6	2.5	68	0	6
Frame	1	3	3	57.5	0	33
Water gun	1	0.2	0.2	102	0	34
Water pump	2	0.2	0.4	38	0	12
Lidar	1	0.8	0.8	83	0	60
Bumper	1	0.2	0.2	105	0	33
Omni Antenna	1	0.2	0.2	73.5	-25	40
Radar	1	0.2	0.2	69	17	55
Camera	1	0.2	0.2	72.5	0	72.5
Ball Launcher	1	1	1	56	0	35
Camera frame	1	0.2	0.2	70	0	53
Lidar frame	1	0.1	0.1	75	0	45
Total Loadcase			30.1	50.74	-0.08	20.89

The hydrostatic method shows the position of the points of the ship's stability elements, namely CG (*Center of Gravity*), CB (*Center of Buoyancy*), and CF (*Center of Flootation*). This method is also used to determine the condition of hull depth and tilt angle on ships longitudinally and transversely. The results of the hydrostatic method show that the position of CG, CB and CF is safe since the CG position is neither too high from baseline nor far apart from the CB while the CF position is in the midship section. These positions indicate that

Ares' hydrostatic is considered good and safe for ship operation.

The equilibrium method shows the heel and trim of the ship in static equilibrium position where the buoyancy and gravity are balanced. The results show the trim and heel of zero degrees, indicating that the ship is very stable.

Large angle stability is a method used to determine the capability of the ship to return to its original position when exposed to external forces. The results of the large angle stability analysis were obtained in the direction of the trim around

±0.96 deg. This result is considered safe for ship operation since the maximum permissible trim is 1% of ship’s length which is 0.99 [1]. This result means that the ship’s condition is likely to remain stable and will not disturb the vision system.

Analysis using *Maxsurf Motions* predicts the movement that the ship performs when exposed to waves. The method used for the analysis is strip theory [2]. After we calculated the simulation, we achieved a conclusion in Table VI.

TABLE VI MAXSURF MOTION SIMULATION RESULTS IN 0.15 M WAVE HEIGHT

Root Mean Squared (RMS)	
Speed	1.5433 m/s
Heave motion	0.038 m
Roll motion	0 deg
Pitch motion	0.18 deg
Heave velocity	0.037 m/s
Roll velocity	0 rad/s
Pitch velocity	0.0119 rad/s

(The detailed stability calculation can be seen in Appendix B.1)

From the table above, roll, pitch, and heave amplitude of Ares was used to determine the stability of the ship that will be explained in detail on Appendix B.1. The result shows that Ares meets all the criteria since it is still safe when encountering waves with 0.08 m – 0.2 m height.

### III. MAIN DECK FRAME DESIGN

To accommodate all ship systems, the main deck frame was designed with a rigid structure and be able to withstand the load from all components. In RoboBoat 2024, Barunastra’s main deck frame is strong enough to carry the desired load but relatively heavy due to complicated joint parts in the main deck base. This complexity also made the modularity concept ineffective since it needed a long time for assembly. Based on this evaluation, Barunastra decided to retain the V-slot aluminum alloy 6063 T5 but simplify the design by redesigning the main deck base and replacing the single slot angle bracket with double slot angle bracket. The redesign was expected to have a better strength than last year to maintain at least the same load.



Fig. 2. Simple construction model using single slot angle bracket



Fig. 3. Simple construction model using double slot angle bracket

Before implementing the concept and plan to the actual main deck frame design, the simpler structure model was designed to compare the strength between single and double slot angle brackets. The design was analyzed using two analyses: equivalent stress using Von Mises method to assess main deck frame strength under load and total deformation to determine how much the frame will deform from its original shape. Both analyses were executed using *ANSYS 2024 R2 Static Structural Mechanical Software*, and the results are shown in Table VII.

TABLE VII MAXIMUM EQUIVALENT STRESS AND TOTAL DEFORMATION OF SIMPLE STRUCTURE MODEL

Angle Bracket Type	Max Equivalent Stress (Pa)	Max Total Deformation (m)
Single slot	$6.07 \times 10^6$	$8.2185 \times 10^{-6}$
Double slot	$3.0845 \times 10^7$	$7.2368 \times 10^{-6}$

(The detailed analyses explanation can be seen in Appendix B.2)

Based on the result, the maximum equivalent stress for the double slot angle bracket is higher which means that under the same load, this structure can take a higher pressure before it yields than the one connected using a single slot angle bracket. From the total deformation, the structure connected using a single slot angle bracket has a bigger deformation which means that it is more prone or elastic than the one joined using a double slot angle bracket. These two analyses had proved that a double slot angle bracket is better than a single slot angle bracket in joining the structure. Based on this finding, we designed a new main deck frame using the double slot angle bracket. The main deck frame design was projected to be simpler and lighter yet still capable to carry the maximum allowable load. With those considerations, the design result is shown in the fig. 4 and fig. 5.

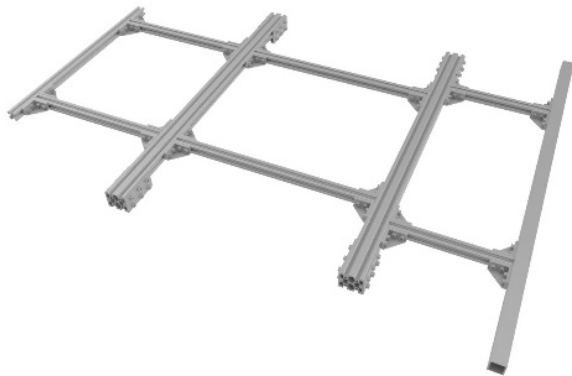


Fig. 4. Main deck frame design

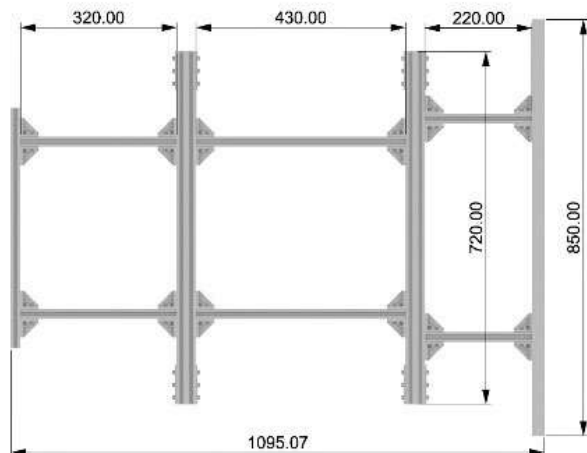


Fig. 5. Main deck frame dimension in millimeters

The same analyses were conducted to compare the strength and reliability of the new main deck frame design with the previous year design under the same designated load. The result is shown in Table VIII.

	<b>Max Equivalent Stress (Pa)</b>	<b>Max Total Deformation (m)</b>
<b>Proteus 2.0</b>	$1.3254 \times 10^7$	$3.6131 \times 10^{-4}$
<b>Ares</b>	$2.6519 \times 10^7$	$1.5123 \times 10^{-4}$

(The detailed analyses explanation can be seen in Appendix B.2)

The result shows that Ares has a higher maximum equivalent stress value which means that under the same load, Ares main deck frame can withstand higher pressure before it yields compared to Proteus 2.0's. Ares main deck is also stiffer and resistant to bending since the maximum total deformation value is smaller than Proteus 2.0's. Beside analyses, another consideration is weight. Both main deck frames have a significant weight difference that will affect the ship's performance. Instead of using the same material, the 2024 main deck frame's weight is 4.74 kg while the new main deck frame is 3.59 kg. This lightweight can give an advantage in increasing the ship's performance while at the same time providing the remaining load space for additional component on board.

#### IV. HULL PRODUCTION

##### A. Production Preparation Stage

The purpose of this stage is to set up the requirement so that the production process can be carried out. This includes a list of materials, methods, and production facilities. All materials used to produce Ares' hull are listed in Table IX.

TABLE IX HULL PRODUCTION MATERIALS

Material	Function
Carbon Fiber	Base material of the ship's hull
Glass Fiber	Base material for mold
Matt tissue	An outer layer of carbon fiber and glass fiber to make a flat surface
Resin Polyester	Glass fiber reinforcer and dryer medium
Resin Epoxy	Carbon fiber reinforcer and dryer medium
6 mm plywood	Construction support of the hull mold
3 mm Polyvinyl Chloride	Construction layer on the mold surface
Polyester Putty	Materials for surface leveling
Wax	Coating between the mold and carbon fiber
G - Adhesive glue	Adhesive between construction part on the mold

All processes were conducted in the production facility provided by our campus, ITS Robotics Workshop, where all parts were produced or repaired using available tools and machines.



Fig. 6. ITS robotics workshop

**B. Material Choice**

After conducting research on glass fiber material used for Proteus hull production, we found that the hull could be lighter by changing the material into carbon fiber. This conclusion comes since carbon fiber mechanical properties

outperform glass fiber's [3]. It is also suitable for applications that should meet strength, stiffness, and lightweight requirements. Therefore, carbon fiber is chosen since Ares hull was planned to have the same displacement with Proteus yet having the lighter weight.



Fig. 7. Carbon fiber sheets

**C. Production Method**

The method used to produce ship hulls is divided into two, which are making molds (Mold) and making products (Hulls). The method that we used in making molds was negative molds whilst the method used in making hull products was manual hand lay-up. The mold method is considered efficient since it directly uses negative mold without having to make a positive mold first while manual hand lay-up is chosen since it is cheaper than vacuum method in cost and there is no need to use compressors and other vacuum equipment.



Fig. 8. Ares' hull product



**D. Hull Production Stages**

**1) Mold Fabrication**

The process of making molds began with plotting the ship's design at each station to form the body plan, followed by plotting the shell plate parts. The plotted design was applied to six millimeter plywood and three millimeter PVC, then cut using a CNC machine to form all sections. All sections were then assembled, and PVC shell plates were attached to form the hull shell plate. The shell plate surface was caulked, smoothed, and coated using a gelcoat to produce a smooth surface. As the gelcoat layer was half dry, the resin process was carried out by coating the skin using polyester resin and strengthening it using glass fiber and fiber tissue. After 24 hours of resin drying, the surface was sanded and caulked again to ensure dimensional accuracy. When the desired mold dimension was obtained, the mold was ready to be used for the next process.



Fig. 9. Mold production process

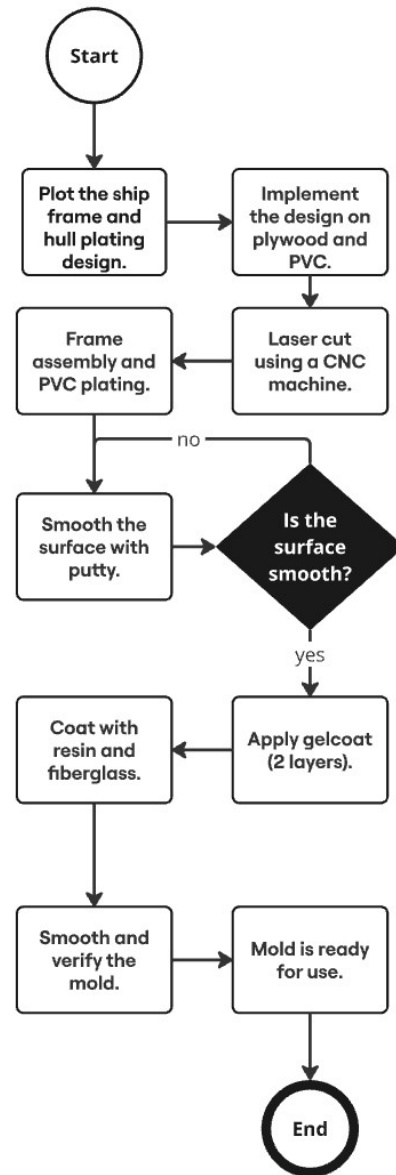


Fig. 10. Mold production flowchart

2) *Product Manufacture*

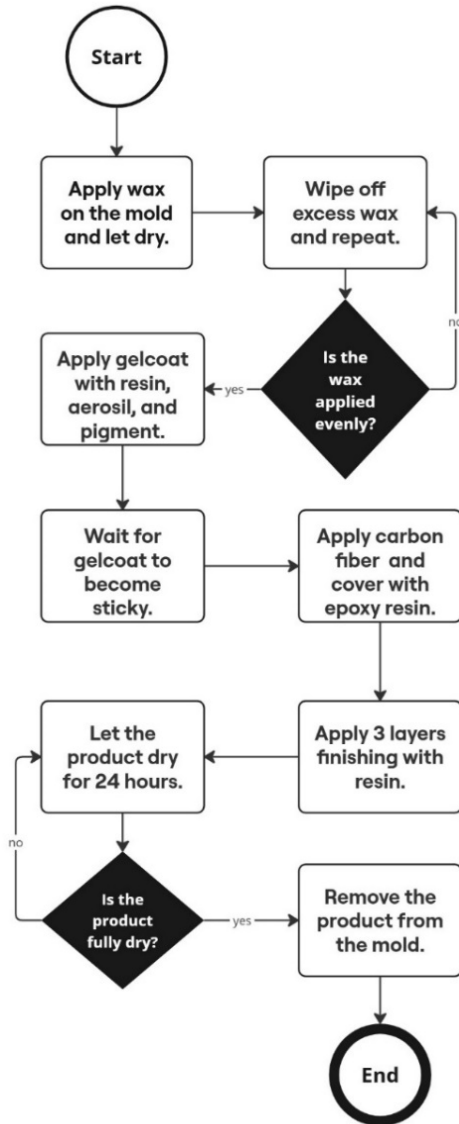


Fig. 11. Hull production flow chart

As the mold process completed, the first step was to coat the mold with wax evenly and let it dry for an hour. The dried wax was then removed using a tissue and the process was repeated twice to ensure the non-stick function. Afterwards, the mold was coated with gelcoat (mixed resin epoxy and *aerosil*) twice until the surface was slightly sticky. Carbon fiber was then plotted and coated using resin epoxy. This process was repeated until three layers. In the last layer, the resin was applied thoroughly. After the product had been dried for 24 hours, it was removed from the mold, and the hull was ready to be used.



Fig. 12. Hull production process

**E. Production Results**

Upon completing hull production process, the hull was measured and weighed. The dimension is shown in Table X.

TABLE X DIMENSION OF ONE HULL PRODUCT

Properties	Value
LOA	0.99 m
Beam	0.20 m
Depth	0.31 m
Weight	3.76 kg



Fig. 13. Hull weight

**V. MAIN DECK PRODUCTION**

The Main Deck is a part of the ship that is used as the place for main component assembly, such as electrical box, camera frame, and water-ball shooting assembly.

**A. Main Deck Frame**

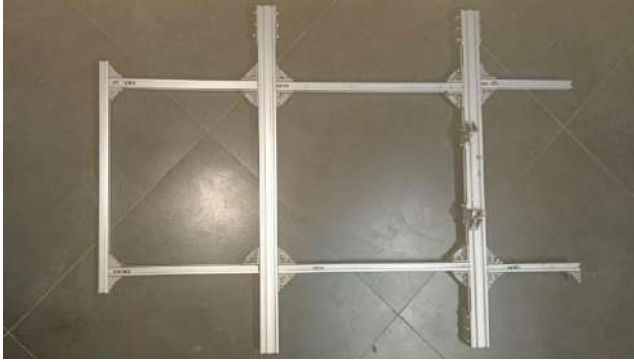


Fig. 14. Main deck frame

Main deck frame is created utilizing single V-slot and double V-slot aluminum. This material is used because of its strength in carrying our component's weight. All parts of this frame were fabricated using a grinding machine to cut the material close to the required dimension, then continued with the cut using a milling machine to decrease the dimension deviation due to the higher precision of this machine. All parts were assembled using double slot angle bracket.



Fig. 15. Double slot angle bracket installation

**B. Main Deck Base**

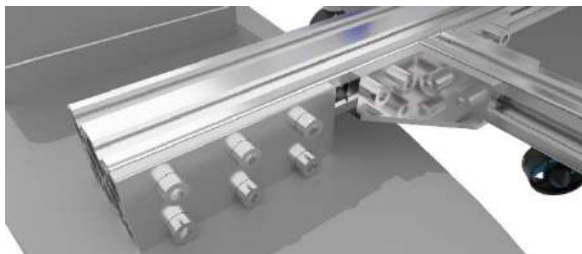


Fig. 16. Main deck base design

To support our modularity, we constructed a base on the hull, allowing the main deck to be removable, reassembled, and transported. The material used is double V-slot aluminum. This

shape was chosen to accommodate the installation of bolts with a rectangle pattern to the hull to ensure its sturdiness, which is shown in fig. 17. Steel epoxy was also applied for more strength.



Fig. 17. Main deck base installation

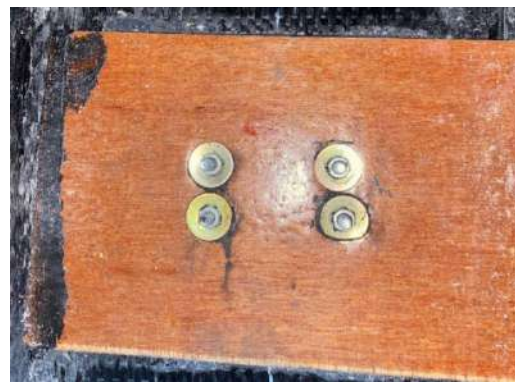


Fig. 18. Main deck base bolt points

For assembly, the main deck frame is placed on the base and connected with the bracket plate in the fore and rear side like shown in fig. 17. 3 mm aluminum plates are used and holed as shown in figure 16. Bracket plates, main deck frame, and base are connected using bolts and T-slide nuts.

**C. Bumper**



Fig. 19. Bumper and roller

The purpose of the bumper is to prevent the ship from being damaged due to collisions on the

forward part of the ship. The bumper is produced by using square hollow aluminum, wood, and foam. The 80 cm hollow aluminum was filled with wood that would strengthen the bumper to avoid deformation when collisions happen. The front side of the bumper is protected with foam attached using bolts and nuts. Both end sides of the bumper were holed for omni wheel rollers installation. The rollers are used to avoid the ship being stuck at the ends of the bumper when the ship crashes with other objects. The bumper is then assembled to the fore of the main deck frame using angle brackets, bolts, and T-slide nuts.

- [3] C. Wonderly, J. Grenestedt, G. Fernlund, and E. Čepus, "Comparison of mechanical properties of glass fiber/vinyl ester and carbon fiber/vinyl ester composites," *Composites Part B: Engineering*, vol. 36, no. 5, pp. 417–426, 2005.



Fig. 20. Hull and main deck product installation

## VI. CONCLUSION

Design and Production process which had been done yields a satisfactory result since the hull and main deck frame are significantly lighter than previous year's. Beside the overall weight, the main deck frame is also more reliable and stronger to carry all components on board. From this result, Ares can perform better in overall aspect than Proteus 2.0 for RoboBoat 2025 challenges.

## VII. REFERENCES

- [1] International Maritime Organization, *International Convention for the Safety of Life at Sea (SOLAS)*, 1974, ch. II-1, Subdivision and Damage Stability, reg. 5-1.4, 1974.
- [2] P. J. Bandyk, "A body-exact strip theory approach to ship motion computations," Ph.D. dissertation, University of Michigan, Ann Arbor, MI, 2009.

# Appendix B.1: Test Plan and Result

## Hull Simulation and Analysis

M Farras Rheza Firmansyah, Davin Abhinaya Briet

### I. ANSYS FLUENT

#### A. Scope

To determine Ares' hull reliability, we conducted hull drag analysis to calculate the ship resistance, volume friction and maximum wave-height value experienced by the ship when operating at its service speed.

#### B. Schedule

The simulation was carried out on November 18<sup>th</sup> until December 22<sup>nd</sup>, 2024. Each simulation took around 40 minutes to be done.

#### C. Resources and Tools

The simulation was carried out using *ANSYS Fluent with Meshing 2024 R2 Software*. This software was chosen since the fluid (hull drag and maximum wave high) which will be used are static and material behavior can be approximated as linear elastic

#### D. Environment

Tests for *Hull Drag* were conducted at service speed of three knots or equivalent to 1.5433 m/s,

gravitational acceleration of  $9.81 \text{ m/s}^2$ , hull meshing at 3 mm, and test area meshing at 5 mm.

#### E. Risk Management

**1) Modelling Error:** This problem often occurred when importing files from *Maxsurf* format as the model form is not solid. There are open edges that can make the object could not be read by *ANSYS* because the *ANSYS* only read solid models. This problem made the analysis could not be run or failed. To fix this problem, the model should be exported into another software format before going to *ANSYS* to change all the open edges to close edges.

**2) Software License Restriction:** Due to the student version of the license, there are restrictions affecting the analysis, such as node amount and mesh size. These elements play a vital role for the analysis result. To solve this problem, we reduced the number of nodes until it was accepted by *ANSYS* restriction.

### F. Result

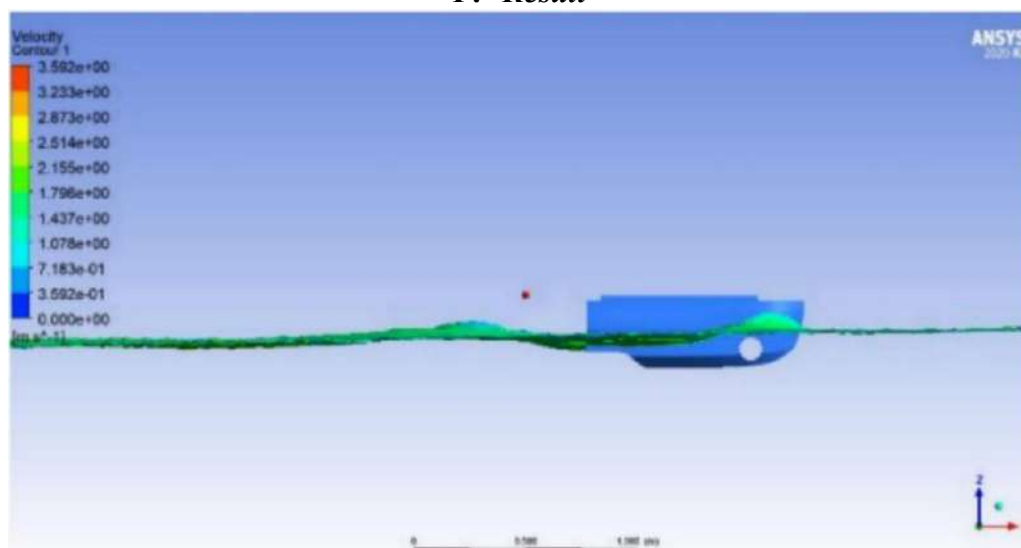


Fig. 1. Proteus side view

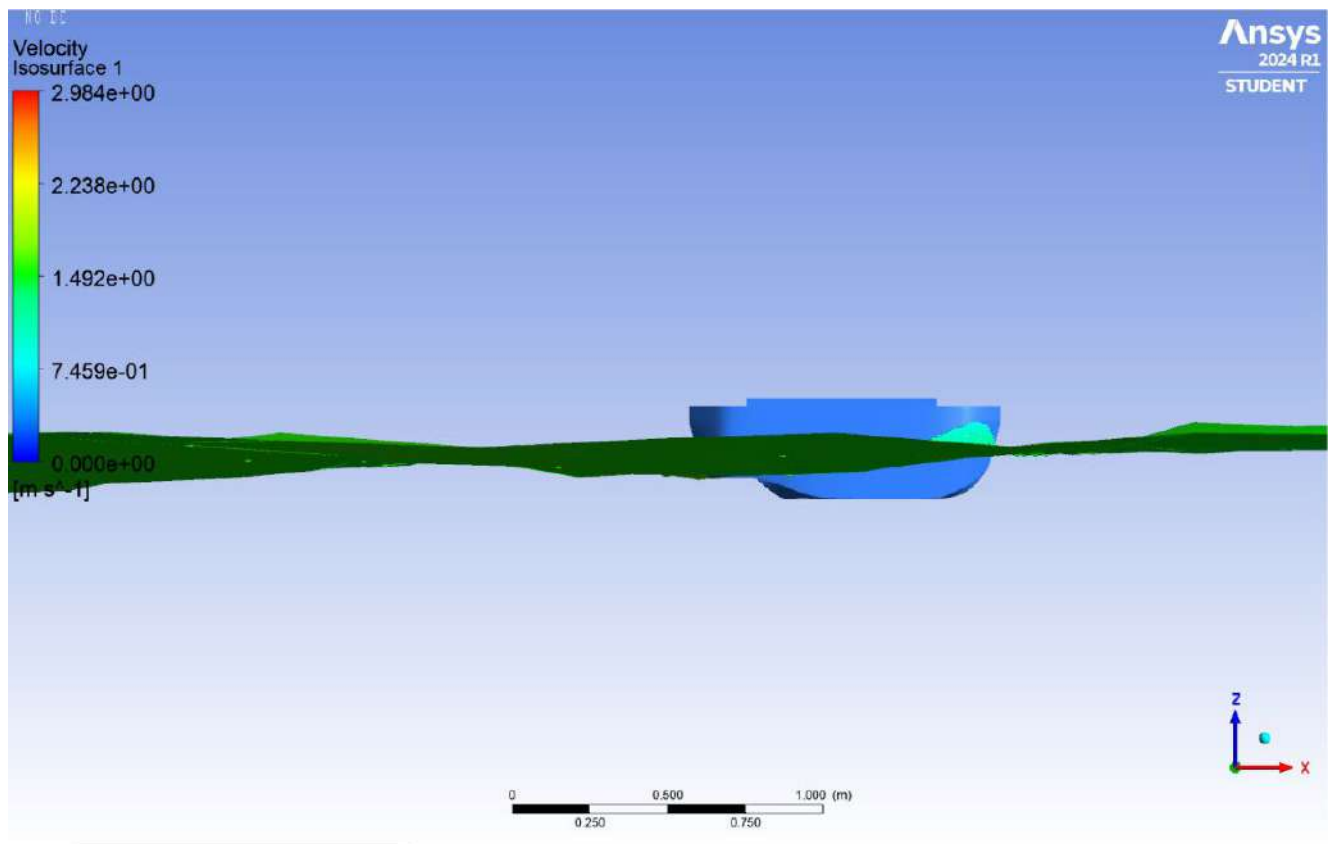


Fig. 2. Ares side view

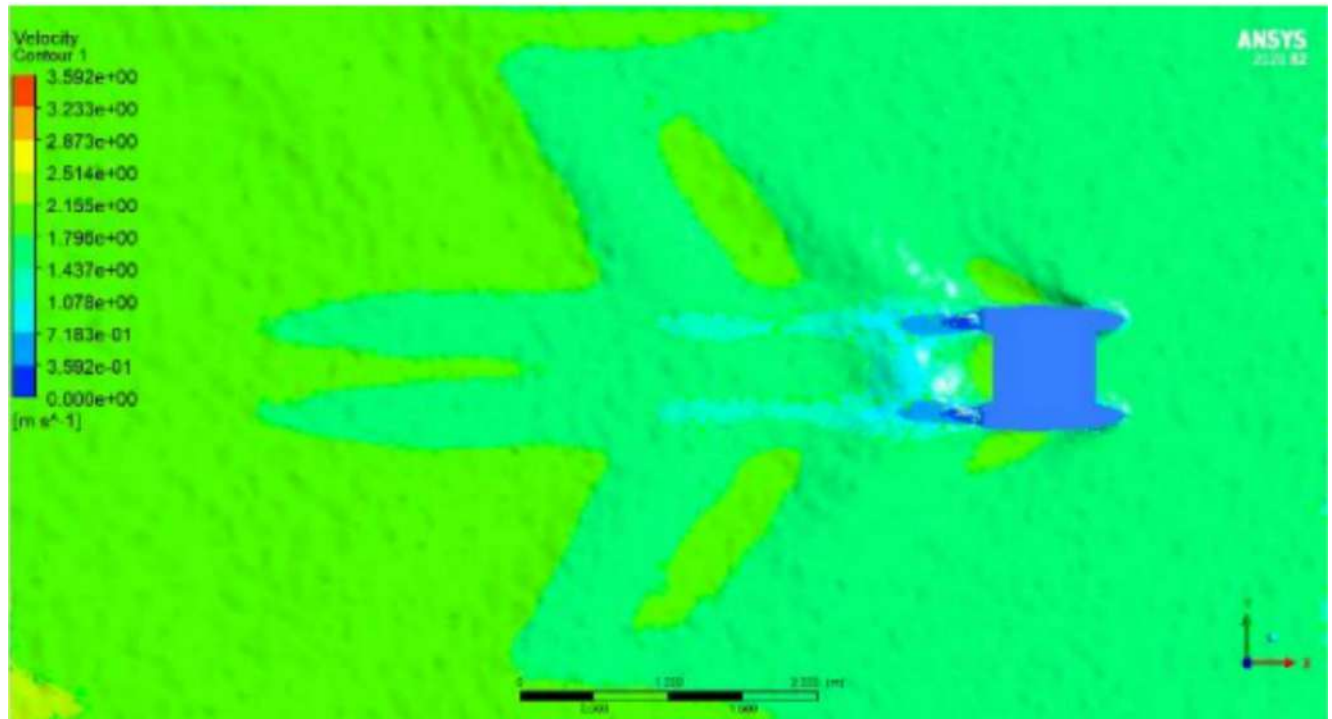


Fig. 3. Proteus top view

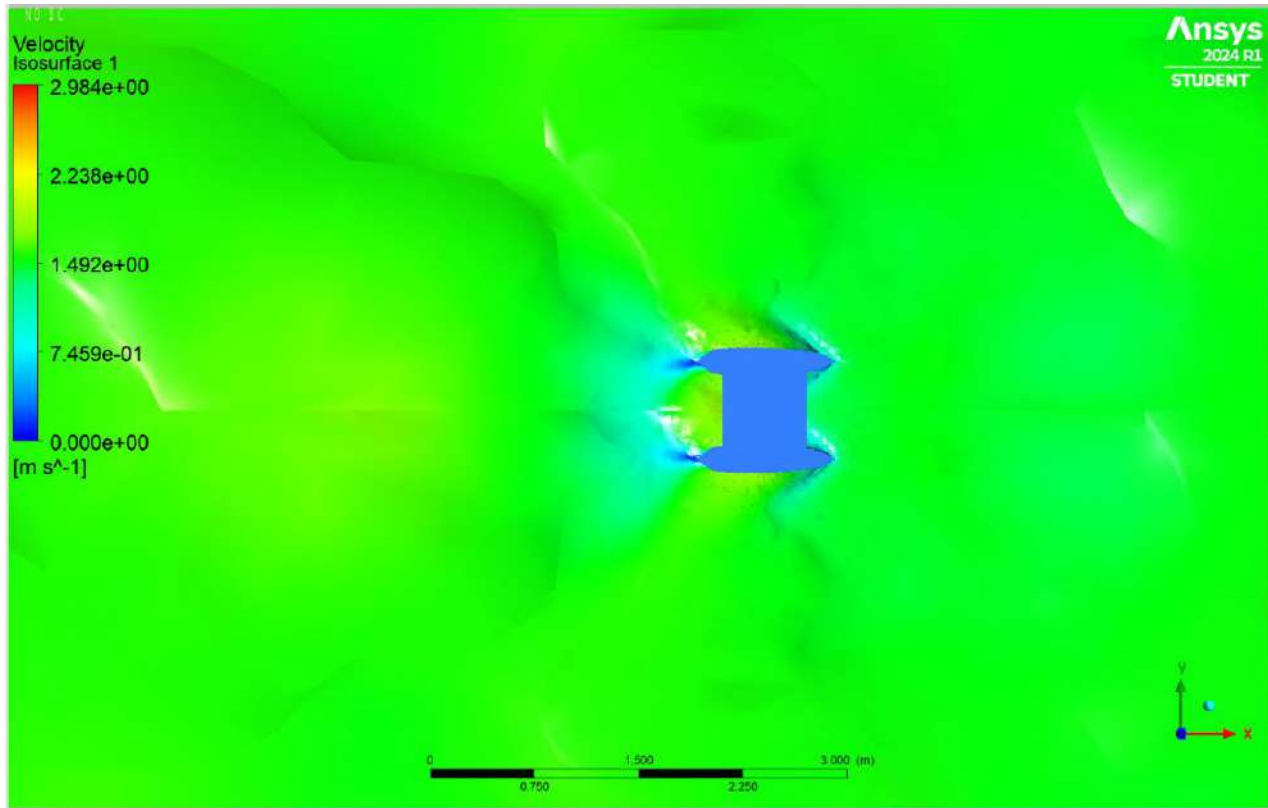


Fig. 4. Ares top view

TABLE I ANSYS FLUENT RESULTS COMPARISON

	Proteus	Ares
Speed	1.5433 m/s	1.5433 m/s
Hull Resistance	31.9745 N	14.3367 N
Air Resistance	2.0358 N	2.1879 N
Volume Friction	0.615356	0.607347
Max Wave Height	0.06631 m	0.09807 m

From the figures and Table I, Ares has smaller resistances than Proteus but bigger in maximum wave height due to the shape of the bow.

## II. MAXSURF RESISTANCE

### A. Scope

Hull drag analysis was conducted to calculate the ship resistance and inspected wave making pattern produced by the ship when operating at its service speed. This analysis was also used to determine the power needed for the ship to operate at service speed.

### B. Schedule

The simulation was carried out on November 20<sup>th</sup> until December 8<sup>th</sup>, 2024. Each simulation took around five minutes to be done.

### C. Resource and Tools

Maxsurf resistance software was used for conducting this analysis. The method we used is slender body [1] due to the hull type which is catamaran.

**D. Environment**

The environment settings of *Maxsurf Resistance* are shown in Table II

TABLE II SOFTWARE SETTINGS FOR RESISTANCE ANALYSIS

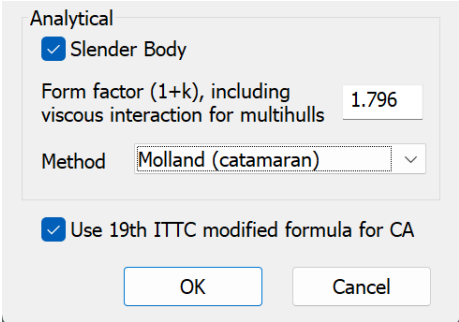
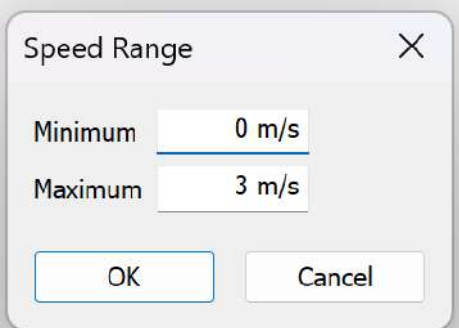
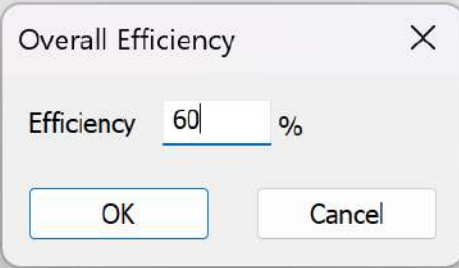
Element	Information
Methods	<p>The method used for this analysis was a <i>slender body</i> (Molland) approach since this analysis was developed for calculating resistance in catamaran vessel type.</p> 
Speed	<p>The <i>Hull drag</i> test was conducted at different speeds ranging from 0-3 m/s with service speed of 1.5433 m/s or equivalent to three knots. This range of speeds is projected to be the top speed of the ship.</p> 
Efficiency	<p>The efficiency of the hull was set on 60% due to propulsion system power loss.</p> 

Fig. 5. Method settings

Fig. 6. Speed range

Fig. 7. Efficiency setting

**E. Risk Management**

**1) Modelling Error**

*Maxsurf Modeller* file could crash when it was operated which made *Maxsurf Resistance* unable to ‘read’ the surface. The solution of this problem was to make new file with the same shape and sizes.

**2) Less Precise Analysis**

*Hull drag* analysis performed by *Maxsurf Resistance* are not 100% precise since it is using numerical approach. Therefore, another software must be used for more precise analysis.



### F. Result

Resistance analysis was conducted at 1.5 m/s for each iteration and the result is shown in Table III and IV.

TABLE III 13 PROTOTYPES RESISTANCE

<b>Resistance of the Prototypes</b>					
<b>Prototypes</b>	<b>Speed (m/s)</b>	<b>Froude No. LWL</b>	<b>Froude No. Volume</b>	<b>Slender body Resistance (N)</b>	<b>Slender body Power (kW)</b>
1	1.5433	0.499	0.862	121.78	0.188
2	1.5433	0.516	0.855	129.57	0.200
3	1.5433	0.500	0.872	273.61	0.422
4	1.5433	0.500	0.856	297.65	0.459
5	1.5433	0.523	0.867	305.13	0.471
6	1.5433	0.489	0.847	261.25	0.403
7	1.5433	0.494	0.849	269.40	0.416
8	1.5433	0.499	0.851	293.90	0.454
9	1.5433	0.499	0.858	303.17	0.468
10	1.5433	0.501	0.861	14.91	0.023
11	1.5433	0.506	0.866	20.64	0.032
12	1.5433	0.505	0.865	17.07	0.026
13	1.5433	0.508	0.879	18.80	0.029

From all the experiments, the 13<sup>th</sup> prototype was the latest experiment since it has a small enough resistance and good wave making. The analysis detail for 13<sup>th</sup> prototype is shown in Table IV.

TABLE IV ARES' HULL RESISTANCE

<b>No.</b>	<b>Speed (m/s)</b>	<b>Froude No. LWL</b>	<b>Froude No. Vol</b>	<b>Slender body Resistance (N)</b>	<b>Slender body Power (kW)</b>
1	0	0	0	--	--
2	0.2572	0.084	0.144	0.46	0
3	0.5144	0.169	0.289	1.88	0.001
4	0.7717	0.253	0.433	3.72	0.003
5	1.0289	0.337	0.577	6.29	0.006
6	1.2861	0.421	0.722	14.25	0.018
7	1.5433	0.506	0.866	20.64	0.032
8	1.8006	0.59	1.01	24.17	0.044
9	2.0578	0.674	1.155	27.01	0.056
10	2.315	0.759	1.299	30.05	0.07
11	2.5722	0.843	1.444	33.43	0.086
12	2.8295	0.927	1.588	37.11	0.105
13	3.0867	1.012	1.732	41.07	0.127

TABLE V ARES' HYDROSTATIC TABLE

Item	Value	<i>Slender Body</i>
LWL	94.95 cm	--
Beam	74.47 cm	--
Draft	15 cm	--
Displaced volume	33947.97 cm <sup>3</sup>	--
Wetted area	6842.47 cm <sup>2</sup>	6842.47
Prismatic coeff. (Cp)	0.682	--
Waterpl. area coeff. (Cwp)	0.805	--
1/2 angle of entrance	23.9 deg.	--
LCG from midships (+ve for'd)	-5.3 cm	--
Transom area	0 cm <sup>2</sup>	--
Transom wl beam	0 cm	--
Transom draft	0 cm	--
Max sectional area	523.89 cm <sup>2</sup>	--
Bulb transverse area	0 cm <sup>2</sup>	--
Bulb height from keel	0 cm	--
Draft at FP	15 cm	--
Deadrise at 50% LWL	1.3 deg.	--
Hard chine or round bilge	Hard chine	--
Frontal Area	0 cm <sup>2</sup>	
Headwind	0 m/s	
Drag Coefficient	0	
Air density	0 kg/cm <sup>3</sup>	
Appendage Area	0 cm <sup>2</sup>	
Nominal App. length	0 cm	
Appendage Factor	1	
Correlation allowance	use 19 <sup>th</sup> ITTC formulation	use 19 <sup>th</sup> ITTC formulation
Kinematic viscosity	0.0118831 cm <sup>2</sup> /s	
Water Density	0.001 kg/cm <sup>3</sup>	

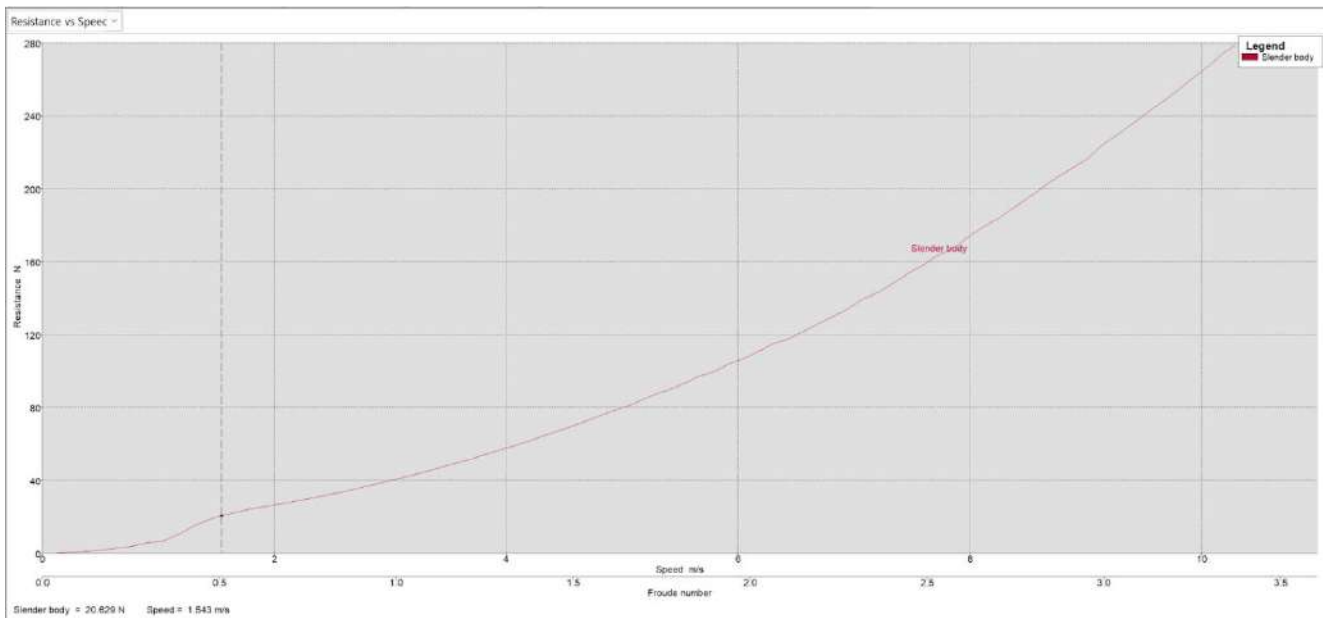


Fig. 8. Resistance vs speed curve (resistance: 20.629 N slender body; speed: 1.5433 m/s)

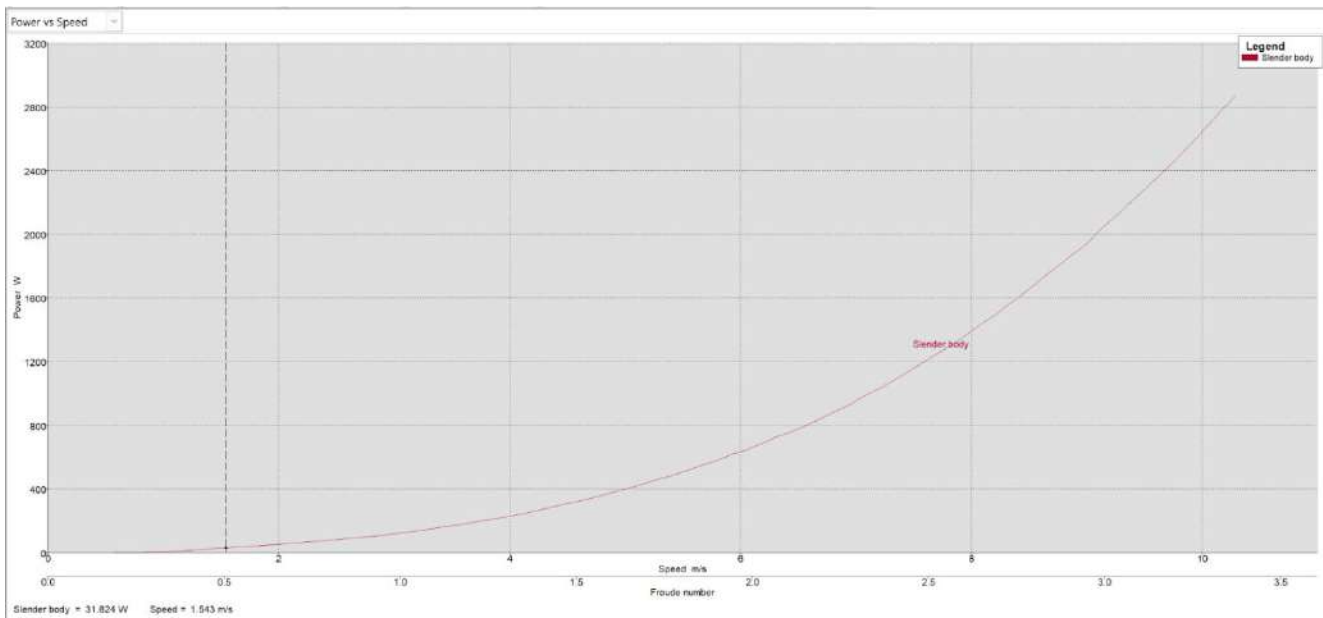


Fig. 9. Power vs speed (power: 31.8240 W slender body; speed: 1.5433 m/s)

After the 13<sup>th</sup> prototype was analyzed and all requirements accomplished, the prototype was compared with Proteus' to benchmark the ability. The *hull drag* analysis results compared to Proteus' is shown in fig. 22 until fig. 25.

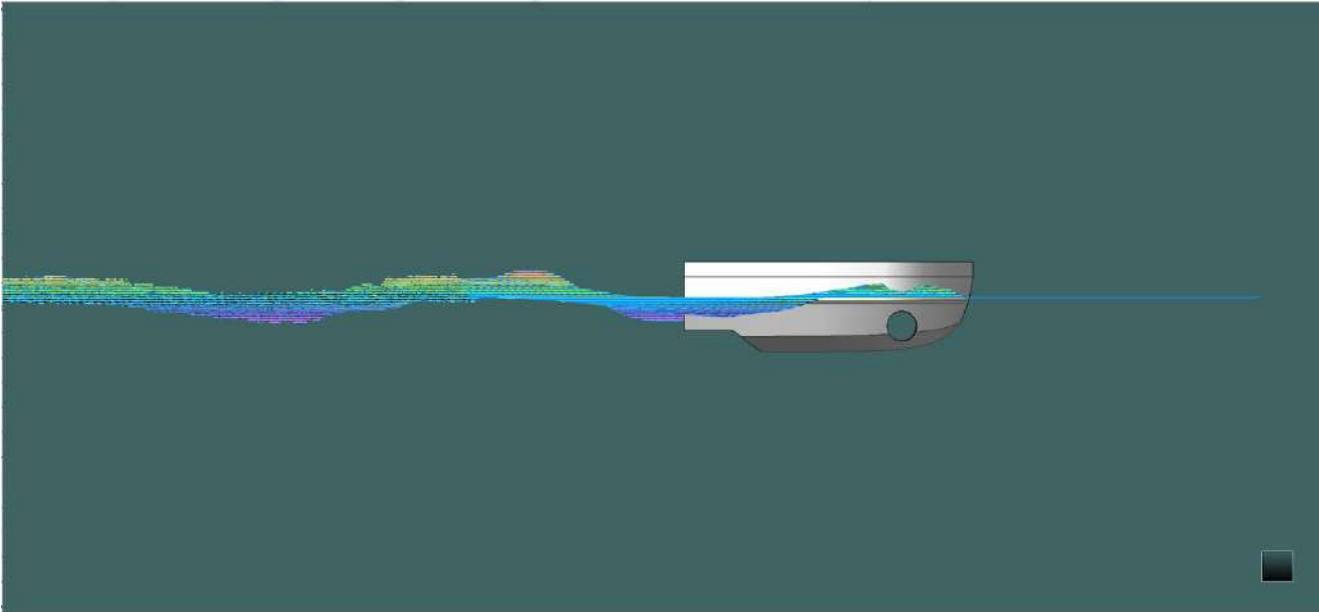


Fig. 10. Side view, Proteus

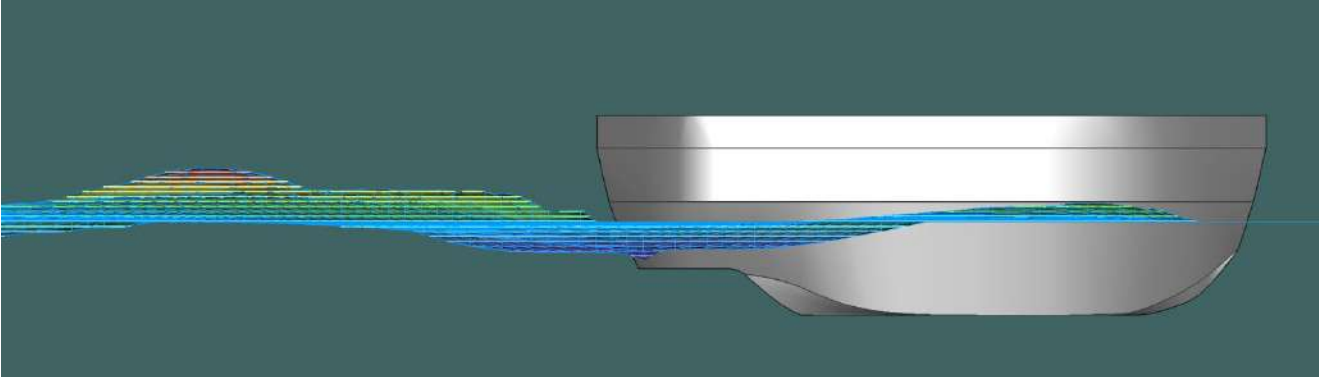


Fig. 11. Side view, Ares

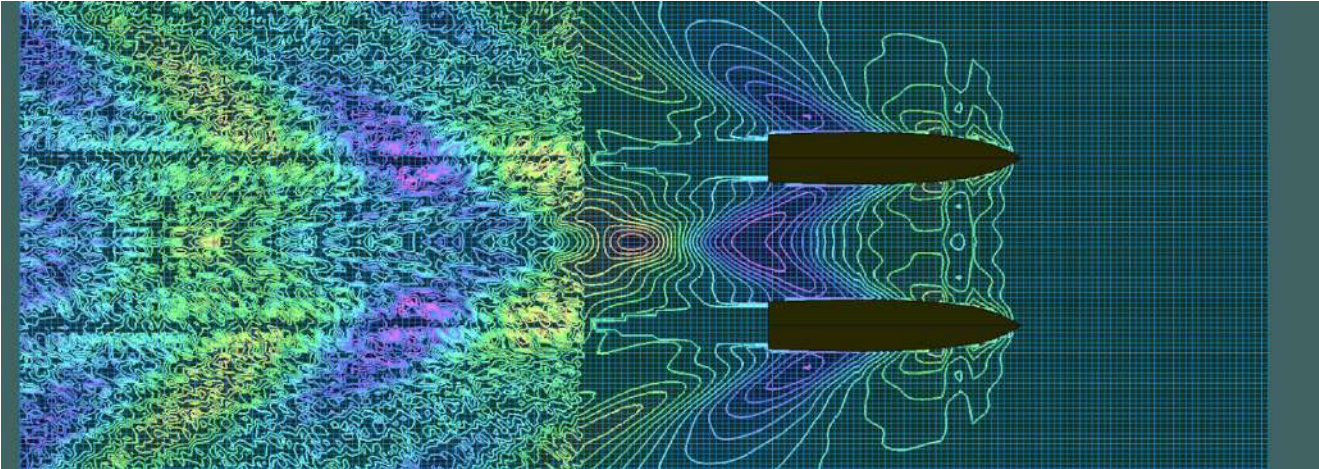


Fig. 12. Top view, Proteus

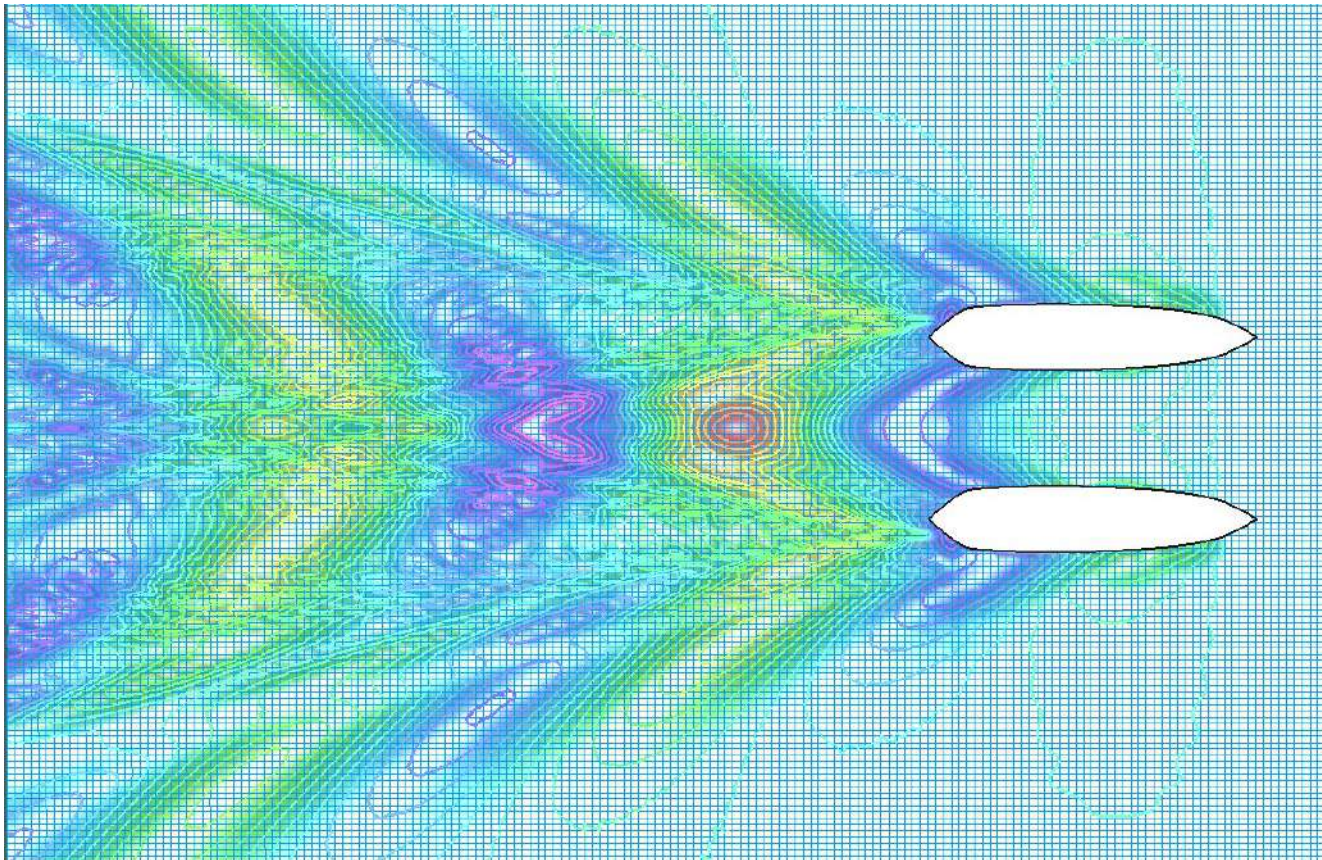


Fig. 13. Ares' top view

From the figure, we can conclude that the wave making simulation by Ares has a smaller amplitude than Proteus which reduces the risk of water from reaching the deck. Therefore, we imply that Ares has better response than Proteus when interacting with water.

### G. References

[1] A. Jamaluddin, I. K. A. P. Utama, and M. A. Hamdani, "Kajian interferensi koefisien hambatan pada lambung katamaran melalui komputasi 'Slender Body Method'," *Kapal: Jurnal Ilmu Pengetahuan dan Teknologi Kelautan*, vol. 7, no. 2, 2010.

## III. MAXSURF STABILITY

### A. Scope

Seakeeping analysis was carried out to calculate hull reliability, focusing on the stability of the ship when carrying the load. This analysis was done using three methods, called *hydrostatic*, *equilibrium*, and *large angle stability*.

### B. Schedule

The simulation was carried out on December 8<sup>th</sup>, 2024, and it took around 2 hours to be done.

### C. Resources and Tools

The simulation was conducted using *Maxsurf stability software*. This software was chosen because it is compatible with *Maxsurf Modeller*. Three main methods to determine ship stability

were chosen: *hydrostatic, equilibrium, and large angle stability.*

TABLE VI SOFTWARE SETTINGS FOR STABILITY ANALYSIS

Element	Information								
Load case	A load case is a list of components that will be used on the ship. The components are arranged according to their usage. We arranged the placement of all components with coordinates along with their weight so that ship stability could be determined.								
	Item Name	Quantit	Unit Mass kg	Total Mass kg	Unit Volume cm^3	Total Volume cm^3	Long. Arm cm	Trans. Arm cm	Vert. Arm cm
	Lightship	2	3.5	7.0			49.80	0.00	17.00
	electrical box	1	7.0	7.0			39.00	0.00	35.00
	t500	2	1.7	3.4			18.00	0.00	-12.00
	t200	2	0.5	1.0			75.00	0.00	-3.00
	tatu	2	1.3	2.7			68.00	0.00	3.00
	onbo	4	0.6	2.5			68.00	0.00	6.00
	frame	1	3.0	3.0			57.50	0.00	33.00
	water gun	1	0.2	0.2			102.00	0.00	34.00
	pump	2	0.2	0.4			38.00	0.00	12.00
	lidar	1	0.8	0.8			83.00	0.00	60.00
	bumper	1	0.2	0.2			105.00	0.00	33.00
	omni antenna	1	0.2	0.2			73.50	-25.00	40.00
	antenna	1	0.2	0.2			69.00	17.00	55.00
	logitech camera	1	0.2	0.2			72.50	0.00	72.50
	ball launcher	1	1.0	1.0			56.00	0.00	35.00
	frame logi	1	0.2	0.2			70.00	0.00	53.00
	frame lidar	1	0.1	0.1			75.00	0.00	45.00
	<b>Total Loadcase</b>			<b>30.1</b>	<b>0.00</b>	<b>0.00</b>	<b>50.74</b>	<b>-0.08</b>	<b>19.73</b>
	<b>FS correction</b>								<b>0.00</b>
	<b>VCG fluid</b>								<b>19.73</b>

Fig. 14. Load case table

Heel setup This setup is used for the inclined test. Initial heel degree and heel direction were set to calculate the ship’s stability.

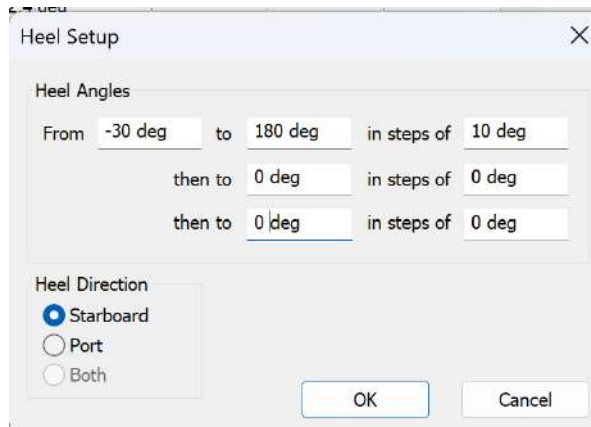


Fig. 15. Heel setup

Trim setup The trim setup is used to simulate the trim condition on the analysis. We chose a free trim to load case to know whether the component position is causing the ship to trim or not.

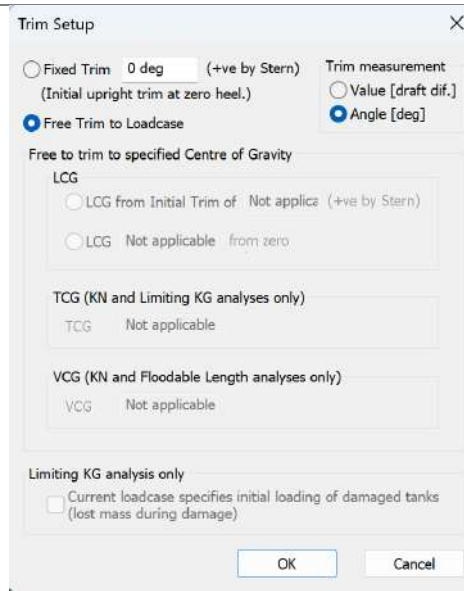


Fig. 16. Trim setup

Draft

This setup is used for hydrostatic analysis. The draft was adjusted since the ship’s actual displacement might be different from the design.

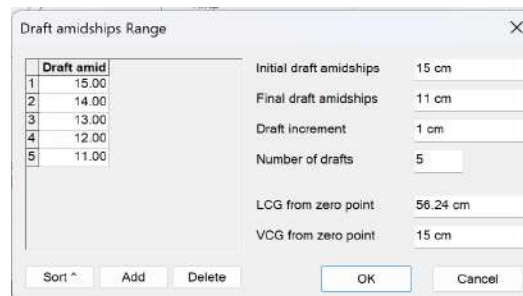


Fig. 17. Draft setting

Density

This setup allows us to calculate the ship’s stability on different density of water such as sea water and fresh water. On this test, we used the density of sea water.

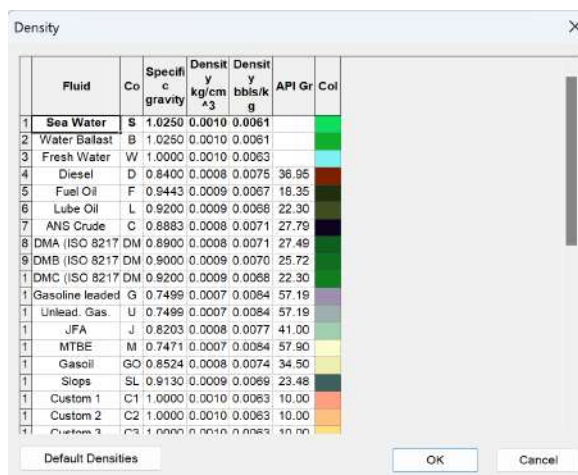


Fig. 18. Density selection

**Criteria** This set up allows us to choose different types of criteria/regulations that we can use for different kinds of analysis. For stability analysis, we used IMO code for the criteria.

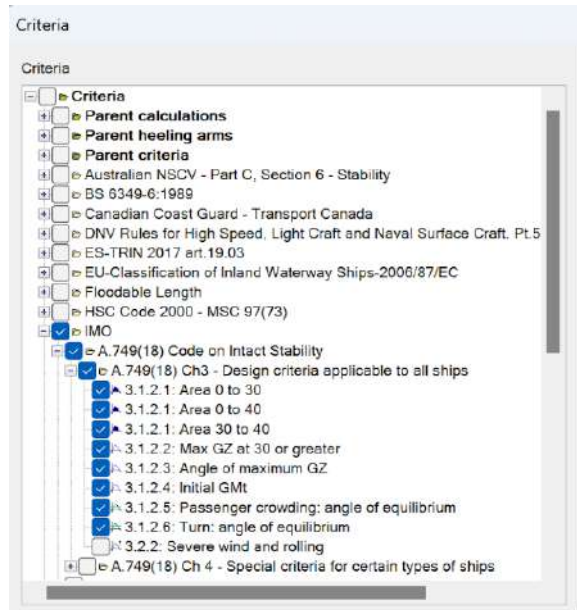


Fig. 19. Criteria selection

**D. Risk Management**

The risk often occurred from the load case adjustment. Load case is part from the design, and it is possible that the load case has different placement due to production errors or components

replacement. To solve this problem, the load case table had been given loads margin to reduce the impact on analysis result if production error happened.

**E. Result**

**1) Hydrostatic Analysis**

This test is carried out to understand the ship conditions on different drafts. Here is the result of upright hydrostatic on Ares:

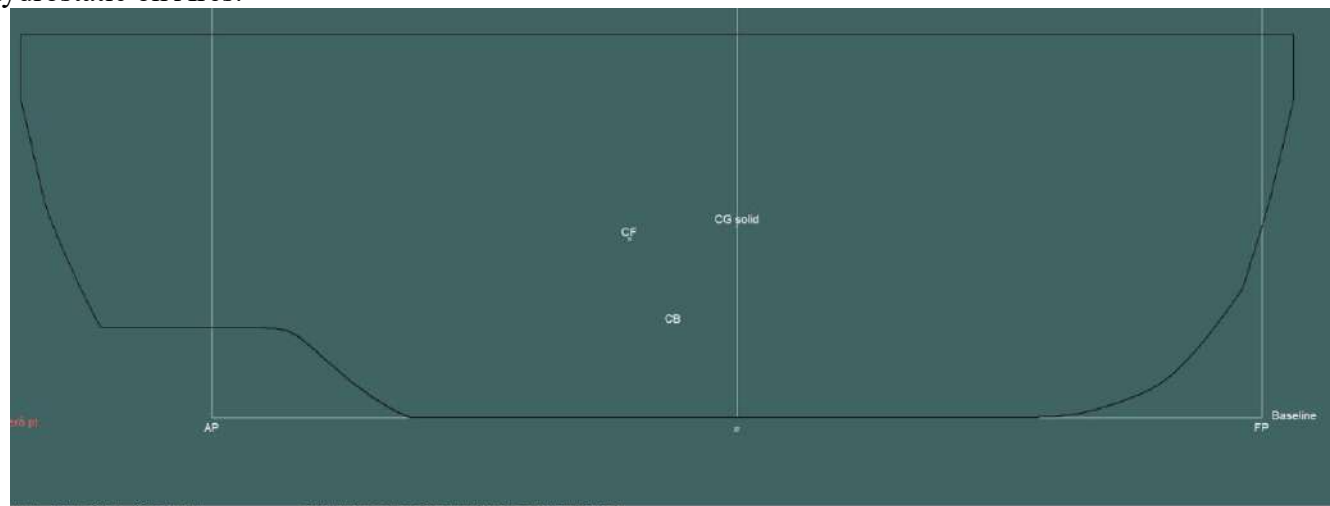


Fig. 20. Ares' upright hydrostatic



The upright hydrostatic method shows the position of the points of the ship's stability elements, CG, CB and CF. The results of the hydrostatic method show that the position of CG, CB and CF is fairly safe since the CG position is neither too high from baseline nor far apart from the CB while the CF position is in the midship section. Furthermore, the hydrostatic analysis can help to predict the ship component arrangement because the CG (Center of Gravity) position has been calculated. Other element listed on the table below can arrange to make the hydrostatic curve.

TABLE VII ARES' HYDROSTATIC RESULTS

<b>Draft Amidship (m)</b>	<b>0.15</b>	<b>0.14</b>	<b>0.13</b>	<b>0.12</b>	<b>0.11</b>
Displacement (kg)	34.8	31.78	28.83	25.94	23.13
Heel (deg)	0	0	0	0	0
Draft at FP (m)	0.15	0.14	0.13	0.12	0.11
Draft at AP (m)	0.15	0.14	0.13	0.12	0.11
Draft at LCF (m)	0.15	0.14	0.13	0.12	0.11
Trim (+ve by stern) (m)	0	0	0	0	0
WL Length (m)	0.95	0.942	0.935	0.927	0.92
Beam max extents on WL (m)	0.745	0.742	0.74	0.737	0.735
Wetted Area (m <sup>2</sup> )	0.684	0.646	0.608	0.57	0.532
Waterpl. Area (m <sup>2</sup> )	0.298	0.291	0.285	0.278	0.271
Prismatic coeff. (Cp)	0.682	0.678	0.672	0.666	0.658
Block coeff. (Cb)	0.612	0.611	0.61	0.608	0.604
Max Sect. area coeff. (Cm)	0.902	0.907	0.912	0.917	0.922
Waterpl. area coeff. (Cwp)	0.805	0.804	0.802	0.8	0.798
LCB from zero pt. (+ve fwd) (m)	0.509	0.513	0.516	0.52	0.525
LCF from zero pt. (+ve fwd) (m)	0.476	0.478	0.479	0.481	0.483
KB (m)	0.085	0.079	0.073	0.068	0.062
KG (m)	0.15	0.15	0.15	0.15	0.15
BMt (m)	0.686	0.733	0.789	0.855	0.935
BML (m)	0.496	0.523	0.555	0.593	0.637
GMt (m)	0.62	0.663	0.713	0.773	0.847
GML (m)	0.431	0.453	0.479	0.51	0.549
KMt (m)	0.77	0.813	0.863	0.923	0.997
KML (m)	0.581	0.603	0.629	0.66	0.699
Immersion (TPc) (tonne/cm)	0.003	0.003	0.003	0.003	0.003
MTc (tonne.m)	0	0	0	0	0
RM at 1deg = GMt.Disp.sin(1) (kg.m)	0.377	0.367	0.359	0.35	0.342
Max deck inclination (deg)	0	0	0	0	0
Trim angle (+ve by stern) (deg)	0	0	0	0	0

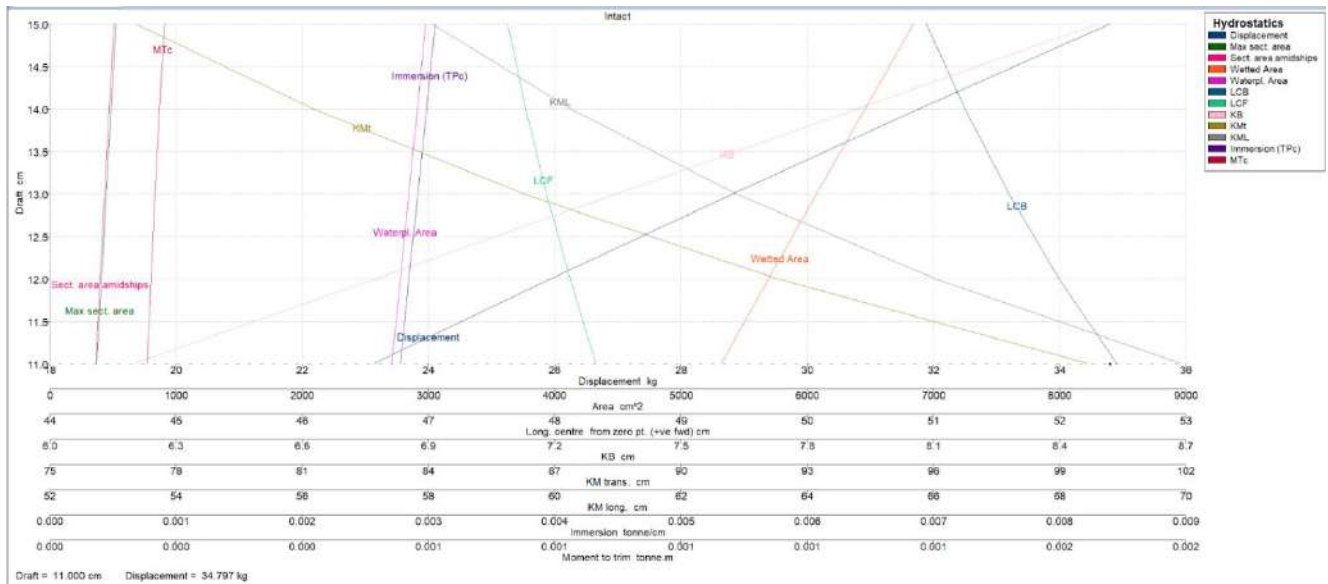


Fig. 21. Ares curve of hydrostatic

**2) Equilibrium Analysis**

This test is carried out to analyze the ship condition on static equilibrium position. Static equilibrium position means the buoyancy force and the gravity force are the same. And the ship will retain the same position without moving.

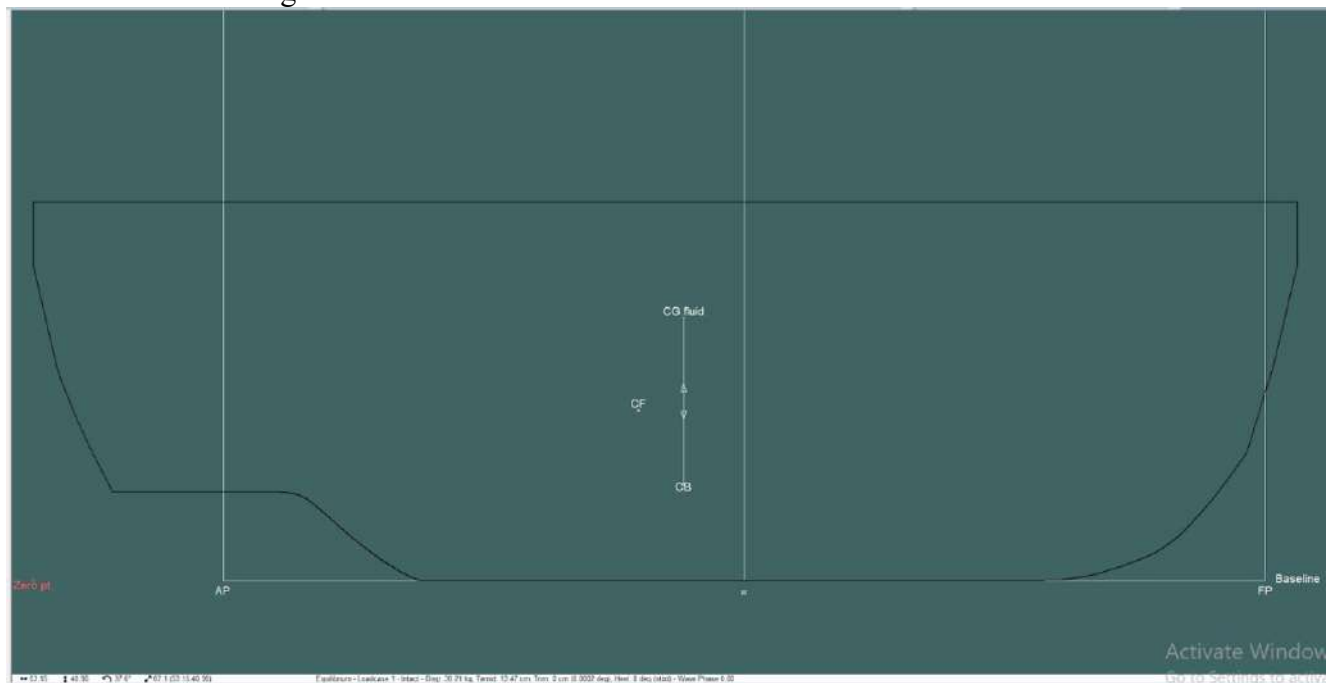


Fig. 22. Results of equilibrium

From the results of equilibrium analysis, the trim and heel value of the ship are 0. Which mean the load case of the ship is well placed.

**3) Large Angle Stability / Intact Stability Analysis**

This test is carried out to determine the ship capability to stabilize itself when opposed by external forces. In this test we set the initial heel for 30 degrees with the load case shown above. Here are the results of the large angle stability:

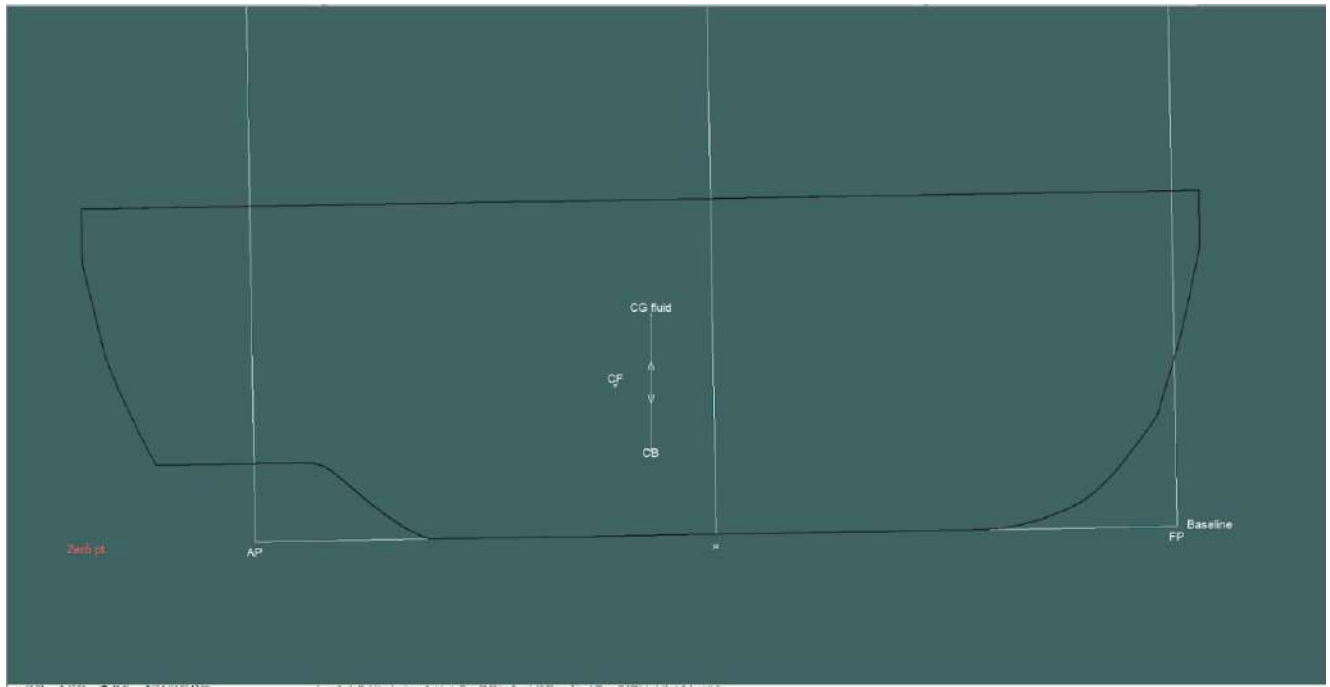


Fig. 23. Ares trim and heel value

	Heel to Starboard deg	-30.0	-20.0	-10.0	0.0	10.0	20.0	30.0	40.0	50.0	60.0	70.0	80.0	90.0	100.	110.	120.	130.	140.	150.	160.	170.	180.	
1	GZ cm	-21.2	-20.7	-11.1	0.08	11.3	20.9	21.3	18.0	14.1	9.89	5.42	0.98	-3.38	-7.71	-6.23	-10.3	-15.9	-22.1	-24.3	-23.7	-13.7	-0.08	
2	Area under	435.	220.	55.0	0.14	56.7	223.	440.	638.	799.	920.	997.	1028	1017	958.	888.	809.	678.	486.	251.	5.33	-188.	-258.	
3	Displaceme	30.0	30.0	30.0	30.0	30.0	30.0	30.0	30.0	30.0	30.0	30.0	30.0	30.0	30.0	30.0	30.0	30.0	30.0	30.0	30.0	30.0	30.0	30.0
4	Draft at FP	11.4	13.4	12.5	12.5	12.5	13.4	11.4	5.06	-2.80	-14.7	-37.7	-99.5	n/a	-113.	312.	98.5	34.2	-0.86	-12.6	-15.5	-17.5	-17.7	
5	Draft at AP	4.27	10.8	13.5	13.9	13.5	10.8	4.26	-3.39	-13.6	-28.6	-55.3	-131.	n/a	-174.	-391.	-150.	-80.3	-48.7	-34.6	-25.5	-22.5	-22.5	
6	WL Length	98.9	98.6	96.7	93.8	96.7	98.6	98.9	98.7	98.2	95.4	93.6	90.8	84.4	81.1	81.8	89.8	98.3	105.	102.	98.8	99.5	98.0	
7	Beam max e	39.2	75.3	74.8	74.1	74.8	75.3	39.2	38.3	35.0	30.2	28.9	30.4	30.0	30.4	31.9	34.3	33.7	36.5	59.9	72.1	75.8	74.9	
8	Wetted Are	5031	5762	6159	6225	6159	5762	5031	5091	5145	5144	5071	4985	4991	5137	6297	6245	6163	5814	5539	6019	6914	6917	
9	Waterpl. Are	1797	2460	2858	2882	2858	2460	1797	1832	1832	1887	2040	2201	2228	2035	185.	45.8	350.	987.	1447	2033	3108	3108	
10	Prismatic co	0.70	0.69	0.66	0.67	0.66	0.69	0.70	0.70	0.70	0.72	0.75	0.79	0.85	0.81	0.37	0.41	0.54	0.54	0.66	0.76	0.77	0.78	
11	Block coeff.	0.51	0.35	0.41	0.59	0.41	0.35	0.51	0.49	0.52	0.59	0.62	0.72	0.82	0.67	0.23	0.18	0.21	0.30	0.46	0.43	0.42	0.60	
12	LCB from ze	52.2	51.2	50.5	50.5	50.5	51.2	52.2	52.5	52.9	53.1	52.8	52.7	53.1	54.4	72.6	69.5	64.7	58.1	53.9	51.8	51.1	51.0	
13	LCF from ze	47.8	51.0	47.9	47.5	47.9	51.0	47.8	46.4	45.0	44.5	45.1	46.2	46.4	45.4	59.0	60.1	59.6	49.8	48.4	54.1	47.6	47.8	
14	Max deck in	30.2	20.0	10.0	0.96	10.0	20.0	30.2	40.2	50.1	60.1	70.0	80.0	90.0	99.9	96.3	106.	118.	134.	147.	159.	169.	176.	
15	Trim angle (	-4.95	-1.82	0.75	0.96	0.74	-1.82	-4.96	-5.84	-7.50	-9.59	-12.0	-21.3	n/a	-36.6	-83.3	-71.6	-54.2	-30.1	-14.9	-6.90	-3.45	-3.33	

Fig. 24. Ares large angle stability results

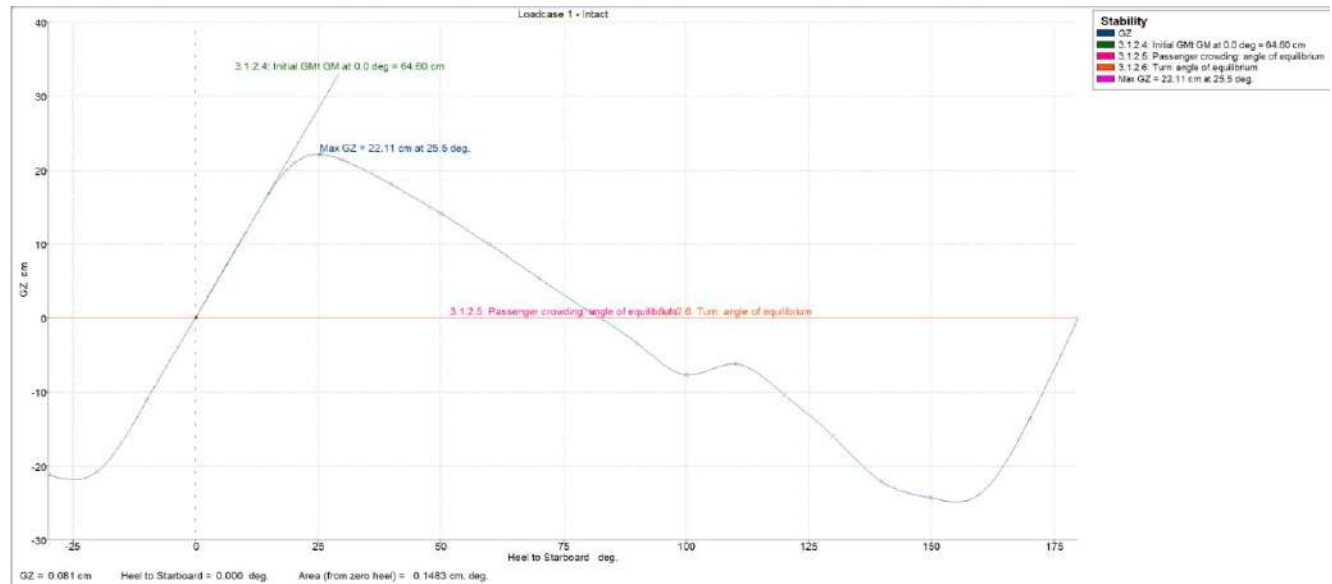


Fig. 25. Ares large angle stability graph

The test results of Nala Ares showed that it has trim value of  $0.96^\circ$  and heel of  $0^\circ$ , which is safe. Other results of the analysis are the large angle stability graph or usually called GZ curve. the calculation to determine the ship stability is obtained as follows [1]:

1. “The area under the righting lever curve (GZ curve) should not be less than 0.055 metre-radians up to  $30^\circ$  angle of heel”.  
 Required = 0.055 m.rad  
 Actual = 0.077 m.rad  
**0.055 < 0.077 .....Pass**
2. “The area under the righting lever curve (GZ curve) should not be less than 0.09 metre radians up to  $40^\circ$  angle of heel or the angle of downflooding if this is less than  $40^\circ$ ”.  
 Required = 0.0900 m.rad  
 Actual = 0.1115 m.rad  
**0.0900 < 0.1115 .....Pass**
3. “The area under the righting curve between the angles of heel of  $30^\circ$  and  $40^\circ$  or between  $30^\circ$  and the angle of down flooding if this angle is less than  $40^\circ$ , should not be less than 0.03 metre-radians”.  
 Required = 0.0300 m.rad  
 Actual = 0.0345 m.rad  
**0.0300 < 0.0345 .....Pass**
4. “The righting lever GZ should be at least 0.20 m at an angle of heel equal to or greater than  $30^\circ$ ”.  
 Required = 0.200 m  
 Actual = 0.214 m  
**0.200 < 0.214 .....Pass**
5. “The maximum righting arm should occur at an angle of heel preferably exceeding  $30^\circ$  but not less than  $25^\circ$ ”.  
 Required = 25.0 deg  
 Actual = 25.5 deg  
**25.0 < 25.5 .....Pass**

6. “The initial metacentric height  $GMO$  should not be less than 0,15 m”.

Required = 0.150 m

Actual = 0.646 m

**0.150 < 0.646.....Pass**

The results of Nala Ares intact stability pass all criteria from IMO, then it can be said that Nala Ares comply all the rules and safe to operate.

**F. Reference**

[1] International Maritime Organization, “Resolution MSC.267(85): Adoption of the International Code on Intact Stability, 2008 (2008 IS CODE),” adopted 4 Dec. 2008.

**IV. MAXSURF MOTION**

**A. Scope**

Motion analysis was conducted to determine ship characteristics when passing through the waves in any directions and frequencies. This analysis is also to determine how the ship responds over the time which can be measured by RAO (*Response Amplitude Operations*) and RMS (*Root Mean Square*) analysis.

**B. Schedule**

This test was held pn December 9<sup>th</sup>, 2024. Each test took around 10 minutes

**C. Resources and Tools**

*Maxsurf Motion* is used because it can predict the ship motion data from the ship and how the ship responds with several waves’ motion.

**D. Environment**

TABLE VIII SOFTWARE SETTINGS FOR MOTION ANALYSIS

Element	Information
Analysis type	The analysis type that we used was strip theory.

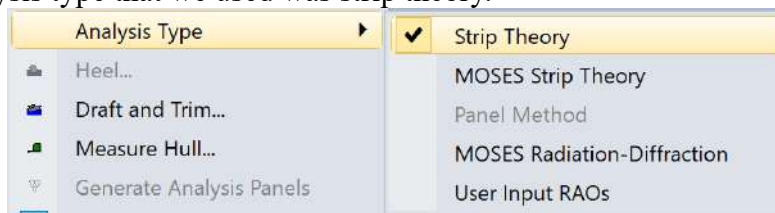


Fig. 26. Analysis selection

Vessel draft and trim We set the trim and draft to zero trim.

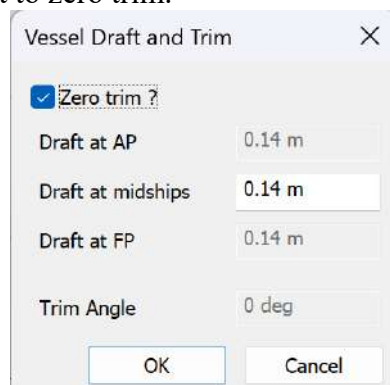


Fig. 27. Draft and trim setting

**Measure hull** This setup was used to slice the hull vertically to make a section along the hull and we set the section to twenty-one.

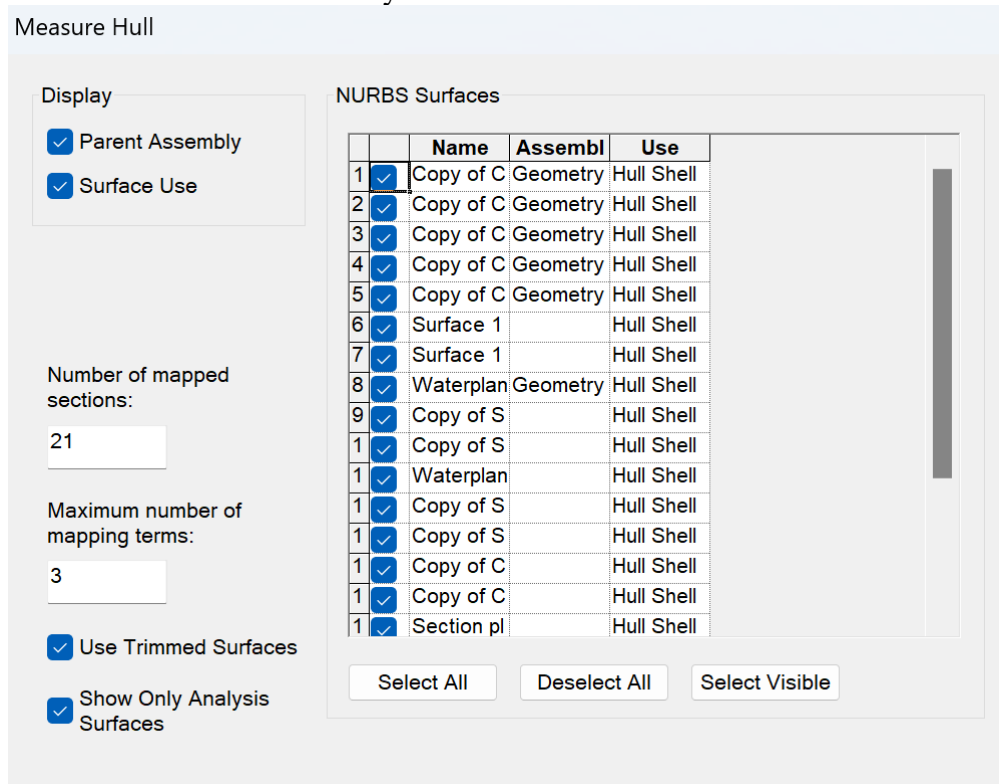


Fig. 28. Surface selection

**Speed** The speeds were set ranging between 0.5 - 3 m/s with addition of service speed.

	Name	Speed [	Analyse
1		0.5000	<input checked="" type="checkbox"/>
2		1.0000	<input checked="" type="checkbox"/>
3		1.5433	<input checked="" type="checkbox"/>
4		2.0000	<input checked="" type="checkbox"/>
5		2.5000	<input checked="" type="checkbox"/>
6		3.0000	<input checked="" type="checkbox"/>

Fig. 29. Speed setting

**Heading** Headings are the direction of the wave when hitting the hull in this setup, and we used 0°, 135°, and 180°.

	Name	Heading	Analyse
1		0.0	<input checked="" type="checkbox"/>
2		135.0	<input checked="" type="checkbox"/>
3		180.0	<input checked="" type="checkbox"/>

Fig. 30. Heading setting

**Spectra** This setup is used to set the wave height, and we used the waves height from 0.08 m to 0.20 m.

	Name	Type	Char. height [m]
1		JONS	0.080
2		JONS	0.150
3		JONS	0.200

Fig. 31. Type and wave height setting

**E. Risk Management**

The risk comes from certain models such as modular catamaran because sometimes *Maxsurf Motion* only detects one hull and does not detect the other one and it will give a bad impact on the result. To solve this problem, we managed the distance of each section to be slightly farther.

**F. Result**

Seakeeping analysis is meant to be used to calculate the comfort of the ship experienced by

the passenger, in this case the vision system (Camera and Lidar). The analysis is carried out using Maxsurf motions to fulfill some criteria mentioned in [1] below:

1. Roll amplitude means  $\leq 12^\circ$
2. Pitch Amplitude Means  $\leq 3^\circ$
3. Heave motion means  $\leq 2$  m/s

This analysis result that we use are at service speed of 1.5433 m/s, Bow Quartering / Heading ( $135^\circ$ ), with JONSWAP wave spectrum. Here are the results of the analysis:

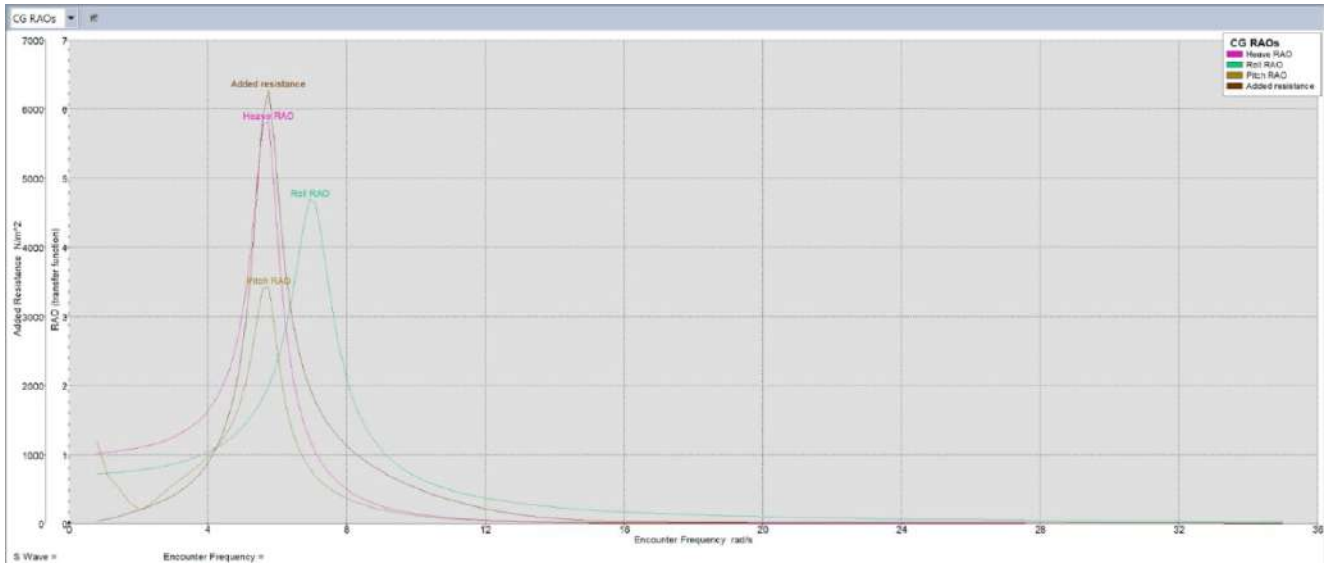


Fig. 32. RAO curve

From the analysis criteria above, we can summarize the data into these table below:

TABLE IX SEAKEEPING ANALYSIS HS = 0.08 M

Item	RMS
Speed	1.5433 m/s
Heave motion	0.021 m
Roll motion	0.095 deg
Pitch motion	0.099 deg
Heave velocity	0.02 m/s
Roll velocity	0.00533 rad/s
Pitch velocity	0.00602 rad/s
Item	S. Amplitude
SM (Lidar)	0.055 SM
MSI (Lidar,120 minute)	0 %
SM (Camera)	0.05 SM5
MSI (Camera, 120 minute)	0 %

TABLE X SEAKEEPING ANALYSIS HS = 0.15 M

Item	RMS
Speed	1.5433 m/s
Heave motion	0.038 m
Roll motion	0.18 deg
Pitch motion	0.18 deg
Heave velocity	0.037 m/s
Roll velocity	0.00995 rad/s
Pitch velocity	0.01119 rad/s
Item	S. Amplitude
SM (Lidar)	0.135 SM
MSI (Lidar,120 minute)	0.002 %
SM (Camera)	0.134 SM
MSI (Camera, 120 minute)	0.002 %

TABLE XI SEAKEEPING ANALYSIS HS = 0.20 M

Item	RMS
Speed	1.5433 m/s
Heave motion	0.051 m
Roll motion	0.24 deg
Pitch motion	0.25 deg
Heave velocity	0.05 m/s
Roll velocity	0.01327 rad/s
Pitch velocity	0.01492 rad/s
Item	S. Amplitude
SM (Lidar)	0.203 SM
MSI (Lidar,120 minute)	0.009 %
SM (Camera)	0.202 SM
MSI (Camera, 120 minute)	0.009 %

After acquiring the required data, then we can calculate all the criteria mentioned , the calculation of roll amplitude, pitch amplitude and heave motion can be seen below:

1. Roll amplitude mean =  $0,5 \times 2,5 \times \text{RMS} (< 12^\circ)$ 
  - Hs = 0.08 m =  $0,5 \times 2,5 \times 0,095 = 0.11875$  .....Pass
  - Hs = 0.15 m =  $0,5 \times 2,5 \times 0,18 = 0.225$  .....Pass
  - Hs = 0.20 m =  $0,5 \times 2,5 \times 0,24 = 0.300$  .....Pass
2. Pitch Amplitude mean =  $0,5 \times 2,5 \times \text{RMS} (< 3^\circ)$ 
  - Hs = 0.08 m =  $0,5 \times 2,5 \times 0,099 = 0.1238$  .....Pass
  - Hs = 0.15 m =  $0,5 \times 2,5 \times 0,18 = 0.225$  .....Pass
  - Hs = 0.20 m =  $0,5 \times 2,5 \times 0,25 = 0.31250$  .....Pass



3. Heave motion mean =  $0,5 \times 4 \times \text{RMS} (< 2 \text{ m/s})$

$H_s = 0.08 \text{ m} = 0,5 \times 4 \times 0,021 = 0.04200$  .....**Pass**

$H_s = 0.15 \text{ m} = 0,5 \times 4 \times 0,038 = 0.07600$  .....**Pass**

$H_s = 0.08 \text{ m} = 0,5 \times 4 \times 0,051 = 0.10200$  .....**Pass**

From calculation of seakeeping criteria above we can conclude that Ares capable of receiving waves with height ranging from 0.08 m to 0.20 m safely.

**G. References**

[1] L. Yun, A. Bliault, and H. Z. Rong, *High Speed Catamarans and Multihulls*. Cham, Switzerland: Springer, 2019, doi: 10.1007/978-1-4939-7891-5.

# Appendix B.2: Test Plan and Result

## Main Deck Frame Stress and Total Deformation

M Farras Rheza Firmansyah

### I. SCOPE

Equivalent stress and total deformation analysis were carried out to determine the main deck frame reliability and strength. The test was carried out for both Ares and Proteus 2.0's main deck under the same load.

#### A. Equivalent Stress

This analysis was carried out to determine the frame's yield to ensure that Ares' main deck frame is stronger than Proteus 2.0's in carrying the same amount of load. The result can help us to predict and optimize the pressure points and yield strength of Ares' main deck frame.

#### B. Total Deformation

Since Ares' main deck frame is planned to be less complex and heavy compared to Proteus 2.0's, total deformation analysis and simulation are carried out to compare the overall magnitude of deformation/material displacement of the frame under heavy loads. Mathematically, the vector sum magnitude of all directional displacements at each point model can be calculated as follows:

$$\text{Total Deformation} = \sqrt{X^2 + Y^2 + Z^2} \quad (1)$$

Where X, Y, and Z are displacements along each Cartesian direction.

Total deformation analysis and simulation will use the principle from to determine the amount of deformation on the main deck when subjected to stress, making sure that Ares' main deck frame is secure from structural failures.

### II. SCHEDULE

Simulation was carried out repeatedly from December 27<sup>th</sup>, 2024, until January 18<sup>th</sup>, 2025, allowing for a high number of iterations and changes in the main deck frame configuration. Each simulation took around ten minutes from design input until result retrieval. In total, we have done around fifteen simulations and analysis for both equivalent stress and total deformation.

### III. RESOURCE AND TOOLS

The simulation was carried out using *ANSYS 2024 R2 Static Structural Mechanical Software*. This software was chosen for the analysis since the loads which will be used are static and material behavior can be approximated as linear elastic. The static load will experience stress and deformation in steady-state condition and this software is ideal due to its focus on static loading. *ANSYS* is also efficient and accurate because it directly calculates the total deformation and equivalent stress based on equilibrium equations.

**IV. ENVIRONMENT**

Testing for both main deck designs was carried out under a load of 11 kg or 107.8 N and 0.5 kg or 4.9 N. Detailed settings and environment for this analysis are shown as follows:

TABLE I ANSYS 2024 R2 STATIC STRUCTURAL MECHANICAL SETTINGS

Elements	Information
Material	Aluminum 6063 T5
Surface Contact	We defined how each surface interacts in one model.
Boundaries Condition	Boundaries condition is used to identify which load is applied on the surface and which surface is not affected by any forces or motion.
Solutions	There are some outputs of the static analysis offered by <i>ANSYS 2024 R2 Static Structural Mechanical Software</i> such as, <i>total deformation test</i> , <i>strain test</i> , <i>equivalent stress</i> , <i>fatigue</i> , etc. For this analysis, we only used two output analyses, which are <i>deformation stress</i> and <i>equivalent stress</i> since those analyses are sufficient for knowing the properties of the frame.

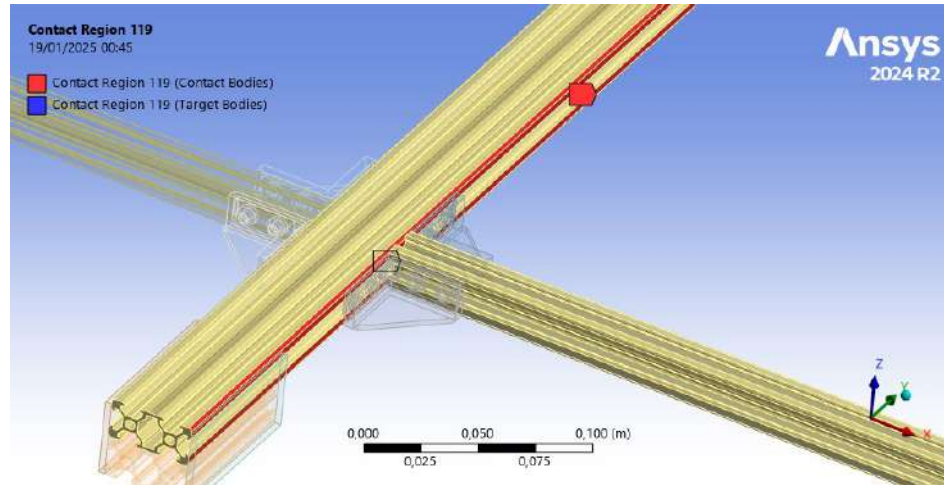


Fig. 1. Surface contact

There are two roles for each contact region—contact bodies and target bodies. Target bodies are references for contact interaction whilst contact bodies have restricted movement and following the target bodies. There are some types of surface contact conditions provided by *ANSYS 2024 R2 Static Structural Mechanical Software* such as bonded, rough, frictional, frictionless, and no separation. For this frame, bonded was chosen as surface contact because each frame connected rigidly.

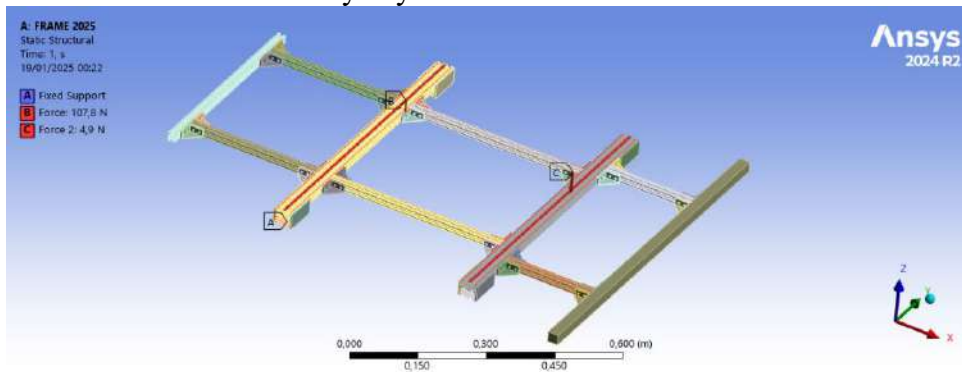


Fig. 2. Boundaries condition

## V. RISK MANAGEMENT

### A. Modeling Error

Meshing was a significant step that was often done inaccurately when doing analysis. Insufficient mesh density and distorted elements could lead to inaccuracies. This was mitigated by carefully modelling both main deck frames and paying close attention to the geometry and meshing.

### B. Interpretation and Human Error

Wrong setup and misinterpretation of results might happen during analysis. This risk was alleviated by having the analysis interpreted by the whole mechanical design team instead of one single person at a time.

## VI. RESULTS

### A. Angle Bracket Testing

Testing was carried out to compare deformation between constructions using single slot-angle brackets and double-slot angle brackets.

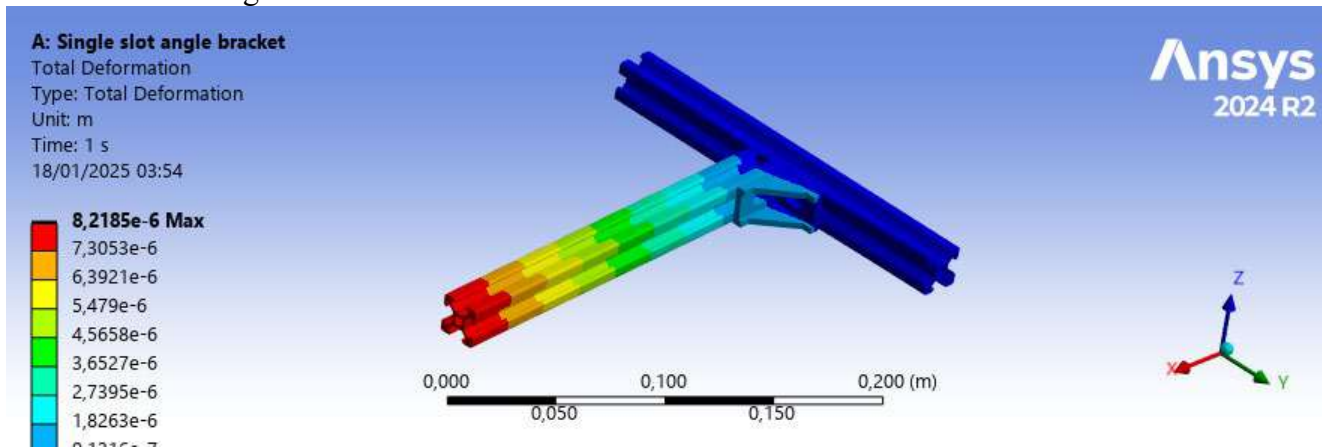


Fig. 3. Total deformation, single-slot angle bracket

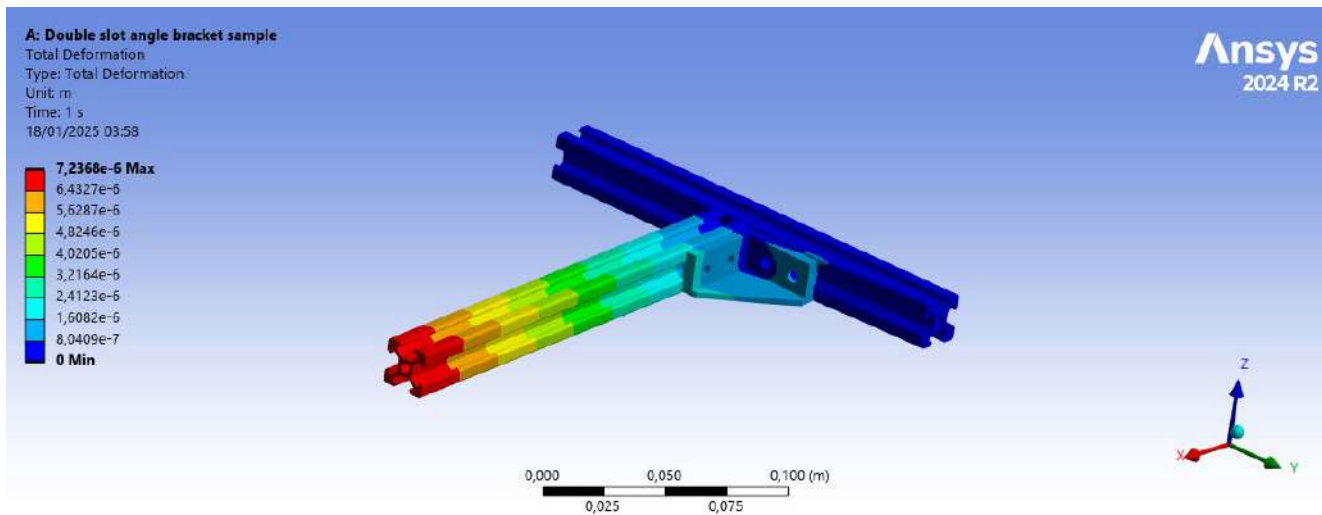


Fig. 4. Total deformation, double-slot angle bracket

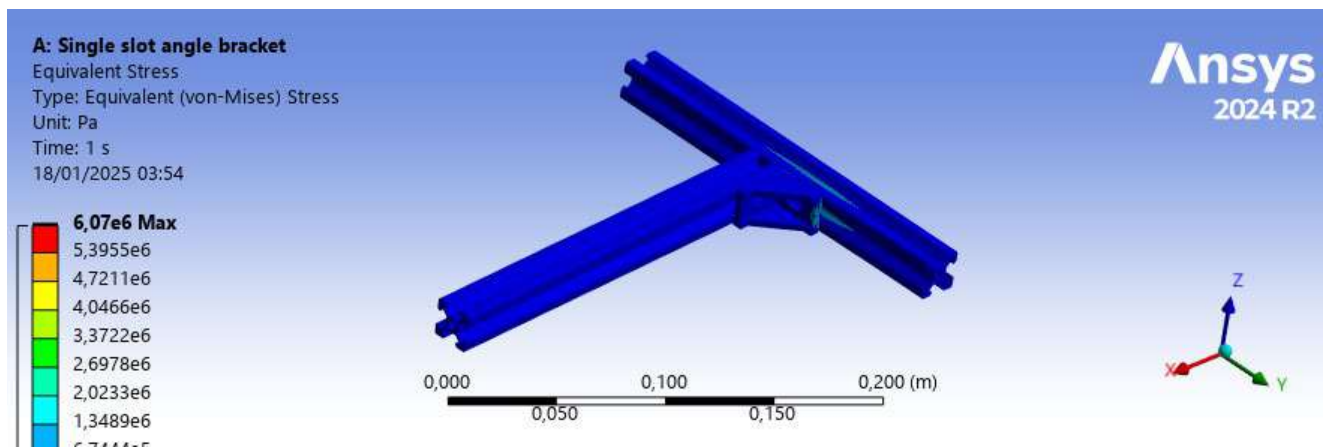


Fig. 5. Equivalent stress, single-slot angle bracket

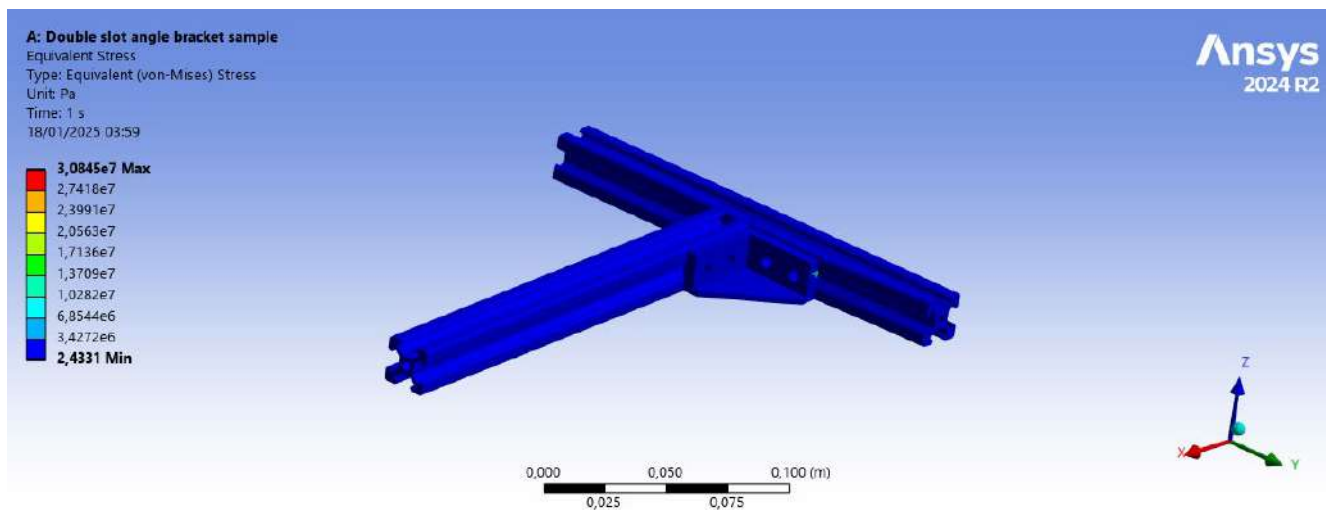


Fig.6. Equivalent stress, double-slot angle bracket

Based on fig. 3 to fig. 6, two identical structures were compared using different angle brackets. The result shows that the double slot angle bracket had a smaller maximum *total deformation* value at  $7.2368 \times 10^{-6}$  Pa compared to the single slot at  $8.2185 \times 10^{-6}$  Pa. This indicates that the double slot angle bracket is more resistant to bending or deflection under load. For the *equivalent stress*, the double slot angle bracket has  $3.0845 \times 10^7$  Pa and single slot angle bracket has  $6.0700 \times 10^6$  Pa. This indicates the double slot angle bracket is

stronger and more reliable while holding the load than single slot angle bracket.

### B. Main Deck Frame Testing

Using the conclusion from the angle bracket testing, the new main deck frame was designed using double slot angle brackets. Therefore, the previous and new main deck frame were compared to prove that the new main deck frame is more reliable. The results are shown in fig. 7 until fig. 10.

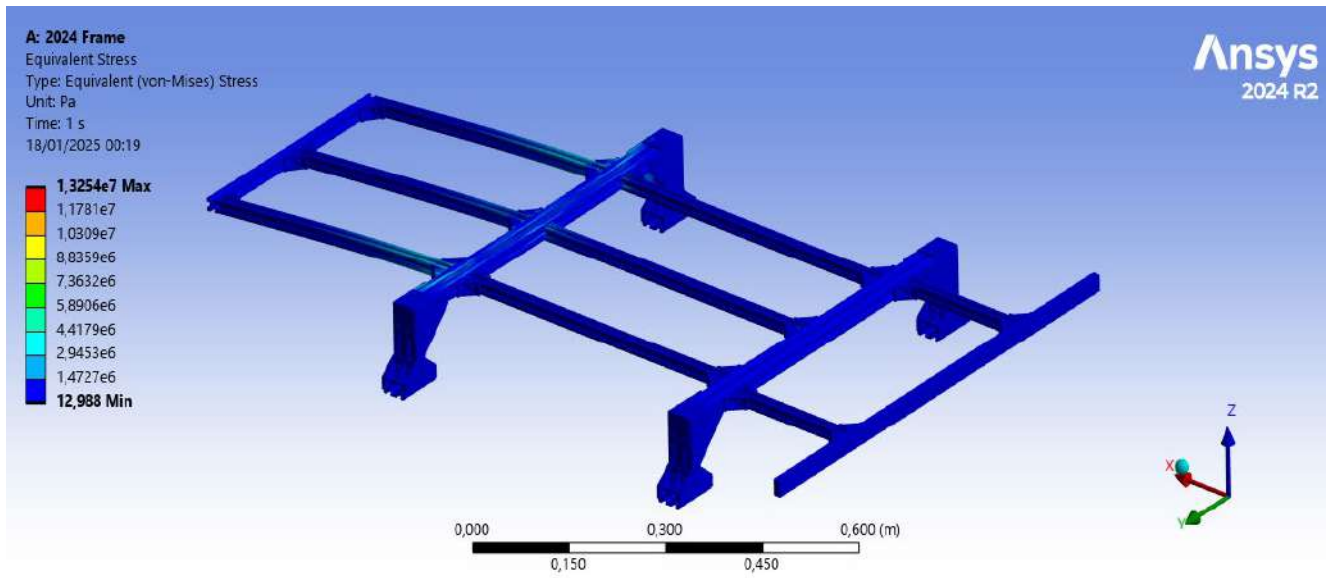


Fig. 7. Equivalent stress, Proteus 2.0

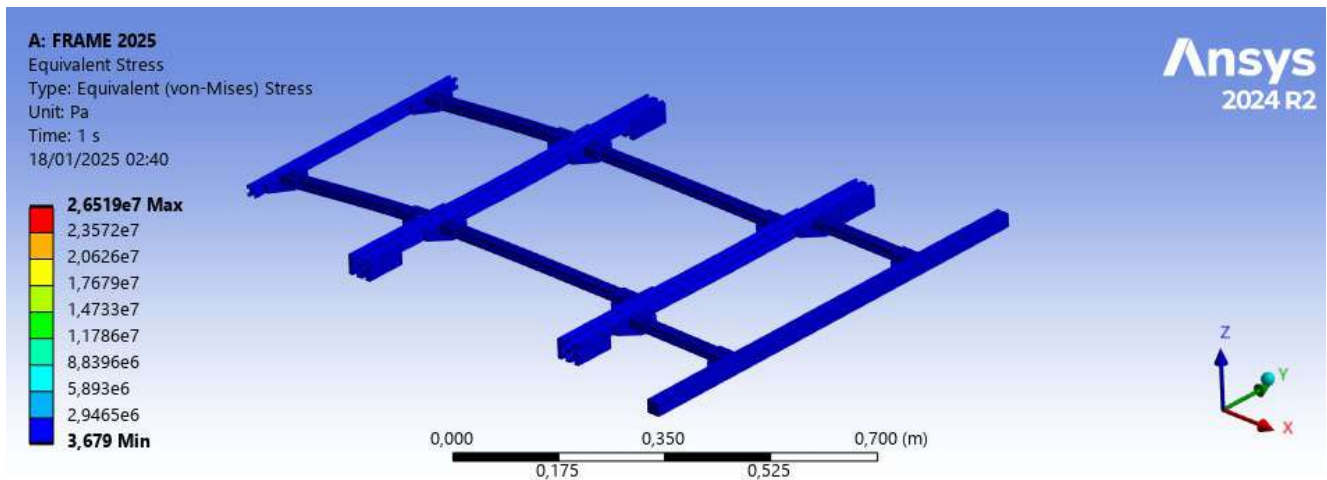


Fig. 8. Equivalent stress, Ares

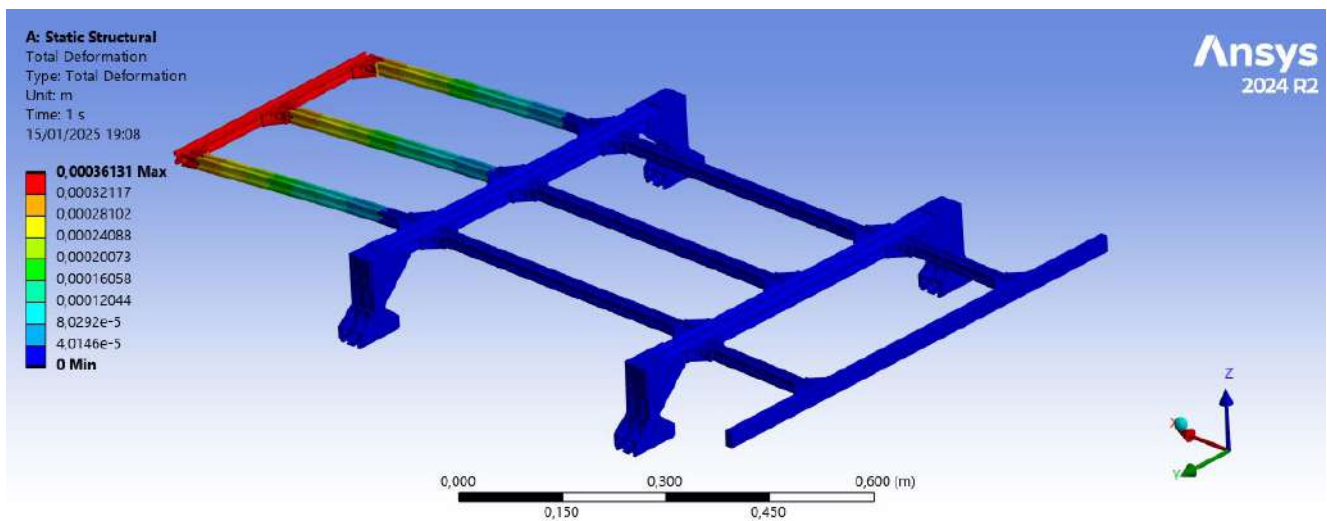


Fig. 9. Total deformation, Proteus 2.0

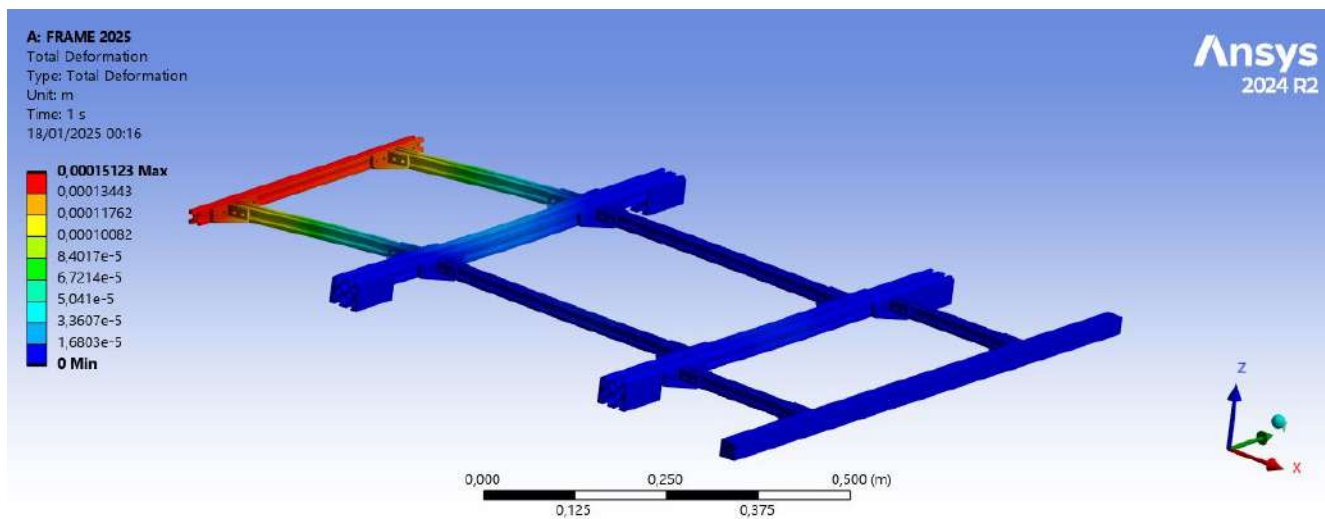


Fig. 10. Total deformation, Ares

According to fig. 7 to fig. 10, Ares' main deck frame has a higher maximum *equivalent stress* compared to the one used in Proteus 2.0's. The value of Ares' main deck frame is  $2.6519 \times 10^7$  Pa, and the value is  $1.3254 \times 10^7$  Pa for Proteus 2.0's. These values indicate that under the same load, Ares' frame can receive more stress than Proteus 2.0's. For the *total deformation* test, the maximum

*total deformation* for Ares' frame is at  $1.5123 \times 10^{-4}$  m and for Proteus 2.0's frame is at  $3.6130 \times 10^{-4}$  m. These values indicate that Ares' frame has less deformation while holding the loads than the previous frame. From all simulation, Ares' main deck frame has been proven to have more strength and reliability. The total comparison between both main deck frames can be seen in table II.

TABLE II Main deck frame properties comparison

	<b>Max. Equivalent Stress (Pa)</b>	<b>Total Deformation (m)</b>
Proteus 2.0	$1.3254 \times 10^7$	$3.6130 \times 10^{-4}$
Ares	$2.6519 \times 10^7$	$1.5120 \times 10^{-4}$

# Appendix C: Control System

Arundaya Pratama Nurhasan, M Andi Abdillah, Muhammad Fajri Romadlon, Sigmayuriza Senaaji Rasendria

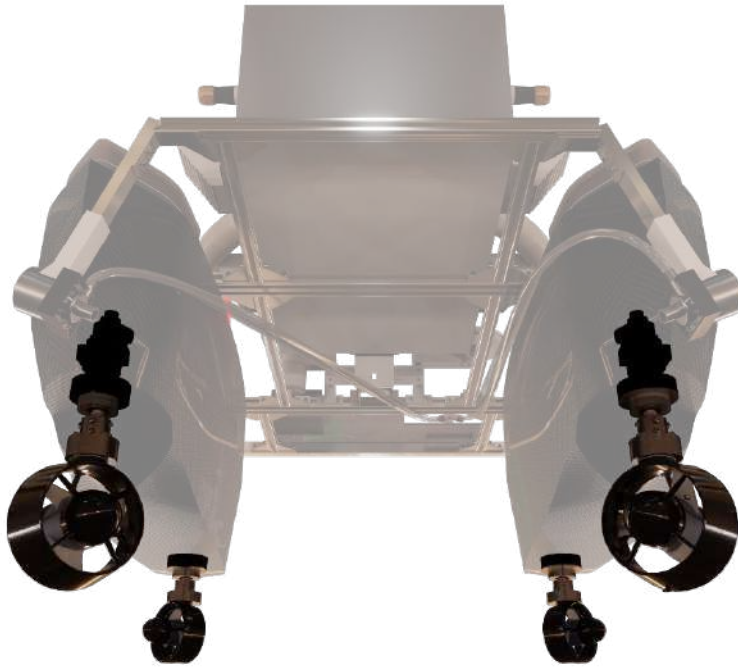


Fig. 1. Ares' propulsion system

## I. INTRODUCTION

In RoboBoat 2024, the bow thrusters in Proteus 2.0 were inefficient since turbulence happened due to the close distance of Proteus 2.0 catamaran hulls. This year, Barunastra moved to combined azimuth and X-Drive configuration with fixed two X-Drive installed at  $+45^\circ$  and  $-45^\circ$  and two stern azimuth thrusters that can rotate from  $-60^\circ$  to  $+60^\circ$ .

This configuration is expected to have high maneuverability and adaptation that allows the ship to operate effectively in various scenarios. To make optimal configuration, an advanced control system is needed to translate navigation commands like surge, sway, and yaw for thrusters.

Two control modes are designed: Azimuth mode when rear thrusters adjust the angle to align the yaw with the desired thrust direction and X-Drive mode, in which all thrusters maintain a fixed angle to support omnidirectional movement. These two modes are supported by the PID controller to ensure stability, accuracy, and responsiveness during operation. The following section will

explain in detail the design and manufacture of Ares' control system.

## II. CONTROL SYSTEM ARCHITECTURE

### A. Vessel Model

The ship dynamics model is the basis for the design of the control system used in ASV. This model describes the relationship between the force generated by the thruster ( $F$ ) and the movement of the ship in three degrees of freedom: surge, sway, and yaw. These parameters are the main reference for calculating the forces and moments required for ASV maneuvers, such as linear movement, heading rotation, or omnidirectional maneuvers. According to [1], connection between force produced by thruster and movement by ship can be written as

$$\tau = B \cdot F \quad (1)$$

$$\tau = [\tau_x, \tau_y, \tau_\psi]^T \quad (2)$$

Where: Vector of surge force ( $\tau_x$ ), sway ( $\tau_y$ ), and yaw moment ( $\tau_\psi$ ).



$B$  : thruster transformation matrix that depends on the thruster angle ( $\theta$ ) and the distance to the ship's center of mass ( $d$ ). And for this ship configuration matrix  $B$  can be defined as:

$$B = [\sin(\theta_1) \cos(\theta_1) d_1], [\sin(\theta_2) \cos(\theta_2) d_2], [\sin(\theta_3) \cos(\theta_3) d_3], [\sin(\theta_4) \cos(\theta_4) d_4]$$

$$F = [F_1, F_2, F_3, F_4]^T: \text{force vector produced by each thruster.}$$

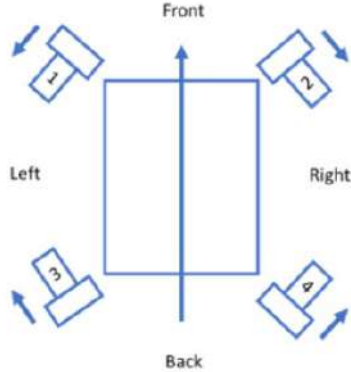


Fig. 2. Thruster configuration

Then Parameters  $\theta_i$  and  $d_i$  are determined according to the thruster configuration:

- Front thruster ( $F_1, F_2$ ) :  $\theta_1 = +45^\circ, \theta_2 = -45^\circ$
- Rear thruster ( $F_3, F_4$ ) : depending on operating mode, azimuth with flexible angle and X-Drive using fix 45 angle.

This model allows the control system to distribute the forces from each thruster precisely to achieve the desired movement. In X-Drive mode, the  $B$  matrix is used to produce a precise omnidirectional force distribution, while in azimuth mode, the rear thruster angle is dynamically adjusted to optimize yaw control.

Implementing this model into the control system ensures that every navigation command such as surge, sway, and yaw can be accurately translated into thruster action. For example, in a heading maneuver, the yaw moment is calculated based on the heading error, which is then converted into thruster forces using the  $B$  matrix. Similarly, for omnidirectional maneuvers such as station-

keeping, the  $B$  matrix allows the ship to balance surge, sway, and yaw forces to maintain a desired position despite environmental disturbances such as wind or ocean currents.

By basing the control on this model, the ship can adapt to a wide range of operational scenarios, from fast linear movements to precision maneuvers at low speeds. The combination of dynamic models and control algorithms provides high flexibility to carry out complex competition missions with optimal efficiency.

## B. Control Mode

Control modes play a critical role in regulating the movement and stability of an ASV in various scenarios. These modes determine how the thrusters are used to achieve some maneuvers, such as precision navigation, station-keeping, or path-following. The ASV implements two main control modes, namely azimuth Mode and X-Drive mode, each optimized for different needs.

### 1) Azimuth Mode

This azimuth mode, the angle of the two rear thrusters ( $\theta_3, \theta_4$ ) will change dynamically to produce yaw without changing the direction and value of thrust. The control angle is calculated using the PID controller based on the yaw error ( $e_\psi$ ). This mode ensures that yaw adjustments are responsive, allowing the ship to reach the desired heading quickly and accurately. With independent angle adjustments, the rear thruster can be optimized for yaw control while maintaining overall thrust efficiency.

Azimuth mode is ideal for use in environments where precise angle adjustments are required, such as when avoiding obstacles, or making sharp course changes during a mission.

### 2) X-Drive Mode

This mode used fixed angles for all thrusters  $\theta_1, \theta_2 = 45^\circ$  and  $\theta_3, \theta_4 = 45^\circ$ . The transformation matrix  $B$  is used to calculate the omnidirectional force distribution:

$$F_1 = -surge(\sin(45)) - sway(\cos(45)) + yaw(d_1) \quad (3)$$

$$F_2 = -surge(\sin(45)) + sway(\cos(45)) - yaw(d_2) \quad (4)$$

$$F_3 = surge(\sin(45)) - sway(\cos(45)) - yaw(d_3) \quad (5)$$

$$F_4 = surge(\sin(45)) + sway(\cos(45)) + yaw(d_4) \quad (6)$$

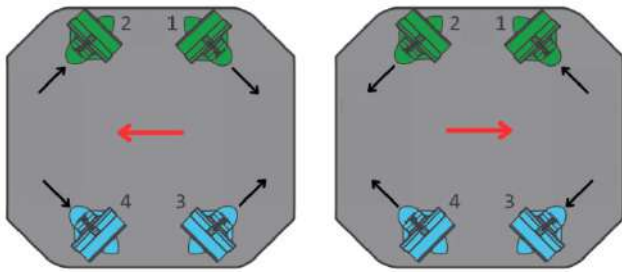


Fig. 3. X-Drive configuration

Fig. 3. shows the configuration of each thruster for sway motion. Black arrows indicate the water flow direction created by each thruster while red arrow shows the movement of the ship. This approach provides very high flexibility and is particularly suitable for low-speed maneuvers that require precise position control. For example, in station-keeping, the ASV can maintain a fixed position by balancing surge, sway, and yaw forces against environmental disturbances.

With the combination of azimuth mode and X-Drive mode, ASV can achieve a versatile control system that can adapt to complete mission requirements. Azimuth mode good in angular precision and rapid maneuvering, while X-Drive mode provides exceptional flexibility for omnidirectional movement and accurate position control. Together, these modes ensure the ASV's ability to navigate in complex environments with high efficiency.

### C. Feedback Control Design

Two control modes which have been explained in detail in main pages are supported with PIC controller to stabilize vessel's heading and position. Using sensor data like IMU and GPS, PID controller minimize the errors that are caused by environmental disturbance such as wind and ocean currents.

PID controller calculates the difference between actual value and desired value, then generate control signal to correct these differences. For the ASV, this control signal in the form of yaw moment ( $e\psi$ ) to adjust heading and surge ( $e_x$ ) or sway ( $e_y$ ) to fix position.

PID controller consists of three main components, Proportional ( $K_p$ ), Integral ( $K_i$ ), and Derivative ( $K_d$ ). The proportional part gives direct correction base on the size of error, generating quick response from disturbance. However, it can produce overshoot if the value is too large. The integral component accumulates errors over time to overcome long-term drift and eliminating steady-state errors. The last one is derivative component. It predicts future error and reduce oscillations. Together, these components form the control equation:

$$\tau\psi = K_p(e\psi) + K_i\left(\int e\psi dt\right) + K_d\left(\frac{de\psi}{dt}\right) \quad (7)$$

This equation is not only applied for heading stabilization but also for position correction through surge and sway force.

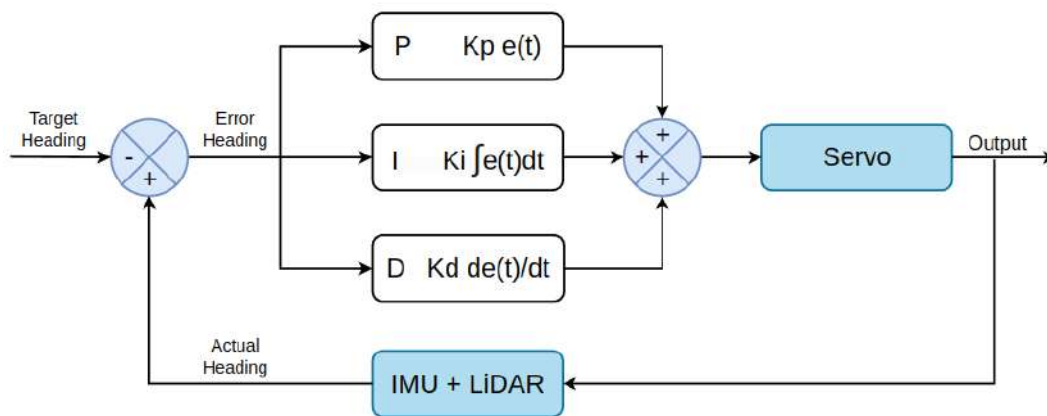


Fig. 4. Control system feedback block diagram azimuth mode

There are some differences in the use of PID which depend on the control modes. In the

azimuth mode, result of the PID calculation is used as the value to control angle of the servo.

However, in the X-Drive mode, angle error is calculated by PID and used as the value to control thruster.

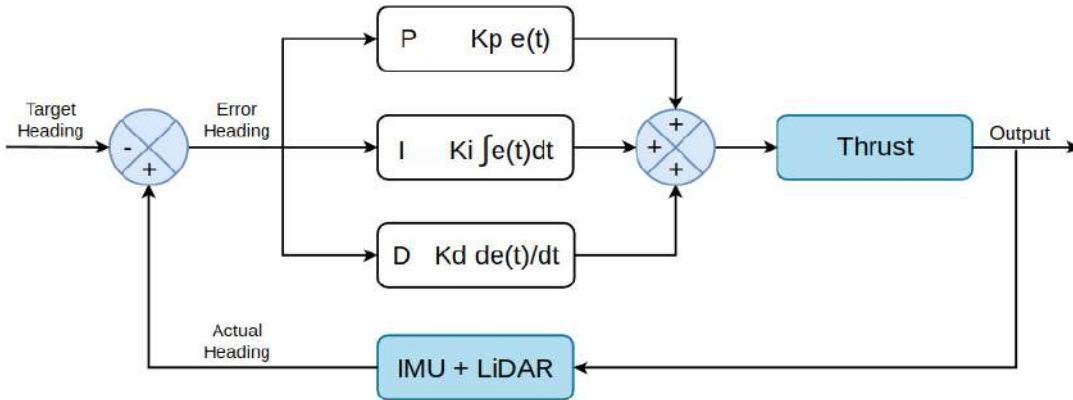


Fig. 5. Control system feedback block diagram X-Drive mode

PID controller operates in a feedback loop running at 50 Hz. This ensures timely processing of data from the IMU used to calculate the current error. The controller output signal is distributed to the thrusters based on the operating mode.

#### D. Operation Modes

The control system on the ASV is designed to handle diverse mission requirements through several operating modes. These operating modes regulate how the ASV moves and maintains its position based on the mission being executed, such as following a certain path or staying at a predetermined point. The two main modes used are Path-Following Mode and Station-Keeping Mode:

##### 1) Path-Following Mode

This mode allows the ASV to move along a pre-designed path, which contains several waypoints. The implementation of this mode depends on the control mode used.

In Azimuth Mode, the control system focuses more on yaw and surge settings, while sway is assumed to be minimum. The ship's heading will be dynamically adjusted to direct the ship to the next track point, so that the ship moves with a constantly changing orientation along the track. A PID controller is used to ensure that the heading remains precise, with the yaw moment calculated based on the yaw error between the desired heading and the actual heading.

In X-Drive mode, the system transforms waypoint coordinates from the global system to the ASV local system. With this approach, the ASV's heading remains constant during the maneuver, while surge and sway values are calculated to bring the ship to the next point. A transformation matrix is used to convert global coordinates to the ASV's local coordinates. This system allows the ASV to move omnidirectionally, making it more flexible in dealing with complex or narrow paths without the need for frequent heading changes. To calculate ASV local coordinate, we can use the following formula:

$$Surge = dy(\sin(-yaw)) + dx(\cos(-yaw)) \quad (8)$$

$$Sway = dy(\cos(-yaw)) - dx(\sin(-yaw)) \quad (9)$$

##### 2) Station-Keeping Mode

This mode is designed to maintain the ASV's position and orientation at a predetermined point despite external disturbances such as wind or ocean currents. This mode is only available in X-Drive mode because the fixed thruster configuration at  $+45^\circ$  and  $-45^\circ$  provides omnidirectional capability that allows the ship to generate forces in all directions. In this mode, the control system continuously monitors the ASV's actual position and actual heading, then compares them with the desired position and heading. The position error and heading error are calculated to determine the required surge, sway, and yaw moment forces.

III. HARDWARE SETUP



Fig. 6. Azimuth thruster mechanical system

The propulsion system of Nala Ares is divided into two which are two azimuths at stern and two X-Drive at fore. The azimuth thruster was installed using shaft inside the stern tube which is made from aluminum alloy. The azimuth movement is created from the shaft gear and servo gear made from synthetic fluoropolymer of polytetrafluoroethylene (PTFE) which are connected to each other while also supported with bearing. The T500 Thruster was attached to the aluminum alloy coin installed with bolts and nuts. This configuration makes the azimuth movement smooth, and thruster angle can be easily controlled using servo according to the gear ratio used. The installation in hull is supported by seal epoxy to prevent it from leaking. The production process involves CNC milling and lathe machines and takes around 2 weeks.

The gears used for azimuth configurations were designed using the gear calculation [2] and the gears were determined that the number of teeth is 30 and its module is 1 mm. Based on pitch diameter equation, The gear pitch diameter is:

$$D = z \times m \tag{10}$$

$$D = 30 \times 1 \text{ mm} \tag{11}$$

$$D = 30 \text{ mm} \tag{12}$$

The outside diameter is:

$$D_o = D + 2 \times m = m(z + 2) \tag{13}$$

$$D_o = 30 + (2 \times 1) \tag{14}$$

$$D_o = 32 \text{ mm} \tag{15}$$

From pitch diameter, the root of diameter is:

$$D_R = D - 2.5 \times m \tag{16}$$

$$D_R = 30 - (2.5 \times 1) \tag{17}$$

$$D_R = 27.5 \text{ mm} \tag{18}$$

From the calculations, the gear for azimuth maneuver was designed in fig. 7.

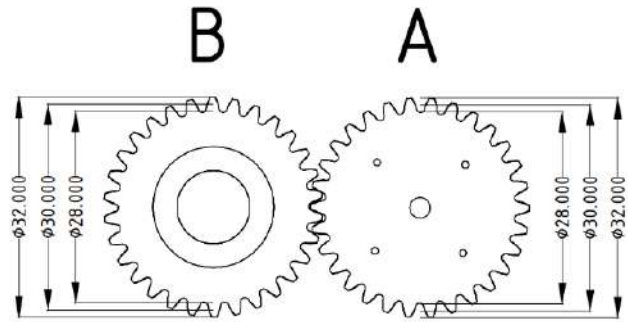


Fig. 7. Azimuth thruster mechanical system

While the azimuth thruster is moved using spur gears connected between shaft and servo, X-Drive installation is fixed in 45°.

IV. CONCLUSION

Ares' propulsion configuration has been designed to accommodate high maneuverability by using combined X-Drive and azimuth configuration. The installation for all thrusters allows the ASV to complete all tasks in RoboBoat 2025 using each control mode and configuration.

V. References

- [1] T. I. Fossen, *Handbook of Marine Craft Hydrodynamics and Motion Control*, 2nd ed. Hoboken, NJ, USA: Wiley, 2021.
- [2] D. W. Dudley, *Handbook of Practical Gear Design*. Boca Raton, FL, USA: CRC Press, 1994.

# Appendix C.1: Test Plan and Result Thruster Efficiency and Speed

M Andi Abdillah

## I. SCOPE

Component efficiency is strongly related to its energy consumption. While maintaining a good performance of the ship, Nala Ares should also have enough endurance to complete all missions using its power source. Thus, energy efficiency is as important as the performance of the ship.

The objective of this test is to choose the best configuration for all four thrusters installed on Ares. The tests consisted of two tests which were battery consumption test and speed test. The purpose of battery consumption test was to determine which configuration has less consumption during its operational time while speed test was to assess which configuration has a higher speed or Ares movement.

## II. SCHEDULE

Both tests were conducted on November 27<sup>th</sup>, 2024, or prior to our first in-water testing for overall mission. These tests took approximately 9 hours overall from changing thruster configurations or installation until testing for each configuration.

## III. RESOURCE AND TOOLS

The ship we used was Nala Proteus 2.0 since Ares was still in production progress. The thrusters we used were T200 and T500 Blue Robotics Thruster.

## IV. ENVIRONMENT

The environment used was campus lake. When we did both tests, the weather was sunny and the water was calm. Therefore, external forces were at their minimum. There were three configurations we tested: the first configuration consists of four T200 thrusters, the second setup uses two T200 thrusters for the X-Drive and two T500 thrusters for main propulsion, and the final configuration employs four T500 thrusters. The power source used for testing was a 4S LiPo battery with a 7200mAh capacity. For the T200 thrusters, Blue

Robotics Basic ESCs were used, while the T500 thrusters utilized Flipsky VESCs.

## V. RISK MANAGEMENT

### A. Thruster Interference

Campus lake is often visited by people on different purposes, from fishing until jogging around the lake. This condition has brought much waste to be thrown at lake, from food waste, plastics, to fishing wire. The waste could be a big problem since they were often struck on the Thruster's propeller although T200 and T500 Thruster has been installed with their own propeller cover. If the propeller thrust is interrupted, the maximum performance would not be acquired. To overcome this risk, Barunastra mechanical division would clear the waste using a fishing net. To prevent the people from putting up a fishing line, Barunastra has collaborated with the campus security team to prevent people from fishing during our trial months.

### B. Bad Weather

Weather will always be a problem when it comes to testing on open fields, such as a lake, and nature can be controlled. In case bad weather, such as heavy rain, happened, the test could not be carried out because the heavy wind would add much to the ship resistance. To mitigate this risk and realizing a rainy season in Indonesia, the testing schedule was started at the morning from 7 A.M. (GMT+7) since the rain in our land, Surabaya, East Java would likely happen in the afternoon. Therefore, instead of overcoming it, we chose to avoid it.

## VI. RESULT

### A. Battery Consumption Test

Battery efficiency testing was conducted by moving the vessel at a constant and equal speed across all three propulsion configurations. Battery voltage was recorded over time, with the results summarized in figure 1-3.

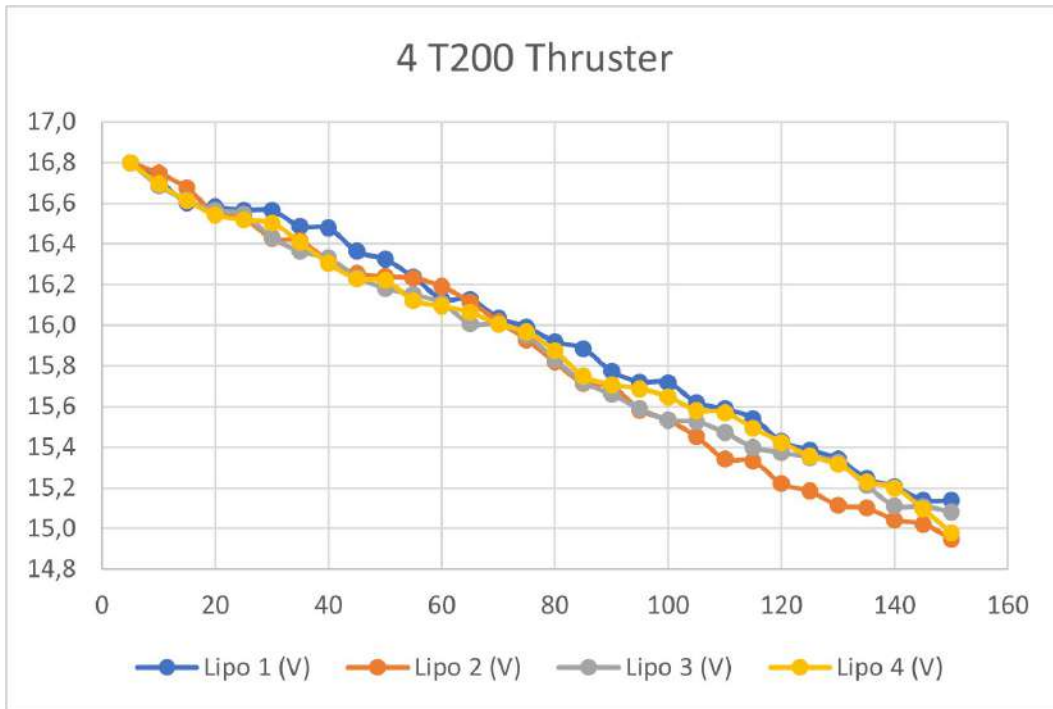


Fig. 1. Battery consumption of 4 T200 configuration

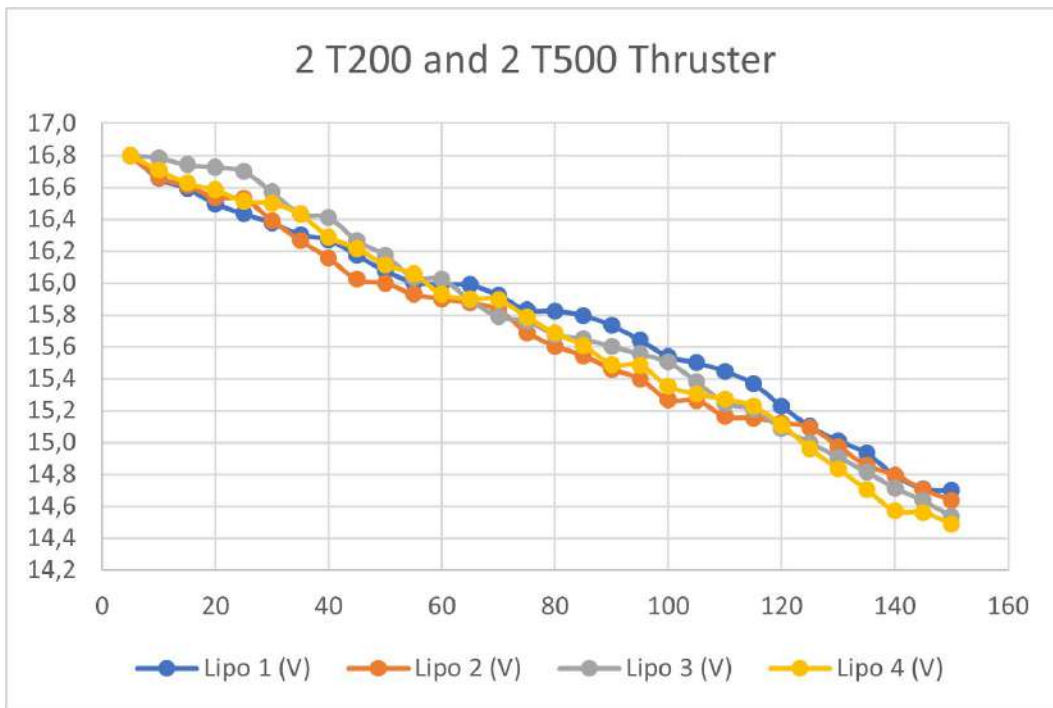


Fig. 2. Battery consumption of 2 T200 and 2 T500 configuration

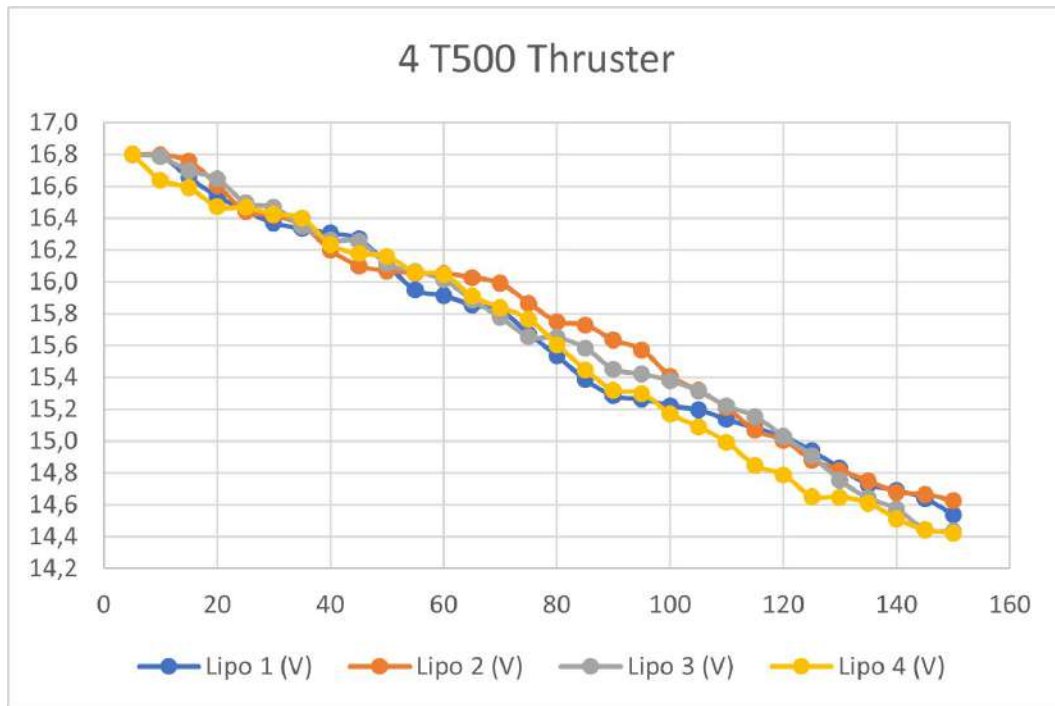


Fig. 3. Battery consumption of 4 T500 configuration

When considering only battery consumption, the configuration with four T200 thrusters demonstrated the highest efficiency due to its lighter total weight compared to the other configurations.

**B. Speed Test**

This test involved moving the vessel straight forward at maximum speed, executing holonomic maneuvers, and performing pivot turns. GPS and a compass were used to ensure more accurate results. The results of these tests are presented in Table I.

TABLE I THRUSTER CONFIGURATION COMPARISON

Configuration	Forward	Holonomic	Pivot
4 T200	4.12 m/s	2.58 m/s	38 RPM
Mixed	6.46 m/s	3.12 m/s	45 RPM
4 T500	7.08 m/s	4.33 m/s	53 RPM

The speed test results confirm the superior thrust power of the T500 thruster across all aspects. The combined configurations of T200 and T500 thrusters performs quite well, showing an improvement over the configurations with 4 T200

Thrusters and 4 T500 Thrusters. Our final consideration is to use the T200 configuration for X-Drive and the T500 for the main thrusters, as this combination offers a good balance of efficiency, speed, and weight.

# Appendix D: Perception System

Medericus Mundi Miseridityo, Sigmayuriza Senaaji Rasendria

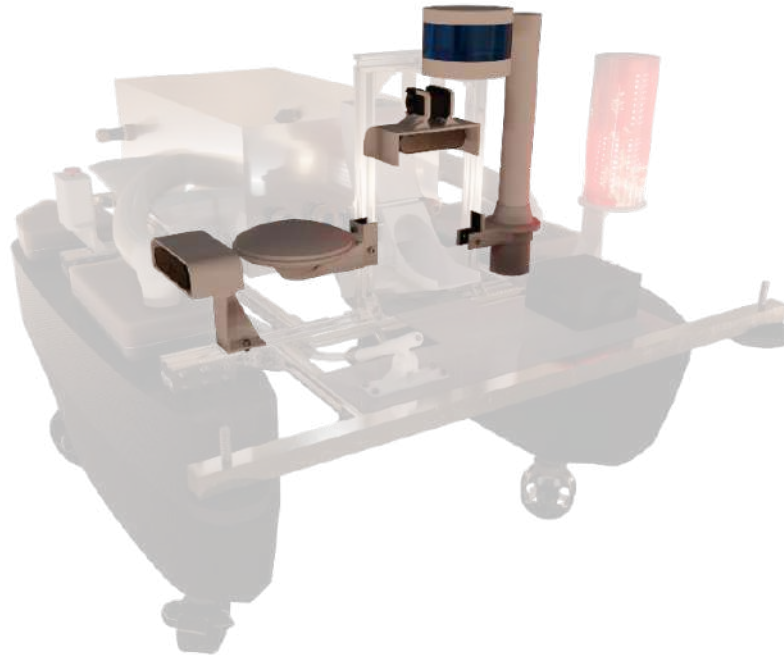


Fig. 1. Ares' perception system

## I. INTRODUCTION

Autonomous Surface Vehicle (ASV) requires a system that can perceive surrounding environments, obstacles, and objectives to be achieved. Barunastra takes an approach to enable the perception system by implementing Computer Vision systems, Localization and Mapping, and Obstacle Avoidance. All the perception data is collected and processed to become knowledge for ASV, and further processes will be done in cognition and behavior systems.

## II. APPROACH

### A. Computer Vision

1) **Hardware:** For the RoboBoat 2025 autonomy challenge, Barunastra ITS uses two cameras: one for the primary and one for the side camera.

The main camera functions for receiving information aligned in the same direction as the

ship, and the side camera focuses on the Speed Challenge task where it needs vision facing the normal angle of the boat (either left or right side), detecting the light tower.

2) **Object Detection:** The primary camera will be processed for object detection by creating a machine-learning model from a trained custom dataset with YOLO (You Only Look Once) architecture [1]. The side camera will focus on the light tower dataset for red and green light detection. The result will contain the ROI (Region of Interest) of the image shown with the bounding box, the name of the class of the detected object, and the probability score of the object.

Ares will use the YOLOv8 deep learning model, combined with the OpenVINO framework, to achieve higher object detection performance with CPU-based inference.



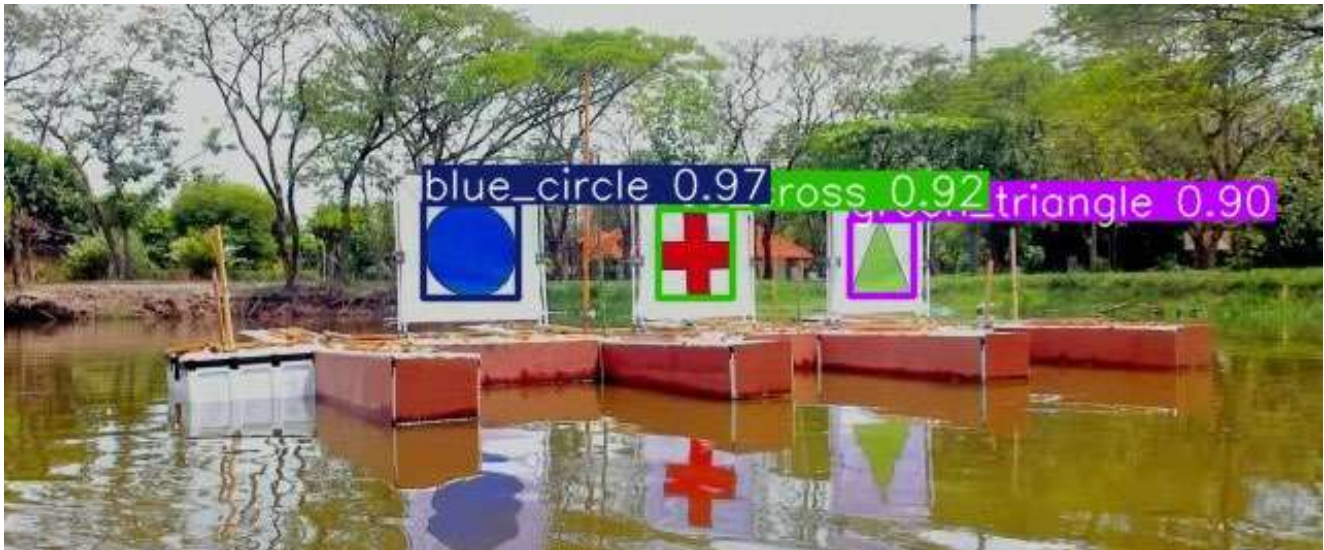


Fig. 2. Object detection result with YOLO

**3) Object Tracking and Counting:** To address the obstacle counting in the Follow the Path task, Barunastra ITS uses the ByteTrack framework and Supervision library, enabling object tracking to detect objects from YOLO. ByteTrack is a multi-object tracking algorithm by which processes comprise object detection, data association, Kalman filtering, and trajectory updating [2]. A Kalman filter will be applied to predict the state of each object by using the object positions and confidence scores from the object detection algorithm, enabling tracking of the object's motion trajectory. The algorithm transitions between states by matching the detecting results with existing predicted trajectories. The unmatched object will be removed, and the tracking for the previously tracked object will be terminated.

Obstacle buoys will be counted by creating a line which counts the tracked objects passing the line. This happens by calculating the tracking directions of an object, and if the direction is from north to south (up to down) and the trajectory tracking is passing the line, meaning that the object has travelled from the bow side of the ship to stern as the boat will constantly moving forward.

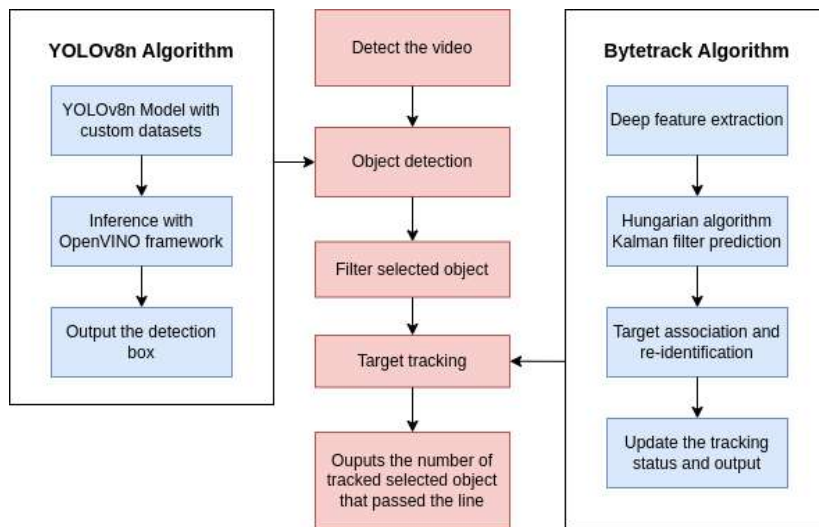


Fig. 3. Object detection, tracking, and counting diagram

**B. Obstacle Avoidance**

We used *Braiteinberg* algorithm uses several sensors connected to the motor, affecting the motor’s speed by the sensor input. It produces a weighted matrix for each sensor input and converts it into motor speeds.

Nala Ares is equipped with a 3D Velodyne LiDAR to detect and avoid obstacles in front of the vehicle; in this case, it is the 2a vehicle model. LiDAR’s laser scan data will be clustered into several angles, and the distance to the nearest obstacle will be calculated, creating a matrix of distances. The data will be calculated by adding weights for each angle to prioritize avoiding obstacles in front of the boat.

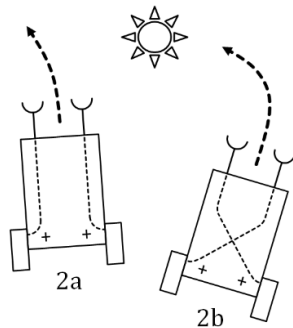


Fig. 5. The Braiteinberg vehicle avoids (2a) and attracts (2b)

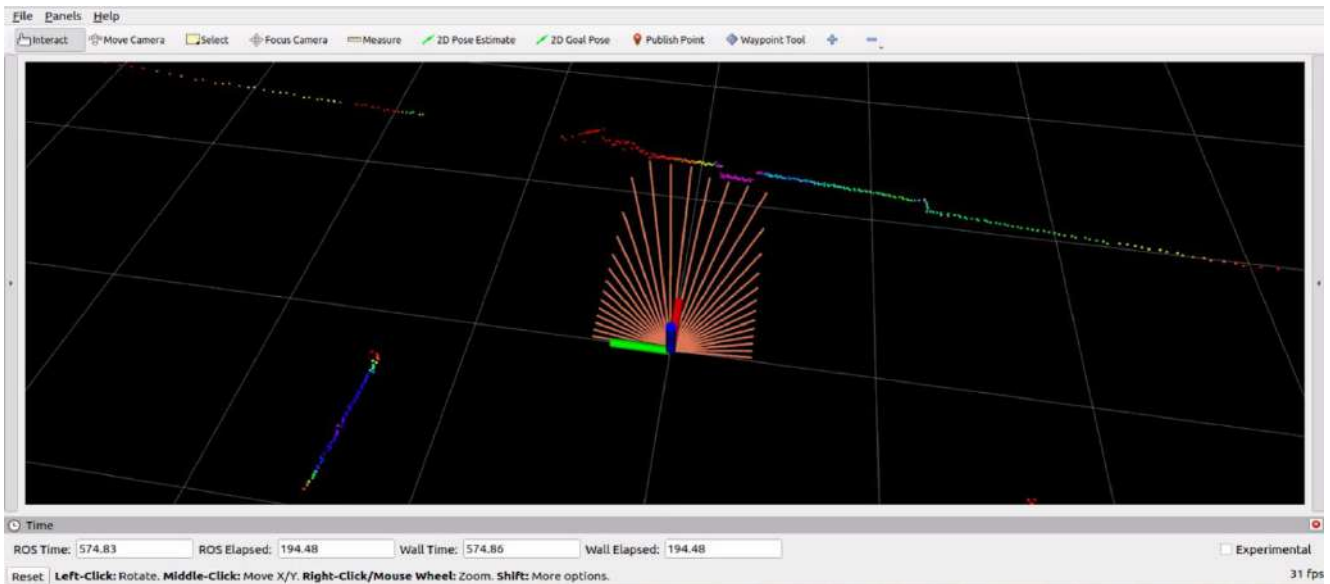


Fig. 6. Obstacle avoidance visualization when detecting objects

---

**Algorithm 1** Obstacle Avoidance Algorithm
 

---

**global variables**

*angle\_start*, start angle for the avoidance  
*angle\_end*, end angle for the avoidance  
*angle\_step*, the step of the distance between angles  
*distance\_list*, array of laser scan distances from angle\_start to angle\_end with respect to angle\_step  
*maneuver\_weight*, an array of desired weights for maneuvering per angle  
*angle\_calculate\_weight*, weight for adding calculation into result angle  
*angle\_result\_weight*, weight for the current angle

**end global variables****begin**

```

angle_calculate = 0
FOR i in number of distance_list
  sector_angle =
    angle_start + angle_step * (i + 0.5)
  angle_calculate =
    angle_calculate + maneuver_weight[i] *
    (1 - distance_list[i]) * sector_angle
END FOR
angle_result =
  angle_result_weight * angle_result +
  angle_calculate_weight * angle_calculate
  
```

**end****C. Localization and Mapping**

Ares will utilize LiDAR to fuse with IMU and GPS, enabling accurate localization and creating a map from observed LiDAR point cloud data compared to last year, which only used data from GPS and IMU that could occur shifting in data localization, causing inaccurate in navigating to a destined goal. Direct LiDAR-Inertial Odometry (DLIO) [4] allows state localization creation by using features of objects from LiDAR point cloud data, calculating the motions and generating state fused with our custom GPS and IMU fuse. DLIO can also create 3D maps by saving motion keyframes and generating more stable maps.



Fig. 7. Map and path trajectory created with DLIO at campus lake

One of the concerns about using the DLIO framework is the chance of only obtaining low-point cloud data in the RoboBoat 2025 course, which will corrupt the localization and mapping

process. Therefore, GPS data is being used as a backup by calibrating both GPS and DLIO states to maintain the map and switch the localization source if either is broken.

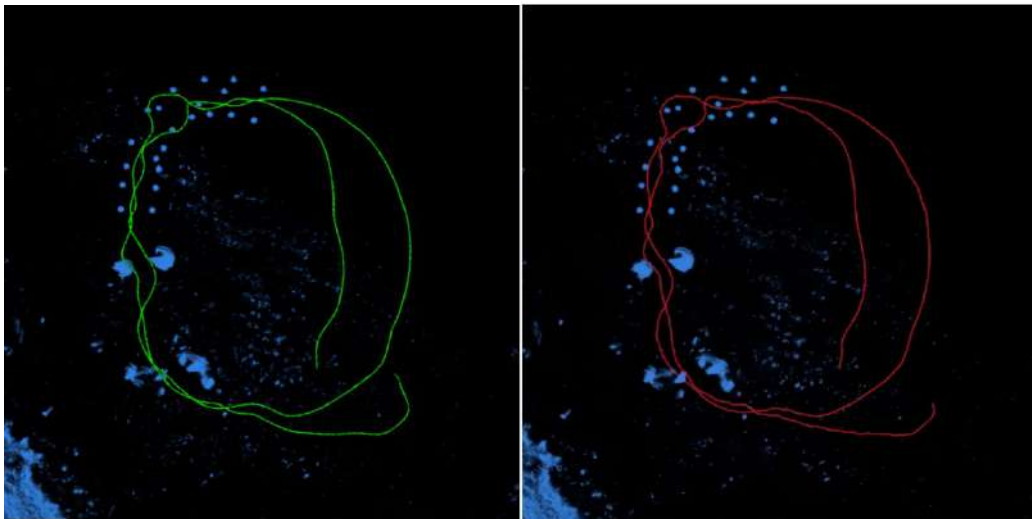


Fig. 8. Localization using GPS and IMU (left) compared with localization using LiDAR and IMU (right)

The result above shows that localization with LiDAR has better accuracy than GPS. GPS has a chance to shift location while moving, resulting in a state located at the supposed object. Conversely, LiDAR can generate a more accurate state because it calculates based on surrounding objects.

### III. HARDWARE SETUP

Some components have requirements to be placed in a high position, especially those that need to emit signals or capture vision, such as

LiDAR, antenna, and the camera. The frame has the main function as a pillar for these components (furthermore will be called “pillar frame”). Previous year, we had less components at the pillar frame and it was enough for us to use light material. However, we have more items attached to the frame for RoboBoat 2025 which make us need to have a stronger construction. The pillar frame uses a material similar to the main deck frame which is single V-slot aluminum. The frame fabrication process starts by cutting the aluminum

close to the desired dimension using a grinding machine, followed by cutting with a milling machine for better precision dimension. The frame was connected using reinforced angle brackets,

bolts, and T-slide nuts at the inside corner of the pillar frame.

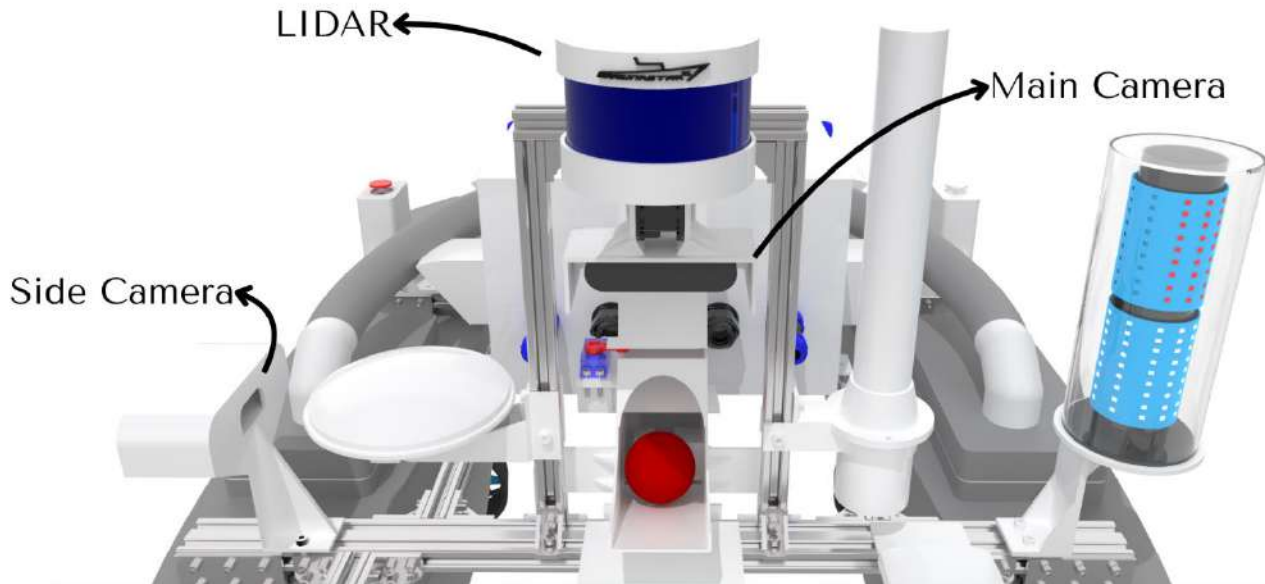


Fig. 9. Perception System

All the bracket parts are used as an item holder to attach to the pillar frame. The LiDAR cover especially reduces direct heat from the sunlight. The brackets were fabricated either using three mm aluminum L-profile/plate if they needed both strong structure and simple design, such as LiDAR bracket base and servo bracket, or using 3D printing with PLA+ filament if they needed both light and easily shaped structure, like covers for LiDAR and camera as well as brackets for antenna and GPS. Aluminum based brackets were manufactured using a grinding machine for cutting the material and a milling machine for clearing the excess material plus drilling a hole for bolt-nut joints. While 3D printed brackets were printed using a 3D printer. For 3D printed brackets which need stronger construction, it was printed using 50% infill whilst the other using 25-30% infill with three hexagonal patterns or gyroid. All brackets were assembled to the frame by using L-type bolts-nuts joints. Dynamixel servo makes it possible for the camera to have an angle rotation

up to 360 degrees. However, due to pillar frame and brackets installation, the camera can only have around 85°.

#### IV. CONCLUSION

Compared to last year, Barunastra's perception vision has a significant upgrade to enhance the knowledge-gathering process. For computer vision, we're using the YOLOv8n ML model with the OpenVINO framework to improve performance on NUC mini-PC and maintain the model by creating valid datasets. ByteTrack is also being used to enable object tracking for more valid data of counting the obstacle for the Follow the Path task. An obstacle avoidance algorithm is added to support global navigation and the Return to Home task, minimizing the chance of the RoboBoat hitting objects. We use the DLIO framework to enhance the localization system but still use GPS for backup localization. Also adding the mapping functionality to plan the autonomous navigation system for RoboBoat 2025 better.

**V. REFERENCES**

- [1] J. Redmon, “You only look once: Unified, real-time object detection,” in *Proc. IEEE Conf. Comput. Vis. Pattern Recognit. (CVPR)*, 2016.
- [2] L. Jinjiang, X. Yonghua, Z. Yu, and L. Haoming, “Vehicle flow detection and tracking based on an improved YOLOv8n and ByteTrack framework,” *World Electric Vehicle Journal*, vol. 16, no. 1, Art. no. 13, 2025, doi: [10.3390/wevj16010013](https://doi.org/10.3390/wevj16010013).
- [3] K. Chen, R. Nemirow, and B. T. Lopez, “Direct LiDAR-Inertial Odometry: Lightweight LIO with continuous-time motion correction,” in *Proc. 2023 IEEE Int. Conf. Robotics and Automation (ICRA)*, London, U.K., 2023, pp. 3983–3989, doi: 10.1109/ICRA48891.2023.10160508.

# Appendix D.1: Test Plan and Result Computer Vision

Medericus Mundi Miseridityo

## I. SCOPE

Choosing the Machine Learning (ML) model for computer vision is one of the main concerns in the autonomy system because it affects how the robot will behave based on this perception subsystem. The model must accurately detect objects while maintaining performance on the processing machine, which, this year, Barunastra uses NUC mini-PC. The model must be tested in a similar condition on the same datasets created on the replica course/arena of RoboBoat 2025.

## II. SCHEDULE

The time needed to complete this testing is about one week around December 20<sup>th</sup> until December 28<sup>th</sup>, 2024. The process included taking datasets from vision taken in arena replica, labelling, training, until testing. The process took a weeklong since there were updates for the placement of the tasks/arena.

## III. RESOURCE AND TOOLS

Efficiently processing the datasets requires a highly computational device to train the ML model. Barunastra ITS uses RTX 4080 Super to train the dataset to the model and uses an Intel Core i7 7th generation CPU processor to benchmark all models and compare them. To label the datasets, Barunastra ITS uses Roboflow, a web-based annotator, to add information to the image datasets.

## IV. ENVIRONMENT

The ML models are trained with the same configurations, e.g. 300 epochs of training, the same dataset, 32 batch size, and the other configurations are set with YOLO's default. Benchmarking uses benchmark tools from YOLO to provide equal and robust configurations for each model.

## V. RISK MANAGEMENT

In creating the dataset for training the ML model, data bias may occur due to the dataset's lack of variety, insufficient data, imbalance dataset, and error in the labelling stage. The images used for the dataset are selected manually to ensure all objects have enough variety. Selected images will be labelled using Roboflow because of its ease of use for manual labelling, preventing errors in labelling compared to the auto-labeller. Data augmentation is also done using Roboflow to multiply the dataset further, creating a wide variety in real-world conditions that may not be as perfect as the dataset.

## VI. RESULT

Several YOLO models were compared using Intel-based CPUs. This is done to mimic the performance of the NUC mini-PC processor. By comparing the performance and accuracy of the models using a custom dataset for RoboBoat 2025 based on trial conditions, it is shown that YOLOv8n has the best performance and accuracy.

TABLE I VISION ML MODEL PERFORMANCE BENCHMARK: VALIDATION AND FPS

Model	Precision	Recall	mAP50	mAP50-95	FPS
<b>YOLOv7-tiny</b>	0.881	0.93	0.948	0.736	10.44
<b>YOLOv8n</b>	0.916	0.925	0.961	0.761	12.816
<b>YOLOv9t</b>	0.907	0.898	0.95	0.749	8.099
<b>YOLOv10n</b>	0.834	0.859	0.907	0.677	10.214
<b>YOLOv11n</b>	0.902	0.925	0.957	0.773	10.966

To maximise the performance of CPU-based inference, we compared several deep learning inference frameworks running in the same YOLOv8n model. It was found that OpenVINO

has the best performance in terms of speed in processing frames while also maintaining detection accuracy.

TABLE II VISION ML INFERENCE FRAMEWORK PERFORMANCE BENCHMARK: VALIDATION AND FPS

Framework	Precision	Recall	mAP50	mAP50-95	FPS
<b>PyTorch</b>	0.916	0.925	0.961	0.761	12.36
<b>TorchScript</b>	0.891	0.928	0.959	0.758	15.66
<b>ONNX</b>	0.891	0.928	0.959	0.758	13.67
<b>OpenVINO</b>	0.891	0.928	0.959	0.758	20.02
<b>MNN</b>	0.891	0.928	0.959	0.76	17.23
<b>NCNN</b>	0.891	0.928	0.959	0.758	15.43

Based on the results above, we chose the YOLOv8n model as our base machine-learning

architecture and OpenVINO as the inference framework for object detection using YOLO.



# Appendix E: Rescue Delivery Mission

M Andi Abdillah, M Farras Rheza Firmansyah

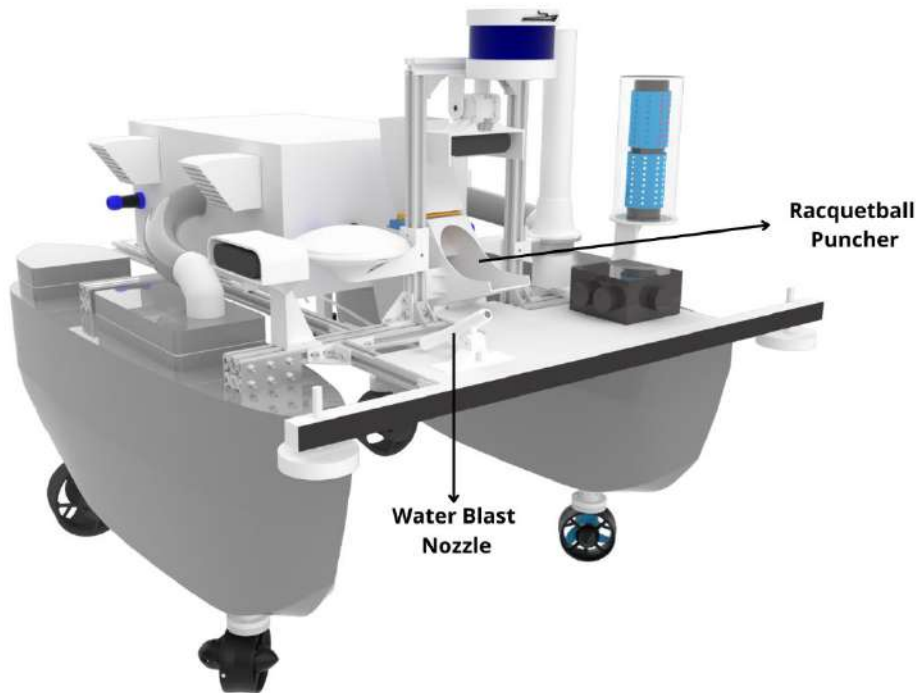


Fig. 1. Ares' rescue delivery mission

## I. INTRODUCTION

The Rescue Delivery Mission for Task 5 in RoboBoat 2025 involves two primary objectives: object delivery and water delivery. Both mechanisms were developed based on evaluations of previous designs and discussions between the mechanical and electrical divisions to identify improvements and ensure alignment with this year's requirements.

For object delivery, the discussion resulted in a decision matrix to compare our two previous mechanisms used in 2023 and 2024 with our new plan, racquetball puncher, which is expected to be lighter since it utilizes solenoid instead of DC Motor. The decision matrix was conducted on a scale of 3 with 3 being the most ideal scenario.

	Ball Catapult	Crane	Racquet ball Puncher
Weight	2	1	3
Size	2	1	2
Ease of Build	2	1	3
Controllability	3	2	1
Total Score	9	5	9

Although the Ball Catapult has the same score as the Racquetball Puncher, the puncher was chosen since it is linear to our goal which is to minimize weight for better performance.

For the water delivery mechanism, the team decided to retain the same system used in 2024. This decision was based on its proven efficiency and reliability, as it successfully met the competition requirements without significant issues.

**II. DESIGN CONCEPT AND REQUIREMENTS**

Prior designing the mechanism for delivery mission, the workflow flowchart was determined as follows.

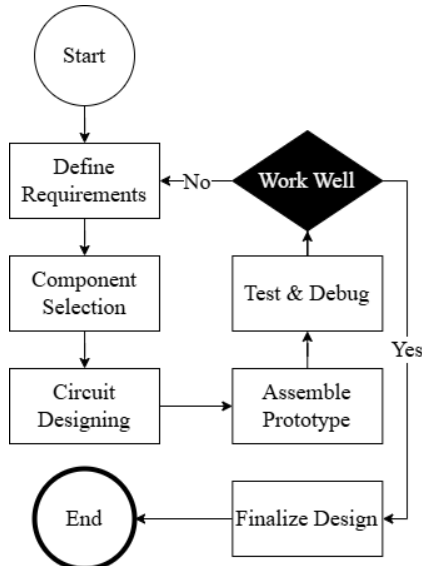


Fig. 2. Workflow flowchart

**A. Object Delivery**

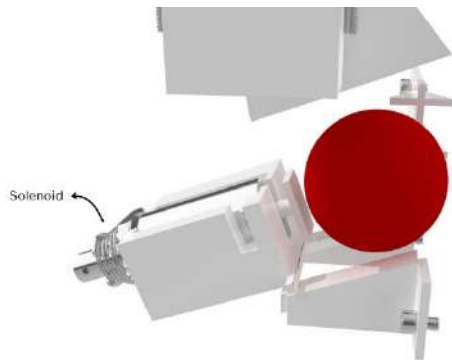


Fig. 3. Solenoid placement

Barunastra’s racquetball puncher is designed to launch racquetballs with high speed and accuracy, while being strong, light, and can be reloaded. It also ensures compatibility for mounting at the correct angle to align with the ASV's structure. The mechanism utilizes a push-pull solenoid for fast and consistent launches. A large electric current causes the iron rod to rapidly move into the solenoid coil, extended by a non-magnetic material, while spring returns the rod to its position outside the coil. As shown in fig. 3, The tip of the iron rod features a 3D-printed square puncher designed to accommodate the ball's round shape, providing an optimal surface for shooting.

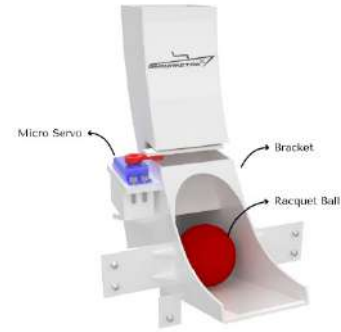


Fig. 4. Racquetball puncher breakdown

In fig. 4, the mechanism relies on an inclined angle to make an arch, allowing the ball to travel farther. A servo-controlled rotating gate manages the reloading and ball-holding mechanism. The launcher bracket was designed with bolt joints for secure installation to the pillar frame. This design aligns with the requirements for a reliable, adaptable, and lightweight launcher capable of delivering racquetballs efficiently during the competition.

**B. Water Delivery**



Fig. 5. Water delivery mechanism

To meet the requirements of the water delivery task, Barunastra's system is designed to accurately and consistently shoot water at designated targets, specifically the black triangle shapes on the orange vessels. The design focuses on delivering a steady and visible stream of water for at least 3 seconds, as required by the competition. The system integrates two water pumps capable of maintaining consistent flow and pressure, ensuring the stream is powerful enough to hit the target from a distance. The nozzle angle remains fixed along ASV operation, as in the previous

design, since the target is positioned directly in front of the ASV.

### III. SYSTEM ANALYSIS

For the object delivery task, the solenoid is first tested using a single supply directly from a LiPo battery. As a result, the ball was pushed with weak force which is not enough for our needs. Enhancing the solenoid's strength can be achieved by applying the principles of electromagnetism and Ohm's Law. Based on the Ampere's law which states:

$$\oint B \cdot dl = \mu I_{enc} \quad (1)$$

While for a long solenoid, the magnetic field is nearly uniform inside and negligible outside. Using symmetry and simplifying the path integral along the solenoid's axis.

$$B \cdot L = \mu \cdot N \cdot I \quad (2)$$

Dividing both sides by  $L$  and letting  $n = \frac{N}{L}$  (Number of turns per unit length)

$$B = \mu \cdot n \cdot I \quad (3)$$

The magnetic field increases with current, number of turns per unit length, and permeability of the core material [3]. Since it is difficult to change the number of turns or the core material's permeability, increasing current can be achieved by raising the voltage, in accordance with Ohm's Law:

$$V = IR \quad (4)$$

With fixed resistance, increasing the voltage allows current to increase. A boost converter capable of converting up to 450V was chosen. Since the current produced by the boost converter is very low, a capacitor was added before the solenoid to temporarily store energy, enabling the production of higher current for short periods. A relay was also added as an electronic switch to ensure safe control by the microcontroller.

## IV. HARDWARE PROTOTYPING

### A. Object Delivery

After conducting a test for the solenoid selection, the next step was to design and build a Racquetball Puncher that matches the requirements. The material selection prioritized lightweight construction with good durability. This year, all parts are fully made from 3D-printed

PLA+ filament. PLA+ was chosen for its toughness and ease of printing. The 3D printing process involved several adjustments, including quality, infill, print speed, support, and material settings. The launcher body is secured between the pillar frame and main deck frame using bolt-and-nut joints. Until the final design, there were three design iterations:

**1) 1<sup>st</sup> Iteration:** The plan was to put a sturdy foundation for the Racquetball Puncher by designing extended supports that attach securely to an extrusion frame, reinforcing the overall structure. The design can be seen in fig. 6.



Fig. 6. First design of racquetball puncher

This design has a limitation in the reloading mechanism. The fixed 90° upright angle causes the structure to contact the ship's camera bracket due to the restricted movement of the camera on the Y-axis. We observed that the overall structure had potential weak points, making it prone to breakage. It was also challenging to position the system precisely within the frame layout while its design also added unnecessary weight to the ship.

**2) 2<sup>nd</sup> Iteration:** Addressing the issue from the previous design, we adjusted the angle between reload and launcher to 50 degrees and removed excessive structural elements. These adjustments aimed to prevent the structure from contacting the camera bracket and to reduce stress on potential weak points. The design is shown in fig. 7.



Fig. 7. Second design of racquetball puncher

The design was still not optimal, as the solenoid actuator was positioned too far forward, obstructing the ball's path. Additionally, the extended ends of the launcher created friction, reducing the shooting range.

**3) 3<sup>rd</sup> Iteration:** We simplified the design to address the issues from previous iterations. The cylindrical structure was replaced with a box to provide more space for the ball's movement. The launch path was shortened to minimize friction, and the solenoid placement was adjusted to ensure the ball could move easily. This iteration proved effective and was adopted as the final design, as shown in fig. 8.



Fig. 8. Racquetball puncher final design perspective (a) and top view (b)

**B. Water Delivery**

Due to the efficiency, we obtained in the water blast mission RoboBoat 2024, we decided to use the same design and mechanism without any changes. The system utilizes two DC water pumps as inlet with 12.5 mm input diameter. Both pumps are submerged at stern and attached to the main deck frame using aluminum hollow and 3D print

as the bracket. The installation of these brackets is precisely at the end of the hull stern to prevent the high resistance between the hulls. Using this placement, the wake from current alongside the hull will not affect much when the ship is going surge forward. The pump installation is shown in fig. 9.



Fig. 9. Pump bracket installation

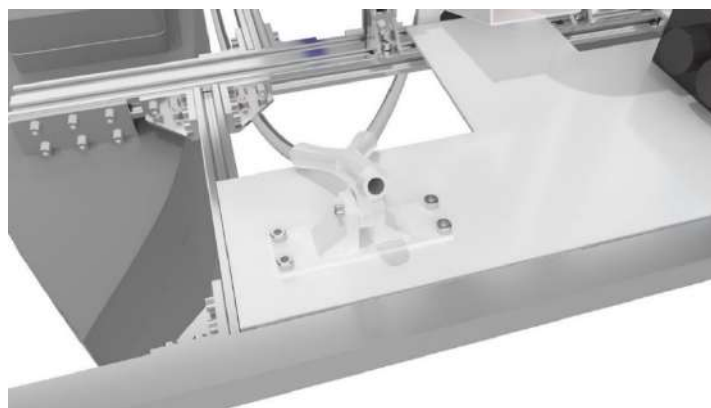


Fig. 10. Main deck nozzle attachment

TABLE II WATER PUMP MECHANISM

Parameter	Value
Working Voltage	DC 12 Volt
Power Rating	8 W
Max water height	5 m
Max flow	10 L/min
Inlet Diameter	15.5 mm
Outlet Diameter	11 mm

TABLE III HOSE SPECIFICATION

	Inside Diameter	Outside Diameter	Length
Left Hose	12.5 mm	15.5 mm	1400 mm
Right Hose	12.5 mm	15.5 mm	1200 mm

The left hose is longer than the right since the placement of the nozzle is in the right side of the main deck. The nozzle has two inputs from two pipes and one input. The input outside diameter is 12.5 mm while output inside diameter is 5 mm. The nozzle was produced using 3D Printing PLA+ filament. The installation angle for this nozzle is fixed at 45° since it yields the farthest projectile.

**V. CONCLUSION**

Racquetball puncher and water blaster has met the requirement for RoboBoat 2025 and the needs

of Barunastra to obtain efficient and lightweight system at the same time. The comparison between racquetball puncher with its predecessors can be seen in the table below.

TABLE IV MECHANISMS COMPARISON

	Ball Catapult	Crane	Racquetball Puncher
Weight	2.7 kg	1.8 kg	1 kg
Power draw per launch	472 J at max power	164 J	108 J at max power
Distance	Max 440 cm	50 cm	Max 115 cm

The table shows that racquetball puncher has the lightest weight and still efficient enough to launch object to the target with the distance more than one meter from the ship.

**VI. REFERENCES**

[1] D. Halliday, R. Resnick, and J. Walker, Fundamentals of Physics, 10th ed. Wiley, 2014

# Appendix E.1: Test Plan and Result Racquetball Puncher

M Andi Abdillah

## I. SCOPE

Solenoid and projectile angle tests were carried out to find the optimal racquetball puncher design. The objective of the solenoid test was to assess which solenoid configuration was best to be used whilst projectile angle test was to determine the best angle installation for racquetball puncher to launch the ball.

## II. SCHEDULE

The solenoid test was conducted on December 20<sup>th</sup>, 2024, for about five hours. After the suitable solenoid was selected, the mechanical system was designed. After the mechanical design was almost done, the projectile angle test was carried out on January 4<sup>th</sup>, 2024, for about six hours to determine the best angle to install a racquetball puncher.

## III. RESOURCE AND TOOLS

The required resources and tools are listed in Table I.

Tools	Function
Battery 3S 12V	Power source
Boost Converter up to 450V	Increase the battery voltage
Capacitor 820 $\mu$ F	Store energy after boost converter
Measuring Tape	Measure the height reached by launched ball
Solenoid	The main launcher component
Relay	The electronic switch
Microcontroller STM32	The relay controller
Ball	The object that will be launched
Protractor	Measure the arc angle of projectile

## IV. ENVIRONMENT

Both tests were conducted inside the Barunastra laboratory without any wind current or other obstructions. For the solenoid selection test, the solenoid was placed on a flat surface and the height of the launched ball is measured vertically using measuring tape. Projectile angle test was conducted in various angles to measure the maximum height of the arc and distance reached by the ball from the launcher point location.

## V. RISK MANAGEMENT

### A. Electric Shock

This risk might happen since the solenoid operated on various voltages which can be hazardous and cause painful shock. Safety precautions, such as wearing gloves, were implemented to prevent exposure to voltage surges from the boost converter. The equipment under test was thoroughly insulated to eliminate the risk of voltage leakage.

### B. Measurement Failure

Measurement failure could occur when the perspective angle is not accurate while seeing or measuring the distance using measuring tape. To overcome this, multiple measurements were conducted, and more team members were involved in the measurement process.

## VI. RESULT

### A. Solenoid Selection

The testing method involved gradually increasing the voltage from 90V to 450V to determine the optimal voltage, considering losses in electromagnetic systems such as core saturation and practical constraints like heat generation, insulation limits, and material properties. Two different types of solenoids were tested with specifications provided in Table II.

TABLE II SOLENOID COMPARISON

	<b>Force at 12V</b>	<b>Plunger Stroke</b>	<b>Body Size</b>
Solenoid 1	5 N	10 mm	30 × 16 × 15 mm
Solenoid 2	14.7 N	10 mm	95 × 30 × 30 mm

Since Solenoid 1 was too small, two of them were connected in parallel to increase the pushing force. During testing, the solenoids were positioned vertically, with a racquetball placed on top. For the result, Solenoid 2 was chosen for its higher launch and greater force

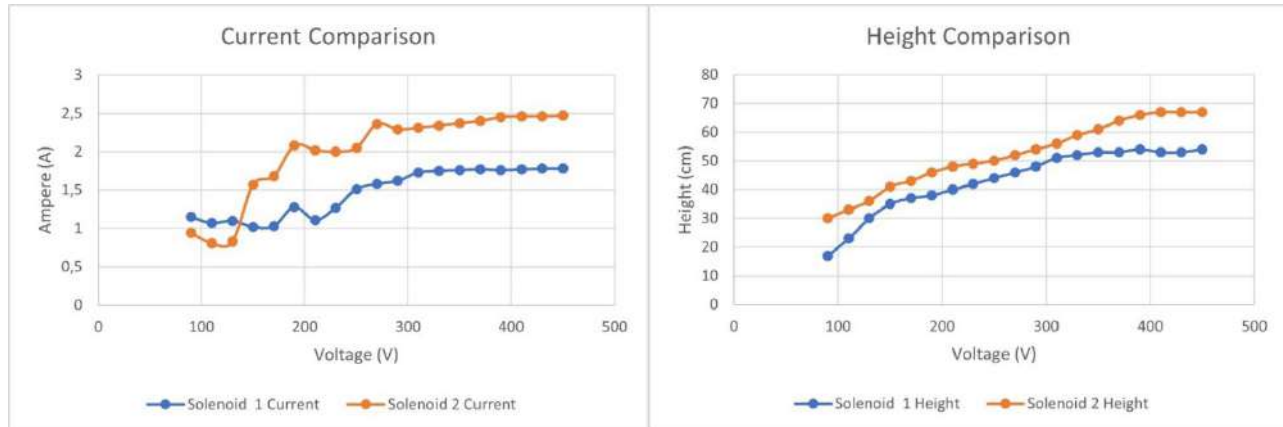


Fig. 1. Current comparison (left), height comparison (right)

Based on the testing results shown in fig. 1, 400V was selected as the voltage input for the solenoid since it reached maximum height and current as it remains constant afterwards.

**B. Projectile Angle**

After installing the solenoid onto a mechanism fabricated using a 3D printer, tests were conducted to strike the racquetball. The testing involved adjusting the shooting angle and recording the distance achieved by the final prototype. The results are summarized in Table III.

TABLE III PROJECTILE TEST RESULT

<b>Angle</b>	<b>Distance</b>	<b>Height</b>
15°	67 cm	4 cm
30°	118 cm	18 cm
45°	135 cm	39 cm
60°	115 cm	52 cm

From the result shown in Table III, we decided to use 45° angle since it gives the farthest distance and 39 cm height from nozzle base is considered enough to shoot consistently.

# Appendix F: Software Architecture and Ground Control

Taib Izzat Samawi

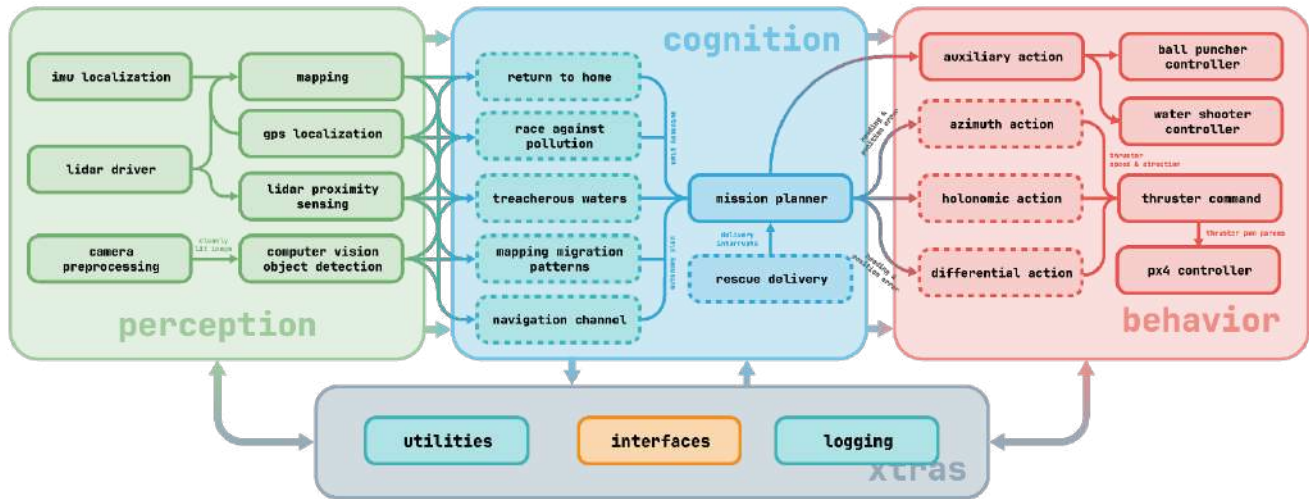


Fig. 1. Software Architecture

## I. INTRODUCTION

We adopt a move-fast-break-things approach to building programs to enhance and optimize the result and performance of our programs. We believe that a high rate of reiteration and experimentation will result in higher chances of finding the best approach to completing missions.

However, as complexity in our program grows, so does the need for a high-level overview mechanism for it. We constantly evolve our software architecture approach to ensure better handling of programs for senior developers and faster learning time/s for junior developers, without making the structure so strict that it contradicts with our experimentation-focused and rapid development approach.

## II. ARCHITECTURE APPROACH

### A. ASV Operating System

In 2018, we migrated from using Windows to Ubuntu as the operating system for both the ground crew and the ASV's main computer. Last year, we used Ubuntu 20.04. Nearing the EOL (End-of-Life) date of Ubuntu 20.04, we decided to slowly refactor our code for an Ubuntu 22.04-based work environment starting in November 2023.

During the transition, we encountered a significant amount of change in our package/tools selection to minimize *dependency hell*:

- We decided to sunset our YOLOv3 and YOLOv4 implementations, focusing more on natively supported YOLO versions for Ubuntu 22.04.
- A migration of our entire Robot Operating System (ROS) programs from *ROS1 Noetic* to *ROS2 Humble* was undertaken to future-proof existing programs for several years to come.

### B. Perception-Cognition-Behavior Stack

A constant reshuffling of our software architecture stack year after year resulted in major refactors and slowdown in software development. To alleviate this issue, we migrated to a purpose-oriented software architecture approach (in which each module in the architecture serves one general task) instead of relying on a package-based software architecture approach (in which each module in the architecture is a separate ROS package) for our ROS2 codebase.

We decided to design our new and hopefully ultimate software architecture based on the concept of the *sensorimotor system* on living



beings. The main idea used for software architecture design is as follows:

- First, the ASV is to receive any external stimulus via one module.
- Second, the ASV is to decide upon the received external stimulus via one module.
- Third, the ASV is to act upon its decisions towards the environment via one module.

This resulted in the creation of 3 modules, which names are lexicographically ordered for easier development. The names of the 3 modules are *Perception*, *Cognition*, and *Behavior*. An extra *Xtras* module is added to store any utilities, interfaces, and or logging software.

Although the exact program flow is not strictly enforced, every ROS2 package in any of the 3 modules is expected to generally receive inputs from the one before it and returns values and or parameters to be used for the module after it.

**1) *Perception*:** This module is to receive any external stimulus and convert them into comprehensible information to be processed by Cognition. This module includes:

- Computer Vision (CV) obstacle detection and tracking.
- LiDAR obstacle detection and DLIO.
- IMU-based localization.
- GPS-based localization.
- CV obstacle counting for Follow the Path

**2) *Cognition*:** This module is to receive processed and distilled information about the environment from Perception and decide the best next action to be executed by Behavior. This module includes:

- Obstacle avoidance programs.
- Delivery mission interrupts (pausing whatever mission is currently running to execute water/ball delivery).
- Decisioning/mission management, used to set priorities and or general sequences of missions.

- Exact planning. controller parameters, and arguments for each mission.

**3) *Behavior*:** This module is to receive movement and or any behavior commands from Cognition and act upon it. This module includes:

- Control action algorithms (Azimuth, Holonomic, and Differential action algorithms).
- Control parameters for each thruster to be sent to PX4.
- Camera servo, water pump, and solenoid ball shooter serial commands.

### III. GROUND CONTROL APPROACH

Communication loss from ground command to ASV generally results in inability to monitor and or terminate its autonomy mode via ground PC (resorting to shutting autonomy down via remote control interruption). If monitoring programs are placed on ground control, loss of communication with ASV oftentimes results in the need for restarting such monitoring software/s.

We decided to use a *Secure Shell* (SSH) connection to the Ares' computer. However, instead of running the programs via the SSH connection, the programs run natively on Ares' computer. The SSH connection is purely used for attaching any terminal sessions active on Ares' computer to ground control. This way, ground control can execute even UI applications via SSH to be shown on Ares' computer instead of the ground control computer.

### IV. CONCLUSION

Changes in software architecture and ground control approach is done to significantly reduce migration and further troubleshooting time and complexity. Barunastra ITS plans to implement the Perception-Cognition-Behavior stack for years to come and improve upon the ground control approach.

# Appendix F.1: Test Plan and Results, Setup Efficiency

Taib Izzat Samawi, Medericus Mundi Miseridityo, Arundaya Pratama Nurhasan

## I. SCOPE

Tests were conducted to verify whether the Perception-Cognition-Behavior software stack increased development efficiency a better ground control approach, which should minimize software restarts, component reboots, and setup times. Testing the setup time (time taken since booting up until all autonomy programs are up and running) is considered enough of a metric.

## II. SCHEDULE AND ENVIRONMENT

Ground control tests were conducted from the start of RoboBoat 2025 progress in November 2024 up until January 2025. During each in-water testing session on *Campus lake* (Campus Lake), a record of the amount of time required to set up autonomy systems using both the old tech stack and the new tech stack were measured.

## III. RESOURCES AND TOOLS

Time to set up Ares' PC and average time taken to restart programs upon errors is measured using a stopwatch. If the new ground control approach yields in reductions of time, the ground control approach is codified to be used during the regatta.

## IV. RISK MANAGEMENT

To prevent unrecorded sessions and to verify the time taken to reboot our troubleshoot an issue, video recording of each trial run is taken to be used to cross-check time records after every on-water testing session.

## V. RESULTS

Out of every on-water testing session conducted, 22 sessions provide enough information that accurately records setup times. These 22 sessions are the ones with both stopwatch and video recordings. Tables I and II describe the details and summary for the setup times of both the old and the new tech stack.

TABLE I DETAILED SETUP TIME DIFFERENCE

No.	Setup Time (s)	
	Old Stack	New Stack
1	308.55	49.48
2	277.85	38.51
3	311.34	48.87
4	308.03	47.32
5	311.02	45.20
6	295.54	52.46
7	313.60	51.53
8	311.97	54.84
9	309.19	54.66
10	316.34	50.49
11	286.73	36.13
12	304.55	48.51
13	306.73	50.30
14	311.01	48.24
15	321.48	53.29
16	289.47	41.95
17	308.09	48.04
18	304.92	52.96
19	307.07	65.14
20	312.50	51.62
21	312.47	39.02
22	307.50	46.66

TABLE II SETUP TIME DIFFERENCE SUMMARY

Attribute	Setup Time (s)	
	Old Stack	New Stack
Mean	305.80	49.48
Min	277.85	36.13
Max	321.48	65.14

# Appendix G: Electrical System

Jonathan Oktaviano Frizzy, Jilan Nabilah Dikairono, M Andi Abdillah, Farrel Rahmadany Akbar

## I. INTRODUCTION

The electrical design for RoboBoat 2024 presented several challenges, including space constraints, system complexity, and inefficiencies in maintenance and repair. These limitations hindered the system's performance, highlighting the need for significant improvements. For RoboBoat 2025, the electrical design of Ares focuses on addressing these issues by emphasizing modularity, flexibility, and efficiency.

Key objectives include minimizing space and weight, reducing complexity while improving the maintainability by integrating advanced features, such as the racquetball puncher for the Rescue Delivery mission. The design strategy leverages data-driven analysis and cross-divisional collaboration to enhance system adaptability and performance. By improving centralized design features, the electrical architecture of Ares is tailored to meet the competition's demands while ensuring reliability and ease of maintenance.

## II. PROBLEM ANALYSIS AND SOLUTIONS

Before designing the electrical architecture for Ares, the team conducted a detailed review of system performance reports, testing logs, and

documentation from Proteus 2.0 in the previous RoboBoat.

In Proteus 2.0, the electrical system was distributed across two separate boxes: one for electrical components and another for essential programming devices, such as the mini-PC and other control units. Although this two-box setup offered advantages in terms of system organization and monitoring, it increased the vessel's overall dimensions and weight. For Ares, the team compresses all components into a single electrical box to align with this year's goal on minimizing space and weight.

This reorganization simplifies the system's layout, reduces the vessel's footprint, and streamlines integration between electrical and programming components. Applications on modular electronic systems in robotics provided valuable insights into how adaptability and compactness can improve system functionality while addressing constraints such as space and complexity. By adopting a single-box design, the architecture also remains accessible for centralized maintenance and ensures efficient cable management.

TABLE I COMPARISON BETWEEN USING 2 BOXES AND 1 BOX

Aspect	Previous 2-Box System	Current 1-Box System
Main Purpose	Separation of electrical and programming components to simplify monitoring and better protection	Minimum space and weight
Enclosure Type	IP67-rated	Waterproof
Space Usage	500 × 400 × 200 mm (electrical box) 400 × 300 × 170 mm (programmer box)	579 × 382 × 217 mm
Weight	± 2 kg (electrical box) ± 1 kg (programmer box)	1.72 kg
Wiring Complexity	Extensive wiring between functions, increasing clutter	Centralized wiring, fewer boards for simplified layout
Maintenance	Easier to isolate systems but longer time taken for interconnections debugging	Centralized but requires careful organization for efficient debugging

Mechanical Constraints	Dimension and stability issues from two separate enclosures	Improved integration due to compact, single-box design
------------------------	---	--

The previous electrical system heavily relied on multiple modular PCBs with independent microcontrollers, resulting in excessive wiring and redundant components. This configuration consumed significant space and increased the time required for debugging and maintenance due to its fragmented layout. To address this, the team redesigned the PCBs to consolidate functionality, reducing the overall number of boards while maintaining modularity. By using smaller power and microcontroller boards, the system achieves a more streamlined layout, allowing for faster fault detection and repair. Additionally, a Pixhawk extension board was introduced to centralize the primary connection for maneuvering directly to the main board. This redesign minimizes the need for long scattered wiring, improving system efficiency.

However, this redesign comes with certain trade-offs. Unlike the previous system, which

featured comprehensive monitoring of all components, the current design limits monitoring to active components only. While this change reduces processing power demands and simplifies the architecture, it sacrifices the real-time insights that were previously invaluable for troubleshooting and system optimization. Nevertheless, monitoring active components alone has proven sufficient for the system’s operational needs, as it prioritizes critical subsystems directly involved in mission execution. By focusing on the components that are actively engaged during operation, the design ensures efficient performance without overburdening the system with unnecessary data collection. This decision reflects a shift in priorities, emphasizing compactness and efficiency over full system visibility

TABLE II PCB COMPARISON

Aspect	Nala Proteus 2.0	Nala Ares
Boards Used	Power, Microcontroller, Emergency Power, Temperature Control, Ultrasonic, LED, Kill-Switch	Power, Microcontroller, Racquetball Puncher, Pixhawk Extension, ESC Holder, LED, Kill-Switch
Microcontroller	STM32F429ZI MCU, STM32F103C8T6 MCU, Arduino Nano	STM32F411CEU6 MCU, Arduino Nano
Special Boards	Dedicated kill-switch board and emergency board for safety management	Compact power and microcontroller board
Controller Setup	STM32 Microcontroller	Pixhawk for maneuvering and STM32 Microcontroller for external function
Monitoring	Fully monitored in real-time for all components	Limited monitoring focusing only on active components to reduce processing power and simplify the system
Weight and Size	Larger and heavier boards due to multiple redundant designs	Smaller, lighter boards optimized for compactness and reduced weight
Flexibility	Modular design but increased complexity due to redundant boards	Improved modularity with specialized boards while simplifying overall design
Wiring	Extensive wiring between multiple boards, leading to clutter and increased troubleshooting time	Centralized wiring with fewer boards, reducing clutter, interference, and easing debugging

### III. DESIGN IMPLEMENTATION

To ensure seamless collaboration across technical divisions, a decision-making framework was implemented. This framework enables continuous evaluation and refinement of electrical elements throughout the development and

implementation phases. By incorporating insights from the mechanical and programming divisions, the electrical architecture is designed to meet operational mission requirements while maintaining redundancy and reliability. The design framework diagram is illustrated in fig. 1.

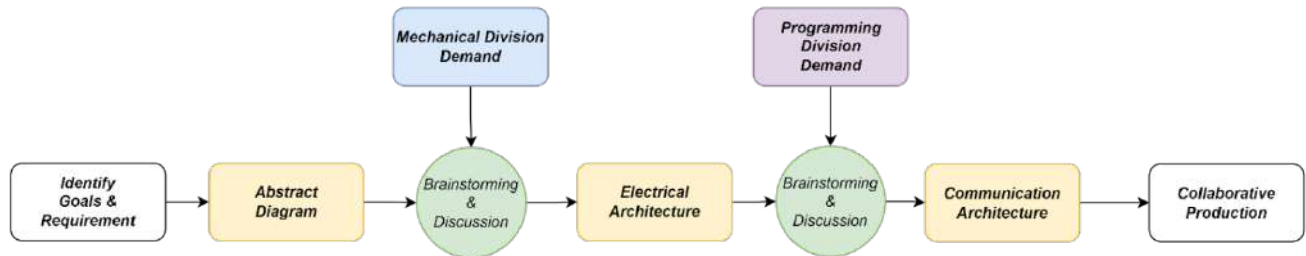


Fig. 1. Design framework solution diagram

Using this framework, the electrical system achieves transparent management at all stages of development. This approach integrates inputs from technical divisions, allowing for real-time evaluation and ensuring that the system’s architecture remains robust and adaptive.

#### A. Abstract System Design

In the early stages of formulating the solution, the design process began with the creation of an abstract diagram that integrates insights from last year’s solution with the objectives for this year’s mission. This initial visualization provides a framework to guide execution in subsequent stages by mapping out the system's overall structure.

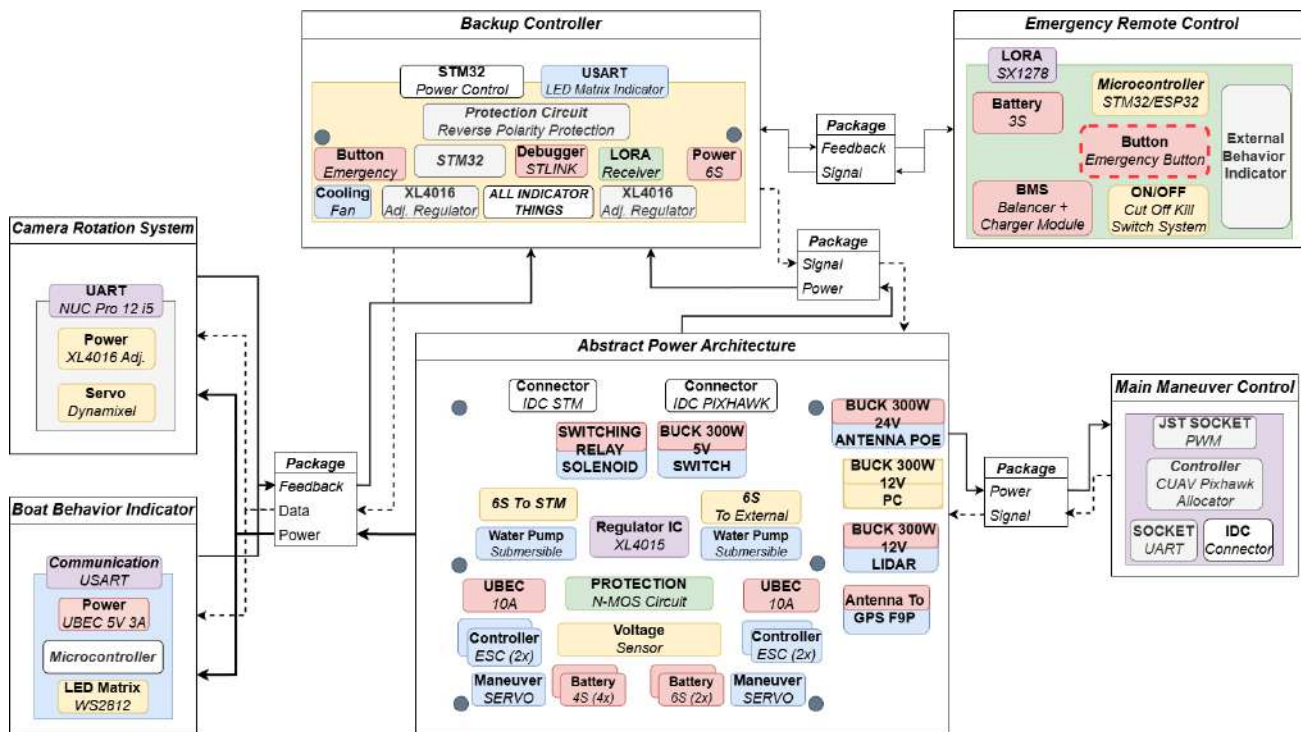


Fig. 2. Abstract design diagram

The abstract diagram [1] offers a comprehensive perspective of the electrical system, addressing key challenges such as space constraints and system complexity. By simplifying the relationships between components, it highlights opportunities for optimization, such as reducing physical size and minimizing the number of components. The design prioritizes modularity, enabling each subsystem to be developed, tested, and installed independently prior integrated into the larger system. Additionally, it ensures that the system can adapt to future competition demands and simplifies ongoing development.

**B. Power Architecture**

The Power Architecture Diagram provides a detailed overview of the power allocation to various ship components based on their priority and operational requirements. Each component is supplied with power according to its energy consumption. By applying principles of modularity and flexibility, the system ensures efficient and isolated power paths for each module. This approach minimizes interference between subsystems, reduces noise, and prevents power waste, allowing components to be replaced or modified without compromising the system's overall integrity.

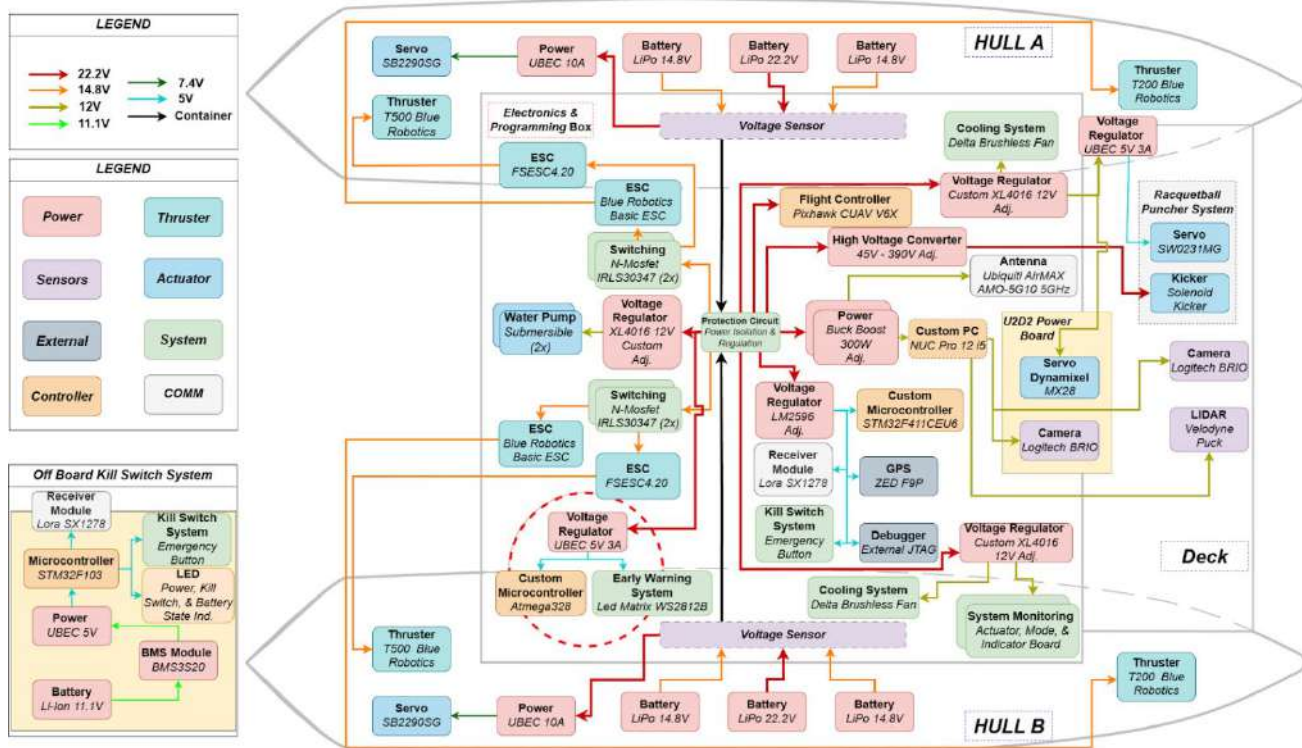


Fig. 3. Power architecture diagram

**C. Communication Architecture**

The Communication Architecture Diagram illustrates the data flow between components and the connectivity settings between subsystems. This architecture is designed to minimize the use

of cables and components by employing technologies that support fast and reliable communication, such as UART, USB, and UDP-based protocols.

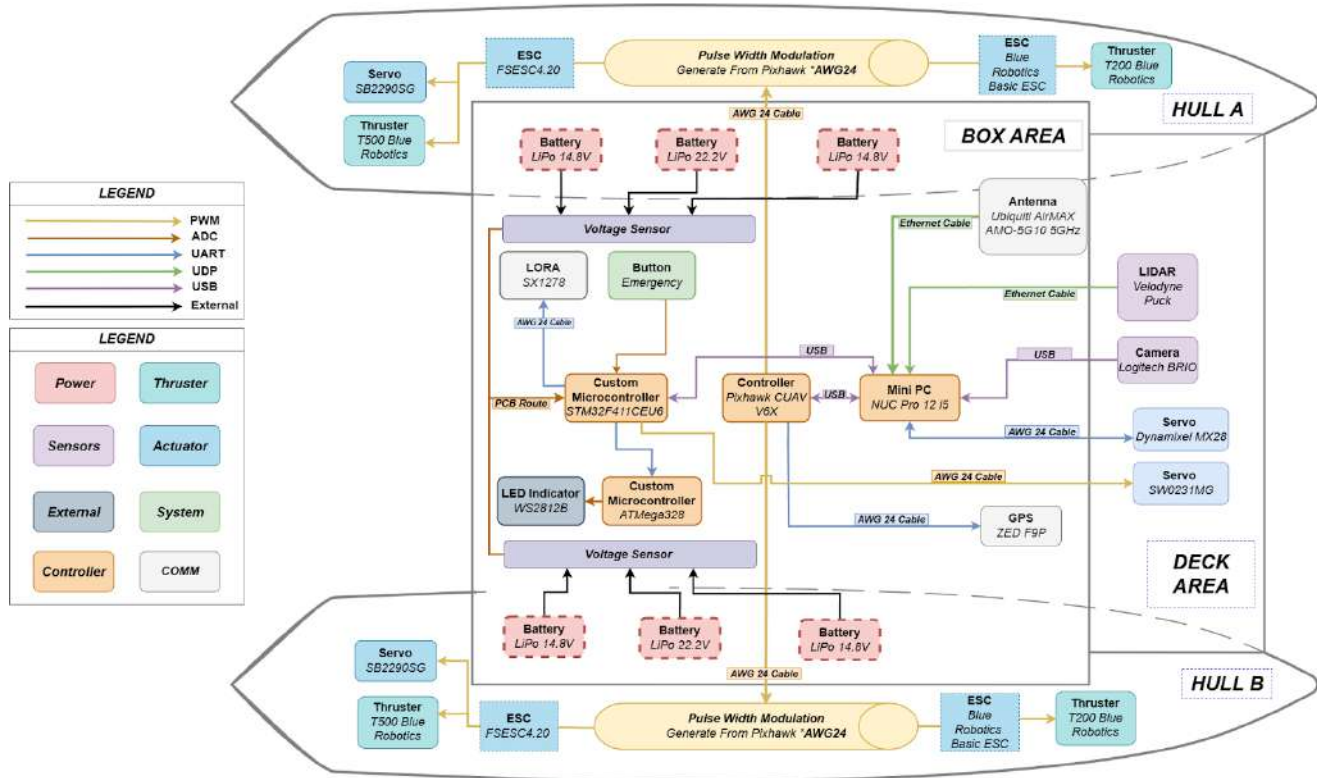


Fig. 4. Communication architecture diagram

Control communication is distributed across multiple microcontrollers, simplifying debugging and improving execution by delegating tasks to localized controls. This approach minimizes signal interference, enhances data exchange reliability, and facilitates troubleshooting during missions. Additionally, efficient communication settings ensure that all components interact with low latency, with controllers optimized to handle varying data widths based on subsystem requirements.

**D. Component Arrangement**

Component placement is crucial not only for efficient functionality but also for ease of maintenance and system reliability. The design approach prioritizes a clear visualization of component arrangement using orthogonal drawings of the ship's design. These drawings illustrate the placement of key electrical components within the spatial dimensions of the vessel. The major change in this year's design is the integration of all electrical and programming components into a single electrical box to minimize space usage and reduce weight.

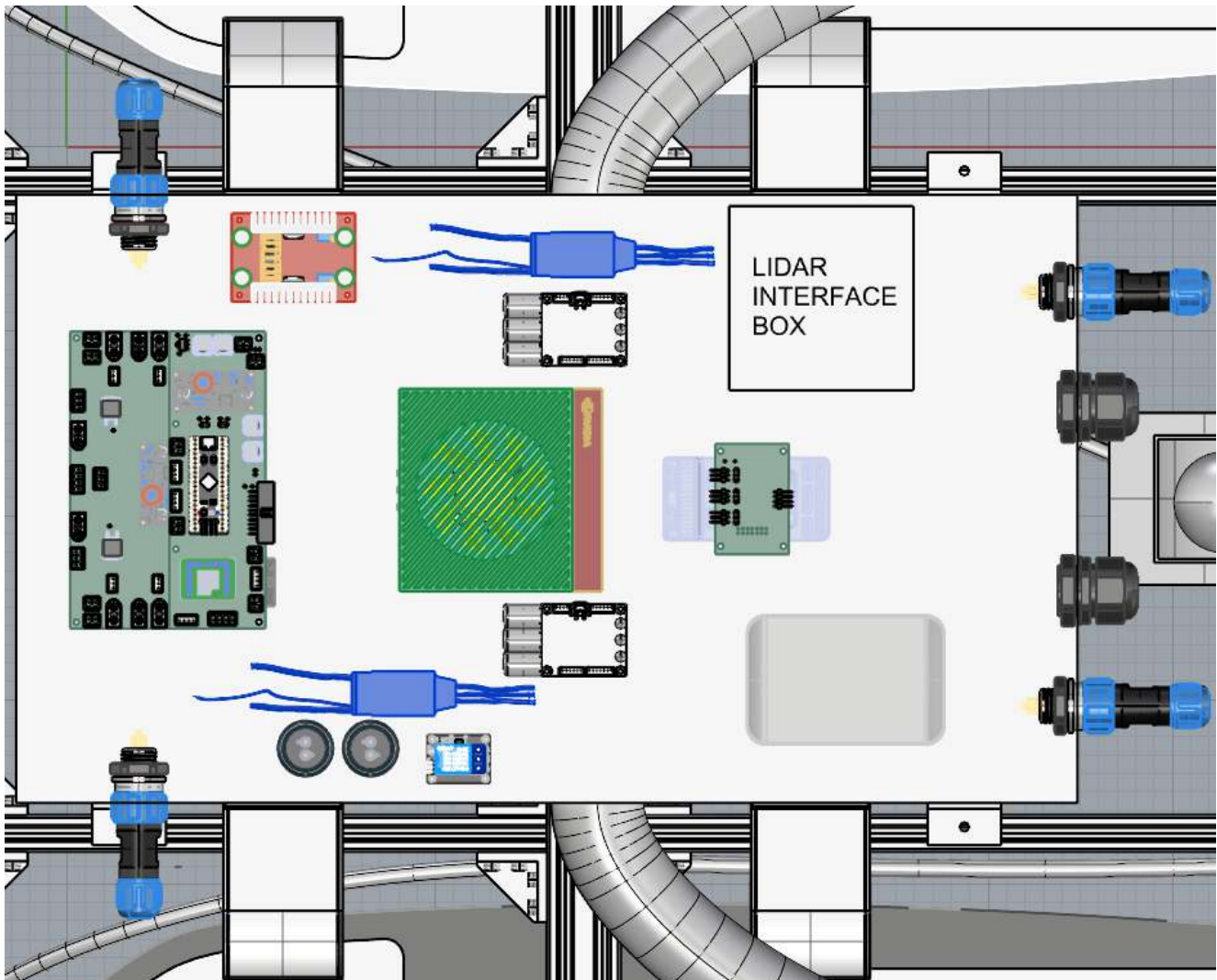


Fig. 5. Component arrangement

Fig. 5 shows the precise arrangement of major components such as the LiDAR Interface Box, PCBs, and other electrical systems, ensuring an optimal configuration. This arrangement reduces wiring clutter, making it easier to identify and troubleshoot faults during operations. This detailed visualization reflects the team's commitment to a collaborative and iterative design process, where each decision is evaluated and verified to ensure efficiency and reliability.

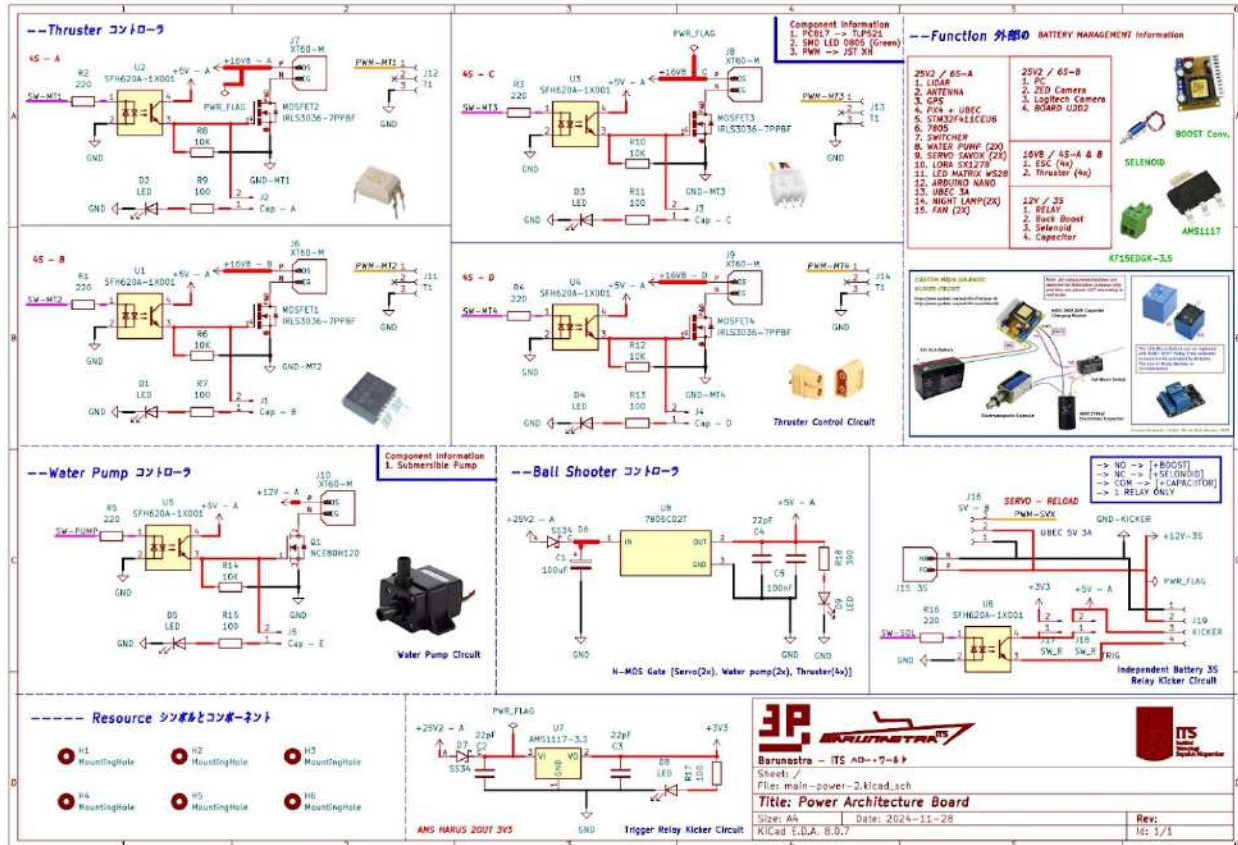
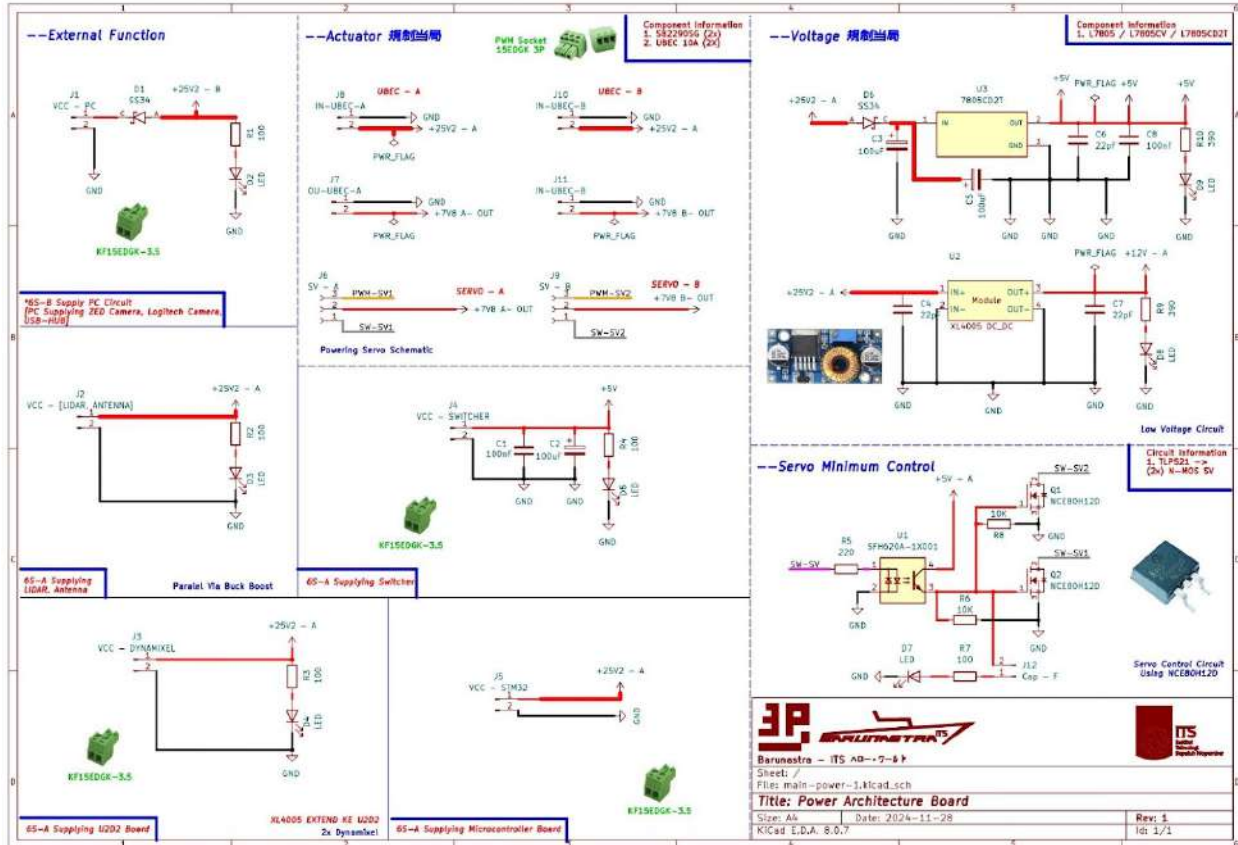
## IV. PRODUCTION PROCESS

### A. PCB Production

In RoboBoat 2025, Ares uses two main PCBs, namely the power and microcontroller boards, which handle critical functions such as thruster power allocation and protection circuits. Additionally, the system includes supporting PCBs like the ESC holder and LED indicator to enhance overall functionality. The production process involved several stages, including schematic design, layout optimization, and 3D modeling to visualize component placement and ensure compactness. The details of the main PCBs are outlined in the schematics below.



# 1) Power Schematics



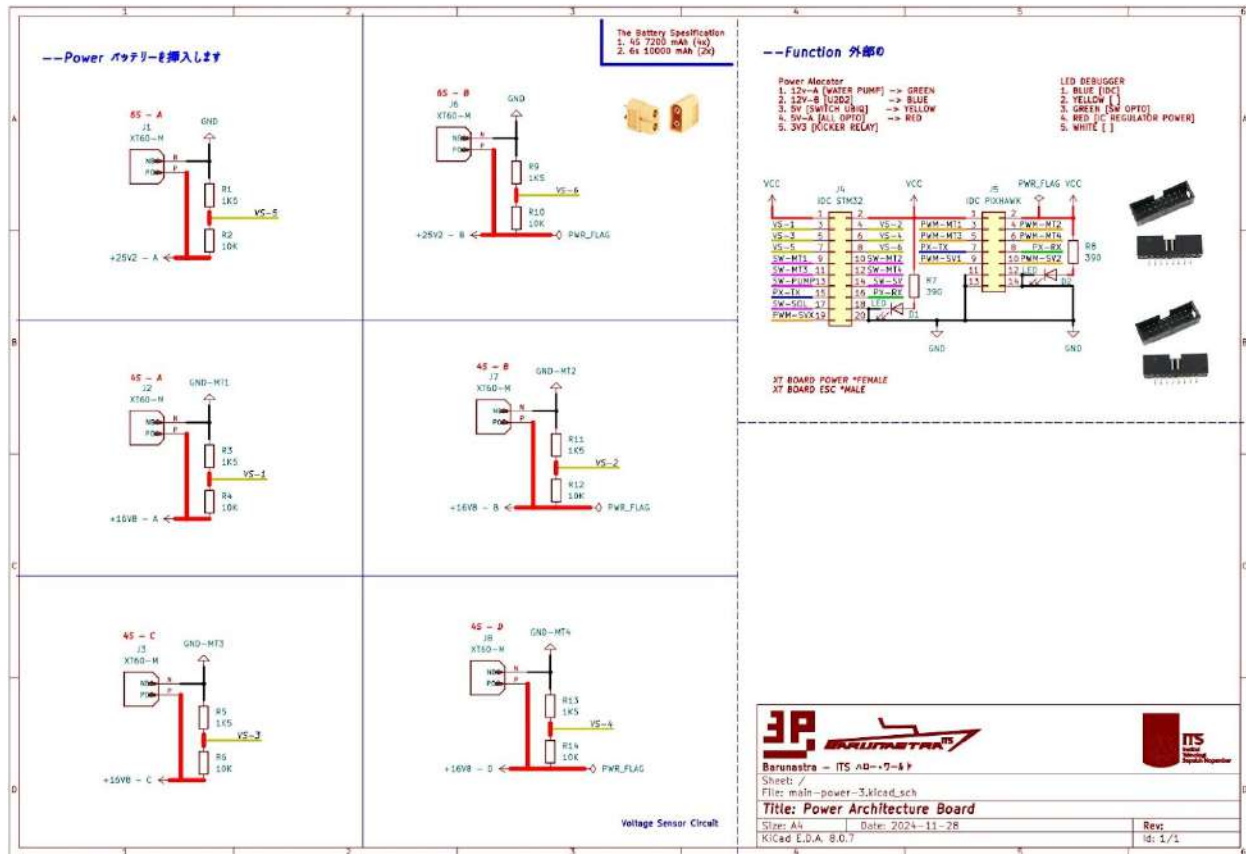


Fig. 6. Main power schematics

The schematic incorporates various main functions, including power input, converters, ESC control, pumps, and the ball launcher. It also includes analog-based sensors and indicators to support debugging processes, such as identifying component damage or system malfunctions. To simplify malfunction detection, debugging indicators have been integrated into each MOSFET circuit, with a pin jumper serving as the display. This schematic is designed with clear

annotations and labels, a text-based power distribution workflow, and visually organized component placement. These features ensure that the system is straightforward to understand, operate, and troubleshoot during testing and missions. The 3D view of the PCB below highlights the arrangement of key components, such as the MOSFETs, connectors, and debugging indicators, offering a detailed perspective of the board's design.



Fig. 7. Power PCB

2) Controller Schematics

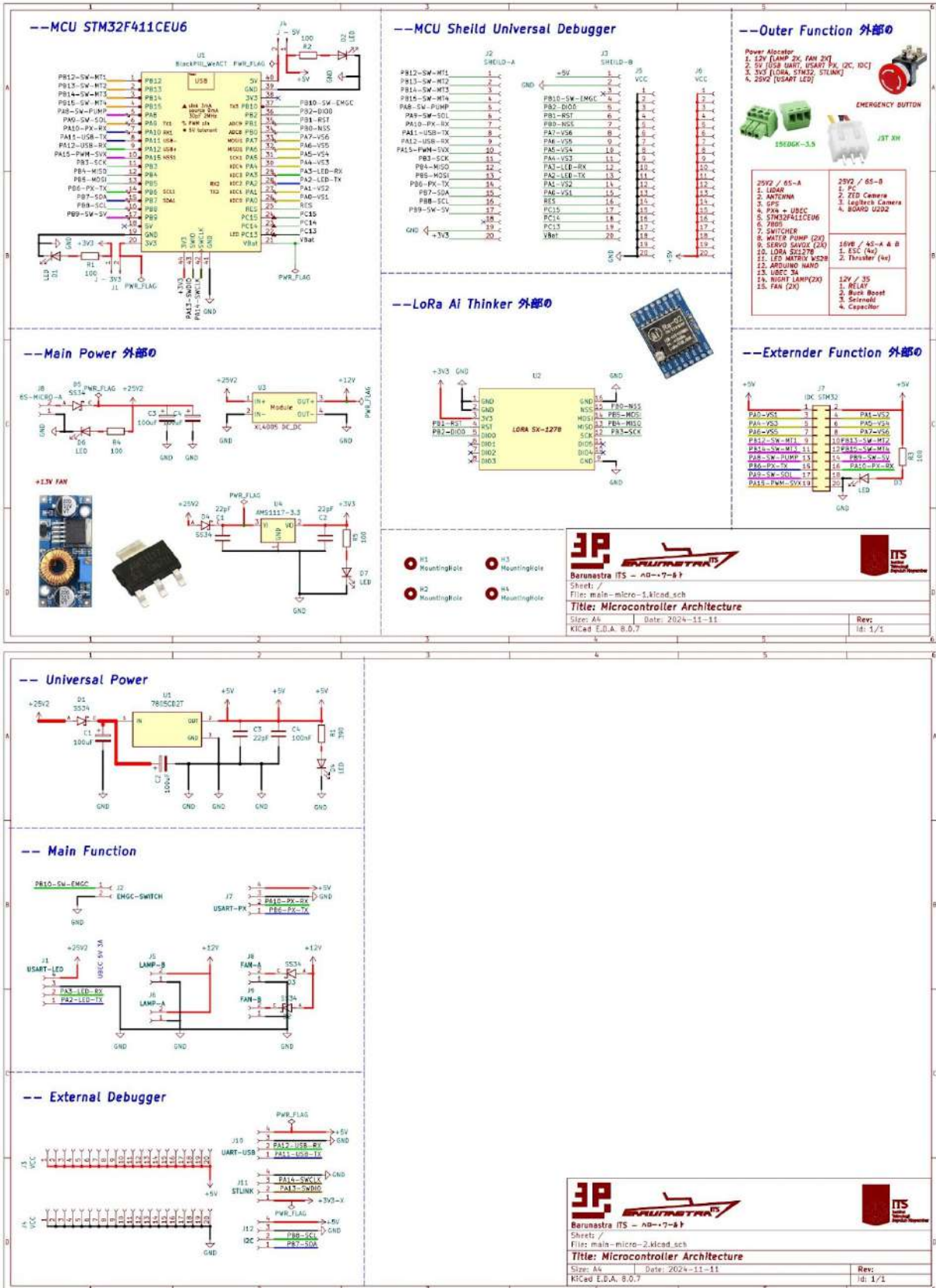


Fig. 8. Controller schematics

The microcontroller board for this competition has been designed to be smaller and more efficient than in previous years. This improvement was achieved by dividing the system into two main controllers: Pixhawk and STM32F411CEU6. Pixhawk serves as the primary controller, managing ship maneuvers, processing GPS data, and transmitting information to the Mini PC. STM32F411CEU6 functions as the secondary controller, handling indicators, protection circuits, and voltage sensor data processing.

The STM32F411CEU6 controller PCB focuses on minimizing system size while maintaining efficiency. Compared to the STM32 NUCLEO

F429ZI used in the previous RoboBoat 2024, the new division of control functions simplifies debugging and enables a more compact PCB design. Technically, the controller schematic integrates key components, including power management for the STM32 microcontroller, an external debugger, and safety communication features such as LoRa for the Kill Switch System for local cut-off functions. These features are designed to mitigate malfunctions in specific systems. The 3D visualization below highlights the layout of critical components, ensuring optimal functionality and accessibility.

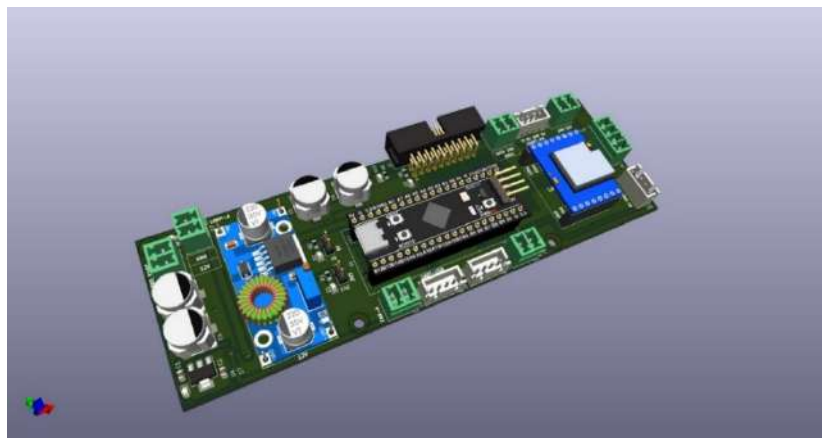


Fig. 9. Microcontroller PCB

**B. System Assembly**

The production and assembly of the Ares electrical system began with collaborative design discussions between the Mechanical and Electrical Divisions. While the hull and frame were pre-produced by the Mechanical Division,

the placement of key components like LiDAR, cameras, ejection systems, and water pumps required joint planning to ensure efficient placement and system compatibility. The process involved three main stages: design review, placement design, and assembly.

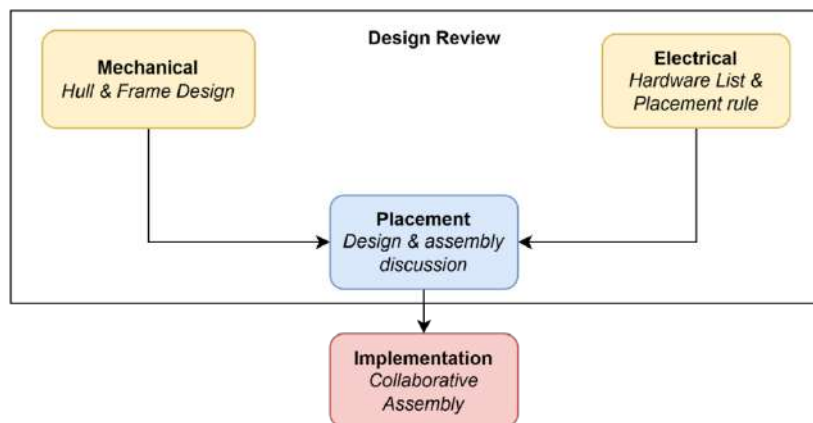


Fig. 10. Assembly diagram process

supply consistent and interference-free power. Calibration during assembly included aligning servo angles with thrusters to optimize maneuverability, while spatial checks ensured sufficient room for components like the camera and delivery system. Quality control involved inspections to confirm components matched the initial design, with wiring standards such as spiral cables applied for arrangement and easier troubleshooting. Following assembly, initial testing in a makeshift testing pool validated system functionality before progressing to larger-scale trials. The entire process spanned three days.

### V. CONCLUSION

The electrical system for Ares has been designed to address the key challenges identified in Proteus

2.0. By simplifying system architecture, consolidating PCBs, and optimizing power and communication layouts, the design aims to improve space usage and streamline functionality. Key improvements, including the single-box configuration, enhanced modularity, and robust quality control, ensure the system adaptability to mission requirements while being reliable and easy to maintain. With these adjustments, the electrical architecture of Ares is well-prepared to support the team's goals in RoboBoat 2025.

### VI. REFERENCES

[1] A. S. Naik, "Abstracting the architecture design system to create new applications," *Engineering and Technology Journal*, vol. 9, no. 6, Jun. 2024, doi: 10.47191/etj/v9i06.14.

# Appendix G.1: Test Plan and Result Communication and Safety Test

Arundaya Pratama Nurhasan, M Andi Abdillah, Farrel Rahmadany Akbar, Jilan Nabilah Dikairono

## I. COMMUNICATION TEST

### A. Scope

This test aims to evaluate which component has the ideal *communication range* and meet the needs of RoboBoat 2025. The first test focused on evaluating the radio controller, comparing the Radiomaster TX16S Mark II to the previously used Radiolink AT9S Pro to assess improvements in range and interference resistance for reliable communication between the operator and the ASV during missions. The second test involved a comparison between the airMAX AM5G19 120° sector antenna and the PowerBeam 5AC 300 to evaluate their range and interference resistance in scenarios requiring long-distance data transmission or operations in environments with potential signal obstructions.

### B. Schedule

Communication Testing was conducted in the the second week of December 2024, coinciding with the component selection process. This test took approximately two days to get the results.

### C. Resources and Tools

This test requires a comparison of the data sheets for each device. The first comparison is between two radio controllers: Radiolink AT9S Pro and Radiomaster TX16S Mark II. The Radiolink controller was paired with the R12DS receiver, while the Radiomaster controller was paired with the RP4TD receiver.

TABLE I REMOTES DATASHEETS COMPARISON

Parameter	Radiolink AT9S Pro	Radiomaster TX16S Mark II
Channels	10 Channels	16 Channels
Protocols	Radiolink Proprietary protocol	Multi-Protocol
Compatibility	Limited to Radiolink receiver	Supported various receiver brands
Display	2.8-inch monochrome LCD	4.3-inch color touchscreen
Firmware	Proprietary firmware	OpenTX or EdgeTX
Gimbals	Standard gimbals (plastic or metal options)	Hall-effect gimbals (precise and durable)
Customization Options	Limited	Extensive (switches, trims, screen layout, etc.)
Signal Range	Up to 2.5 km	Up to 3-5 km (varies with receiver/module)
Battery Type	Built-in 7.4V LiPo (can be replaced manually)	External 7.4V LiPo or 18650 batteries
Sim Support	Yes, via trainer port	Yes, with USB-C for direct simulator use
Weight	~600 g	~750 g (varies with battery type)

The second comparison is between the AM5G19 120° Sector antenna and the PowerBeam 5AC. Datasheet of both devices is listed at Table II

TABLE II ANTENNA DATASHEETS COMPARISON

Parameter	AM5G19 120° Sector	Powerbeam 5AC 300
Gain	19 dBi	22 dBi
Beamwidth	120° (horizontal) x 5° (vertical)	Narrow-focused (6° beamwidth)
Max Range	Wide-area coverage (short to mid-range)	Long-range, focused connection
Dimensions	700 x 145 x 78 mm	362 x 267 x 184 mm

Both data link devices were paired with the Rocket 5AC, which was already connected to the AMO5G10 antenna. Testing parameters such as

distance, signal strength, and latency can be monitored on Ubiquiti's dashboard, as shown in figure 1.

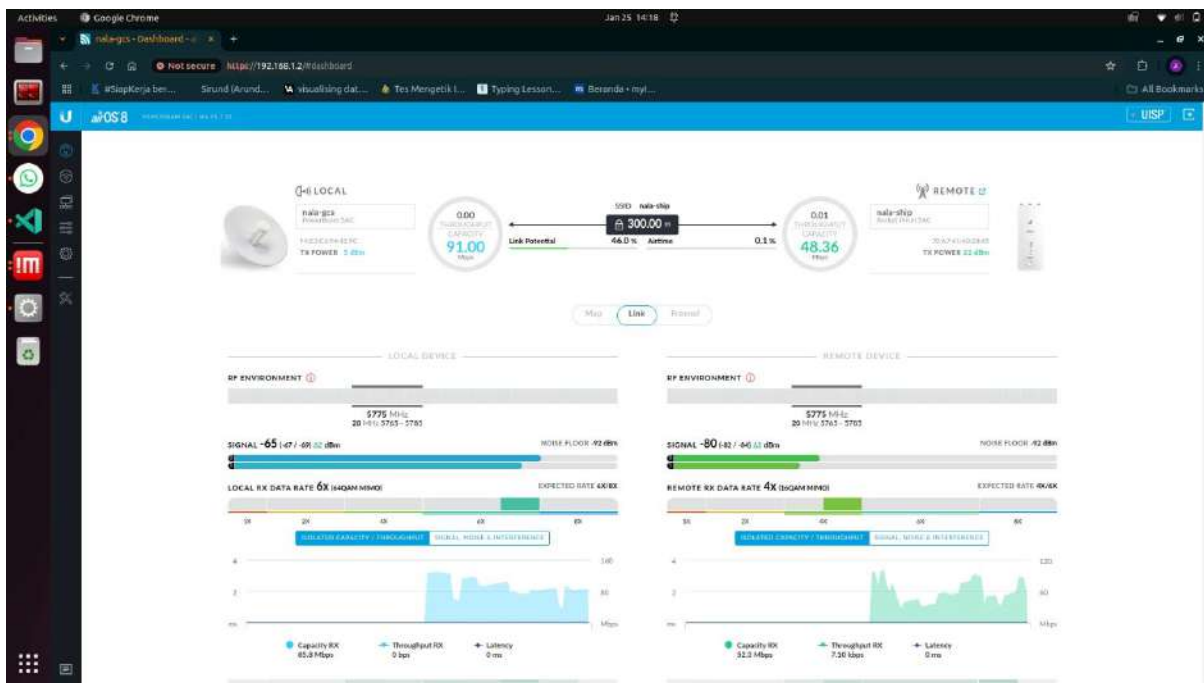


Fig. 1. Ubiquiti dashboard

**D. Environment**

The radio controller testing was conducted on a cloudy day in a spacious area surrounded by tall trees. The testing involved measuring the maximum distance at which each remote maintained a connection with its respective

receiver before disconnecting. The Data Link antenna testing was carried out using the same environment as the radio controller testing. The testing for these devices was conducted independently, unlike the radio controller testing, which could be performed simultaneously.



Fig. 2. Ground testing antenna (left) and Antenna distance testing (right)

**E. Risk Management**

Risks that can occur include RF interference, environment, faulty equipment, potential circuit damage, and human error.

**1) Health and safety risks**

High-gain antennas have the potential to emit elevated levels of radio frequency (RF) radiation, particularly during close-range testing. It is essential to ensure adherence to established RF exposure limits, which can be achieved by performing accurate calculations to determine the safe distance for testing. To minimize the risk of excessive exposure, our teams maintained a safe distance from the transmitting antenna during testing activities.

**2) RF Interference**

The outdoor testing conducted outside the camp

s area may lead to RF interference. Frequencies from other Wi-Fi transmitters, television stations, and other signals can affect the accuracy of this testing as they may disrupt the connectivity between the two devices. To mitigate this, the testing environment was carefully selected in a less congested area with minimal RF interference.

**3) Environmental factors**

Environmental factors, such as weather conditions, physical obstructions, and multipath reflections, can introduce variability and inaccuracies in test results. To mitigate these risks, the test was conducted under controlled and repeatable conditions whenever feasible. Additionally, the weather conditions and the surrounding environment during testing were documented to account for any potential influences on the result

**F. Result**

TABLE III REMOTE TESTING RESULT

Parameter	Radiolink AT9S Pro	Radiomaster TX16S Mark II
Screen Brightness	Dim	Bright
Battery life	13 Hours	8 Hours
Max Range	1.1 km	2.3 km

The Radiolink AT9S Pro has a 62.5% longer lifespan, which is due to different specifications and screen conditions, however, the operating

range of the Radiomaster TX16S Mark II is twice as long. The need for operational range makes the Radiomaster TX16S Mark II more suitable for use

TABLE IV ANTENNA TESTING RESULT

Parameter	AM5G19 120° Sector	Powerbeam 5AC 300
Max Range	1.5 km	3.2 km
Latency at 1Km	0.097 ms	0.083 ms
Signal Strength at 1Km	-86 dBm	-81 dBm



Both data link antennas showed similar latency at a 1 km range, but the signal strength differed significantly, with the PowerBeam 5AC 300 being 5 dBm stronger than the AM5G19 120° Sector. This logarithmic difference indicates the PowerBeam is approximately three times stronger. Additionally, the PowerBeam offers greater range, making it the preferred choice.

**II. SAFETY TEST**

**A. Scope**

This year's long range kill switch focuses on LoRa utilization which will operate interchangeably between transmit and receive. This switch is crucial since it directly affects the hardware capability for responsive long-distance communication with minimum delay. The testing aims to identify the optimal combination of spreading factor (SF), bandwidth, and coding rate to minimize delay and ensure a responsive system for emergency commands.

**B. Schedule**

The kill switch testing was done on January 20<sup>th</sup> when the PCB has been printed and all components had been installed.

**C. Resources and Tools**

The LoRa SX1278 datasheet was used as guidance to understand its technical specifications and limitations. STM32 Cube IDE was used to configure and program the microcontroller. The required resources and tools are listed in Table V

Tools	Function
LoRa SX1278 module	Wireless communication module for long range
STM32F103C8T6 (BluePill)	Microcontroller for managing system communication and operation
Li-Ion 11.1V 18650 battery	Power supply
BMS 3S module	Monitoring and protecting the battery
Kill Switch PCB	Custom PCB for integrating STM32 and LoRa
Main Power PCB	Primary system to be disabled by the kill switch
Emergency button	Manual input to trigger the kill switch system
Buzzer	Audio indicator for system feedback and warnings
Container	Physical housing for protecting and organizing components

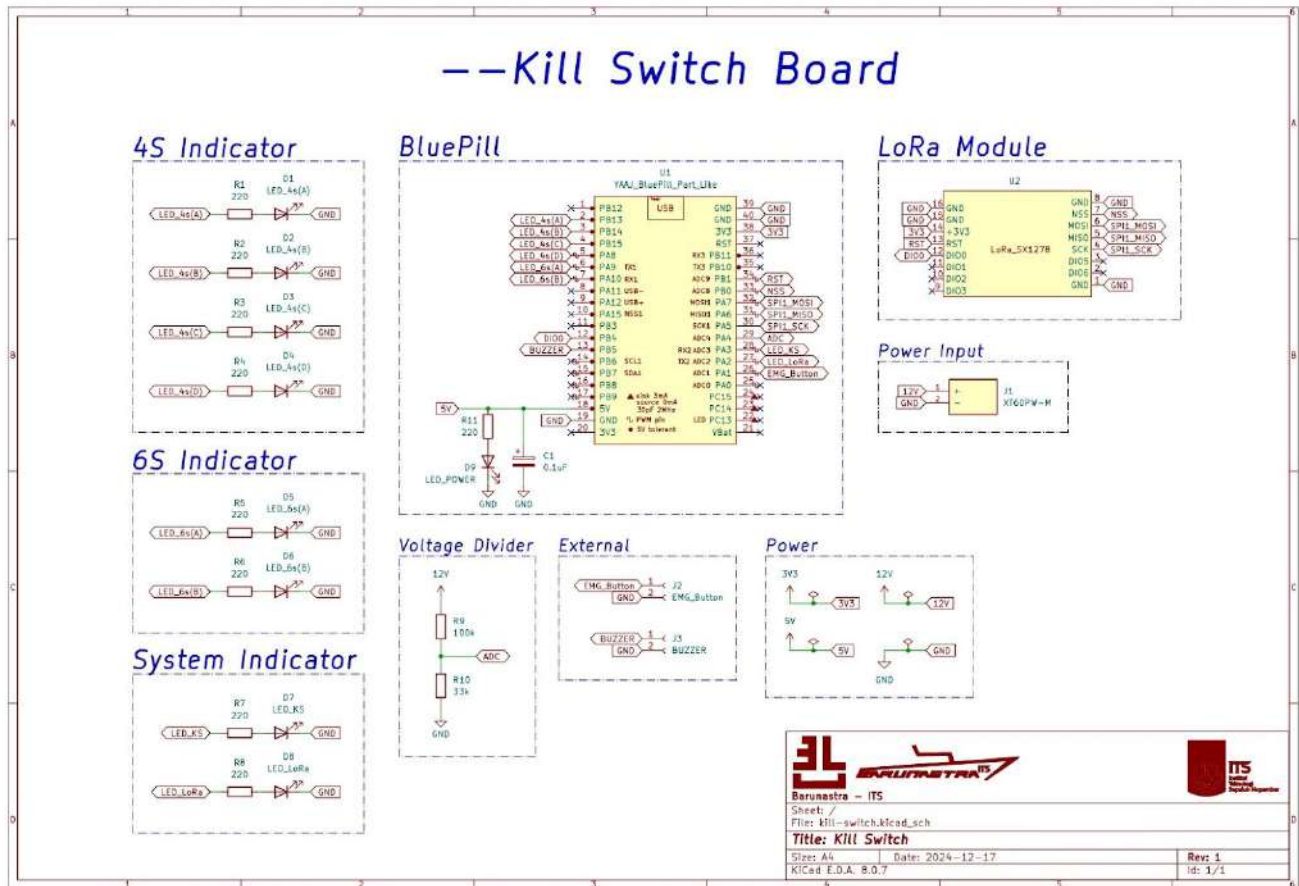


Fig. 3. Kill switch schematics

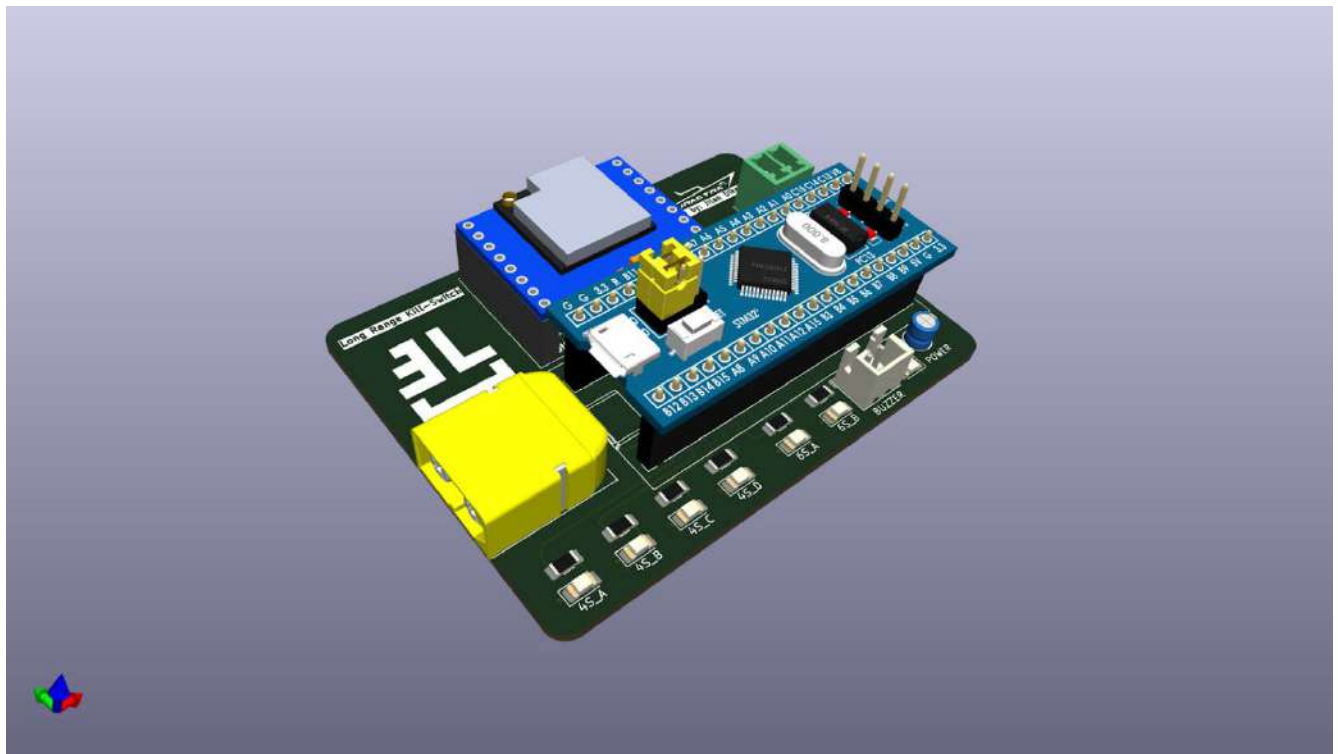


Fig. 4. Kill switch board

**D. Environment**

The testing was conducted in closed areas where the LoRa module sent and received data continuously to the main board. The main board’s LED indicator was used to verify communication. It remained on during normal operation and turned off when the kill switch button was pressed, signaling that the system had entered emergency mode. The frequency configuration was set at 433 MHz with the power output set to a maximum of 20 dBm. Various combinations of parameters, including bandwidth, spreading factor, and coding rate, were systematically tested to determine the optimal configuration that minimized communication delay while maintaining reliability.

**E. Risk Management**

**1) System Delay**

Switching between transmit and receive modes, along with executing other tasks such as managing

the LED and buzzer indicators, could increase system delay. To mitigate this, FreeRTOS was implemented to handle multitasking efficiently, minimizing delays and ensuring responsiveness during emergency situations.

**2) Signal Interference or Loss**

LoRa signal reliability is crucial for the kill switch system. To reduce the risk of signal loss or interference, the power supply voltage and current for the LoRa module were carefully monitored and verified during testing to ensure stable operation under various conditions.

**F. Result**

Testing is done by trying several configuration combinations to see the resulting delay of the 3 bandwidth (125 kHz, 250kHz, 500 kHz).

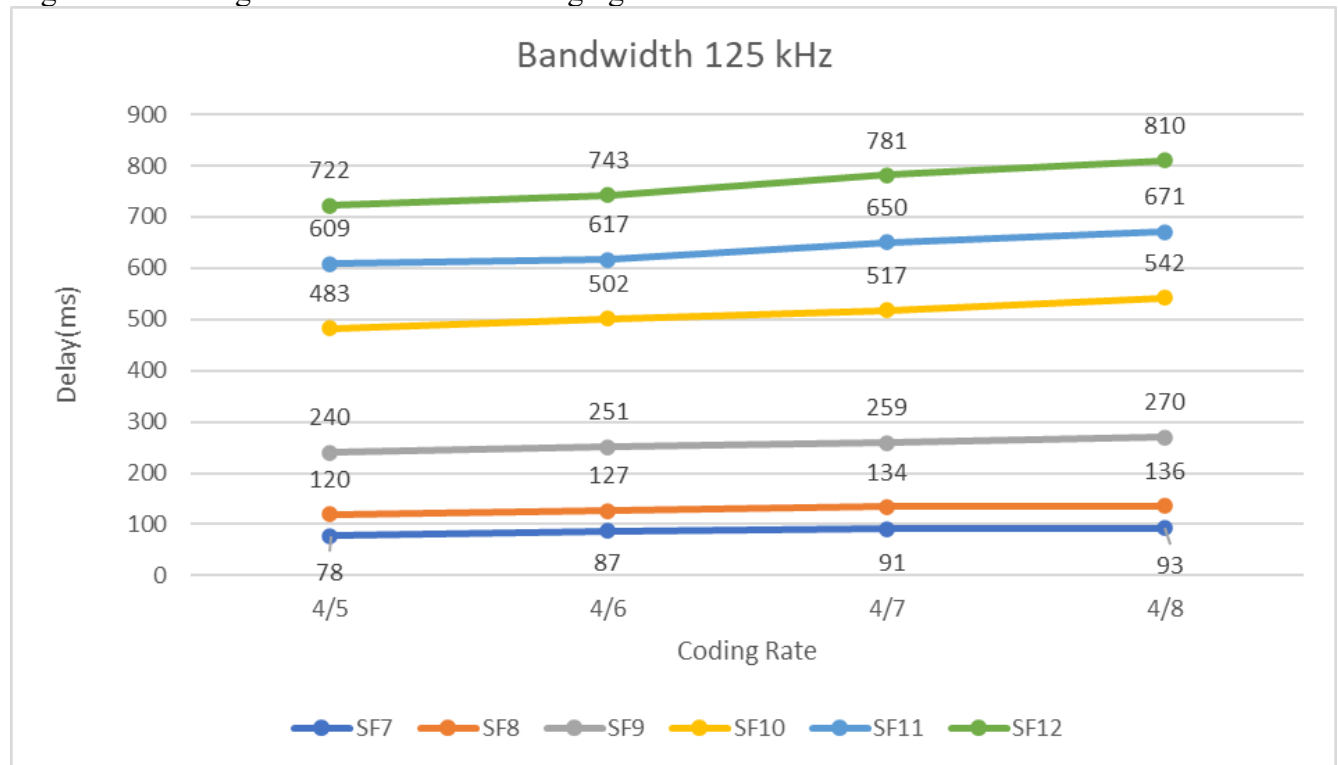


Fig. 5. Delay comparison on bandwidth 125 kHz

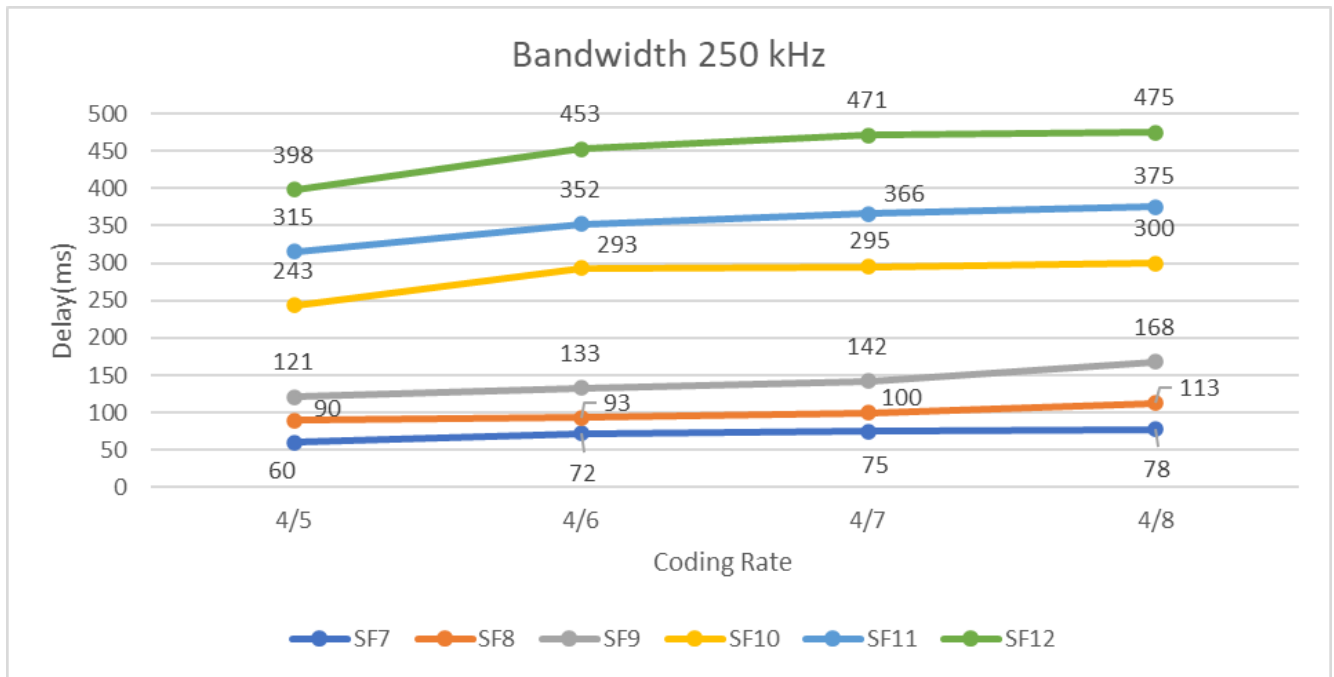


Fig. 6. Delay comparison on bandwidth 250 kHz

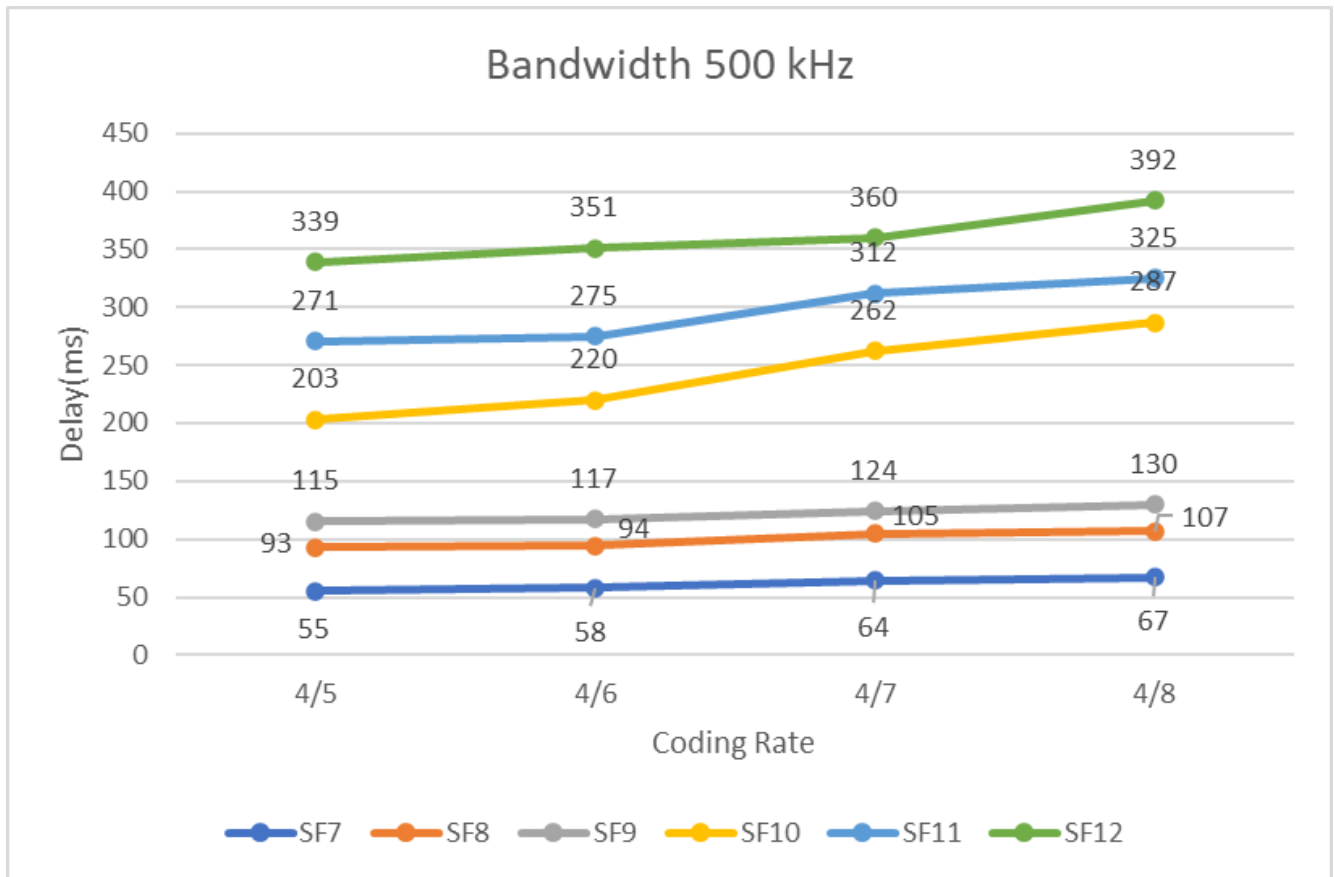


Fig. 7. Delay comparison on bandwidth 500 kHz

The results demonstrate that larger bandwidth results in lower delays for all SFs, and a smaller SF minimizes delay due to faster data transmission. On the other hand, higher coding rates increase delays as redundancy in communication increases. Among the configurations tested, SF7 produced the lowest delay, achieving 55 ms on 500 kHz and 60 ms on

250 kHz, both at a coding rate of 4/5. While 500 kHz offers the minimum delay, 250 kHz was chosen for its balanced performance, ensuring longer lifespan within hardware specifications. This configuration meets the requirements for responsive and reliable communication in critical operations for the kill switch system.

# Appendix H: Trial Arena

Muhammad Fajri Romadlon, Muhammad Rizki Alfa Thaaariq, M Farras Rheza Firmansyah, Dionisius Vito Aubin, Sigmayuriza Senaaji Rasendria, Batara Haryo Yudanto, Davin Abhinaya Briet, Dipta Mulya Suryono

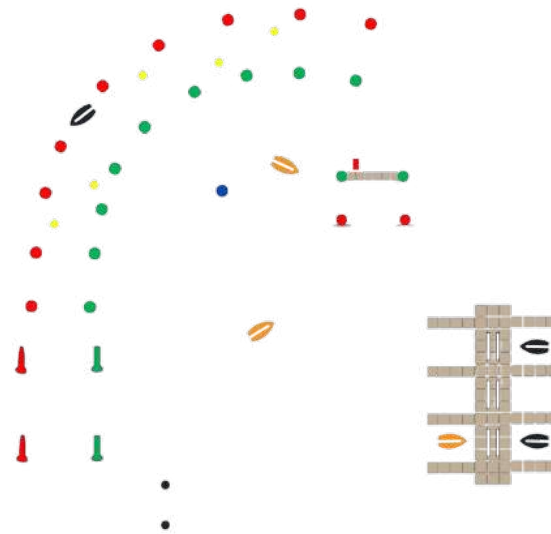


Fig. 1. RoboBoat 2025 arena  
Source: RoboBoat 2025 handbook

## I. INTRODUCTION

An arena mimicking the RoboBoat task challenges is important for testing Ares' performance in the real environment. Besides having a clear image of the competition condition in Sarasota, Florida, USA, this arena can also be used to experiment with all possible strategies to get the highest point possible during the time stated in the competition regulation. Therefore, Barunastra's mechanical division built all the arena by themselves manually to reduce the cost. All arena was produced using secondhand or used materials. The tasks arena we built are Navigation Channel, Mapping Migration Patterns (Follow the path), Treacherous Waters (Docking), Race Against Pollution (Speed Challenge), Rescue Deliveries (Object and Water Delivery), and Return to Home.

## II. REQUIREMENT, DESIGN, MATERIAL SELECTION, AND PRODUCTION

Prior producing the arena, we drafted the concept of all arena items, including the material that would be used. The detailed draft for each mission is detailed in subsequent sections below.

### A. Task 1 - Navigation Channel

In this task, ASV should demonstrate the basic autonomous control and sensing. The ASV should navigate through two pairs of red and green buoys with the determined distance. Therefore, we planned to make our own buoy with the concept shown below

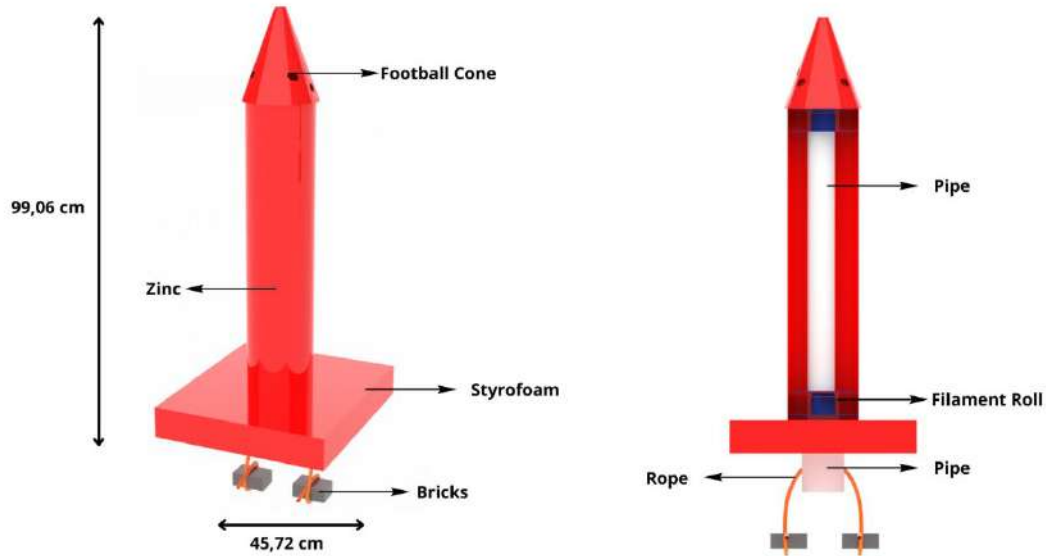


Fig. 2. Navigation channel buoy breakdown

The buoy pillar was made by using several unused filament rollers and covered with a zinc sheet that was tied using wires. The pillar is glued to the base using a glue gun with an offset position below the base. The base uses square Styrofoam to get buoyancy force for the buoy. The buoy was painted following the color regulation. For the red buoy, the football cone is attached on the topside. The bottom of the pillar is tied with a rope to the brick for the anchor. This arena production was done for a week to make four complete buoys.



Fig. 3. Buoy installed in water

**B. Task 2 – Mapping Migration Patterns (Follow the Path)**

This task requires ASV to follow the route while avoiding the obstacles which are buoys (red, green, and yellow) and stationary vessels placed within pathways. While maneuvering through all pathways, ASV should also count the number of yellow buoys and reports to the judges.

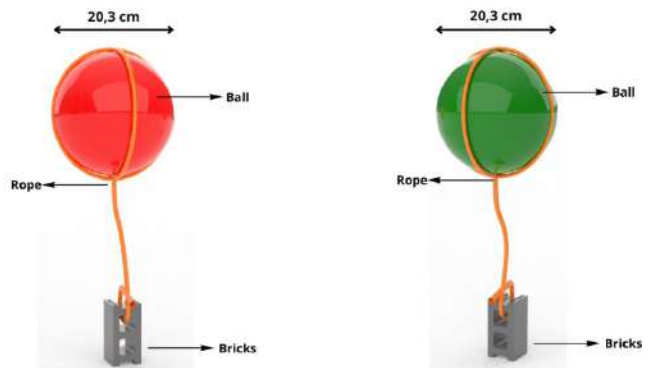


Fig. 4. Buoys breakdown for follow the path mission

We made this buoy by using a cheap plastic ball, rope and glue to make the buoy. The ball was tied using a plus knot and glued to the ball using a glue gun. The ball buoy was painted using a spray gun which color refers to the rule. The ball’s anchor uses a brick attached by a rope. This arena was made for two days to complete task elements.



Fig. 5. Buoy installation for follow the path

**C. Task 3 – Treacherous Waters (Docking)**

ASV should demonstrate the ability to sense, locate, and maneuver into the empty docking bay correctly according to the color or shape decided. Some docking bays will be occupied by stationary vessels. If the shape or color decided is occupied with stationary vessel, the ASV should locate and

enter another bay with the same color or shape which is not occupied by any vessels.

This year's ship dock has a very large size to achieve detailed mission simulation. We designed it to follow the mission rule, ensuring ship safety while colliding, and its long live requirements. Main material for building the dock is a styrofoam box because it gives enough buoyancy force. Both inside and outside the box are attached with plywood to strengthen the wall for collision. The lid of the box is also attached with a wooden plate below to prevent water leaking inside. The construction is supported with 5-inch pipe for a flexible connection to avoid fracture. The outside of the box was given three mm plywood to protect the box when it collided with the ship.

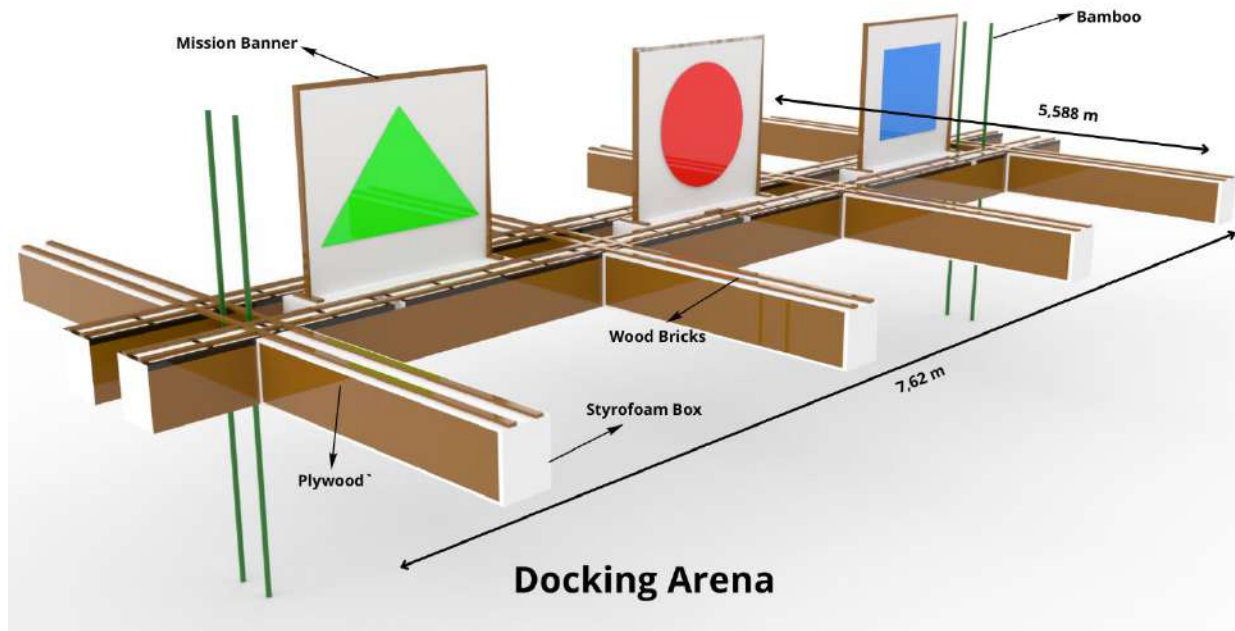


Fig. 6. Docking arena breakdown

For stronger construction, on the top of the docking was given meranti wood tied using wires to resist hogging and sagging moments. Every wire connection was glued using a glue gun to strengthen the connection and prevent water leaks. The middle part of the dock was also constructed using wood as a base of the banner frame. The Banner hangs on the frame that was made by 1/2 inch pipe. The dock installed using bamboo as the dock's anchor. This arena took the longest time to build, which was two weeks until it was fully built.



Fig. 7. Docking arena installed in water



**D. Task 4 – Race Against Pollution (Speed Challenge)**

ASV should demonstrate the hull form efficiency along with its propulsion system. Once ASV enters a holding bay and observes a light panel, the light will change from red to green after a random interval indicating the start of the race clock. Once started, ASV should quickly pass through gate buoys, circling around blue marker buoy, and exits back through the same gate buoys.

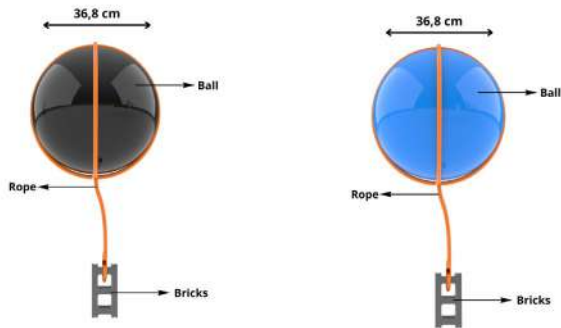


Fig. 8. Speed challenge ball breakdown

We made this arena like Mapping Migration Patterns (Follow the Path), but we used a bigger ball. For the speed challenge, the platform was built like a docking mission. The light indicator is using LED matrix, and the construction was built

using the 1/2 inch pipe and aluminum plate as its bracket. This arena took two days to be built.



Fig. 9. Speed challenge installed in water

**E. Task 5 – Rescue Deliveries (Object and Water Delivery)**

ASV should demonstrate the ability to locate the stationary vessels and deliver the object or water according to the marker carried by the stationary vessel. If the marker is black triangle shape, ASV should blast a steady and visible stream of water to the black triangle shape for at least 3 seconds. However, if the marker is black plus shape, ASV should launch a ball, either striking the plus sign or simply dropping the ball into the hull of the vessel.

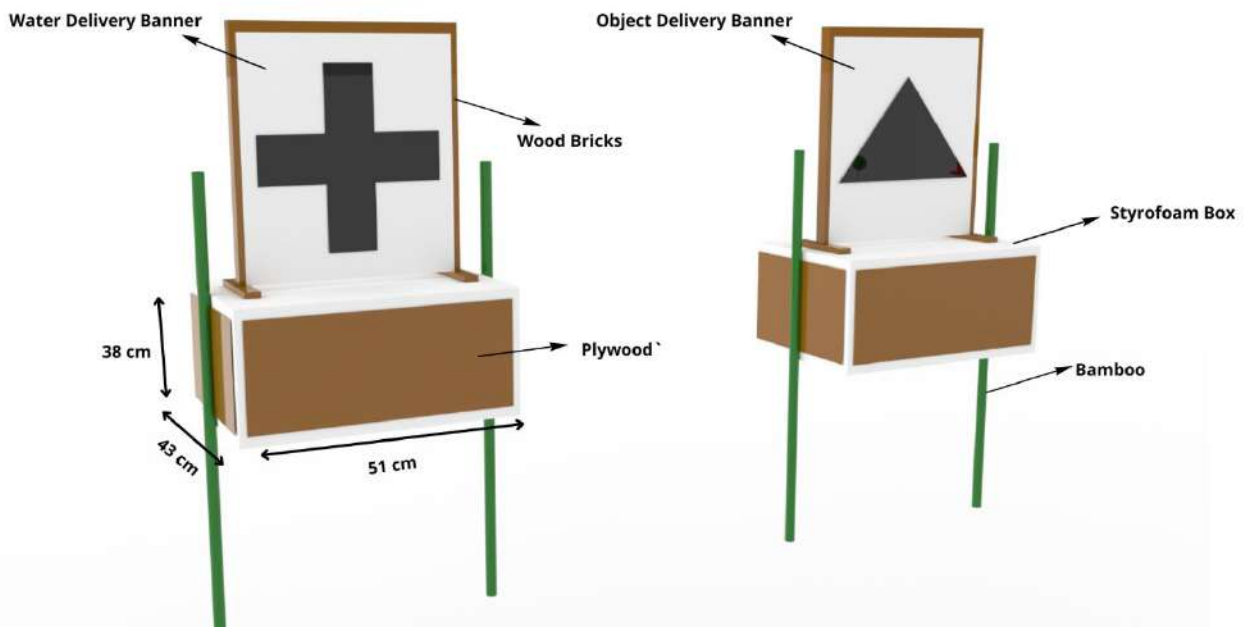


Fig. 10. Water and object delivery arena breakdown

On this mission, we used a styrofoam instead of vessel to carry the banner. The banner frame was made of wood and assembled with screw joints. We use bamboo as its anchor to resist the rolling moment. It needed three days to make three water deliveries and three ball delivery objectives.



Fig. 11. Object delivery arena installed in water

### ***F. Task 6 – Return to Home***

This task uses the same methods as follow the path's task which is the ball tied using rope and glued to the ball anchored using stone bricks. It takes one day due to the less elements it needs.

### **III. CONCLUSION**

All arenas have been created to mimic the RoboBoat 2025 arena which will be completed in Florida, USA. By utilizing the local campus lake, all arenas could be installed in accordance with the dimensions determined by RoboBoat 2025, and the arena is ready to be used anytime for in-water testing of ASV.



Fig 12. Arena installation overview

# Appendix H.1: Test Plan and Result

## On-Water Testing

Muhammad Fathoni Al Fadh, M Farras Rheza Firmansyah, Davin Abhinaya Briet, M Andi Abdillah, Jilan Nabilah  
Dikairono, Arundaya Pratama Nurhasan

### I. SEAKEEPING ANALYSIS

#### A. Scope

To determine the stability and response of the ship, the *seakeeping* analysis was conducted to Ares' hull with full load condition in wave pool simulation to get a sample of the ship motion in real situation. This test also determines the effectiveness of the *station-keeping* algorithm to maintain the position and adjust heading.

#### B. Schedule

This analysis was conducted on January 22<sup>nd</sup>, 2025, after all the components and system are fully installed on the ship. This analysis was carried out in one day for a total of seven hours at the National Hydrodynamics Research and Innovation Agency (BRIN).

#### C. Resources and Tools

This analysis was carried out at wave pool simulation with a fully equipped ship and the rope was attached on the ship for safety and to prevent it from damaging all the laboratory's equipment. Furthermore, we set the *station-keeping* algorithm for the seakeeping analysis test. While the simulation was started, there were some people needed to support the simulation and it was divided into some roles such as programmer who

ran the autonomous of the ship, electrical who ensured that all electrical components were working properly, and mechanic who stayed on the edge of simulation pool to ensure the ship was physically ready for analysis. The facility used a camera sensor for tracking and recording the motion of the ship during simulation.

#### D. Environment

This analysis was conducted on a simulation pool Maneuvering and Ocean engineering Basin (MOB) at BRIN Hydrodynamics Laboratory with 65 meters length, 35 meters wide, and 2.5 meters depth. This size allows Ares for running *seakeeping* tests.



Fig. 1. BRIN facility

#### E. Risk Management

Despite the simulation being conducted at a proper laboratory, there were some risks that occurred during the simulation.

##### 1) Missing Ship Coordinate

To get precise results, the ship should be matched with the camera sensor on the simulator machine. The problem occurred when the ship was not staying in the determined position, and it could cause the result data to have less accuracy. Hence, some team members were holding the ship position until the calibration process was done.

##### 2) Ship Movement Disturbance

Before simulation was carried out, the ship should be steady in the center of the camera vision until the calibration was already done. Ares was often tossed about by the small waves due to the size is relatively small. This problem was solved by controlling the ship using remote control.

**F. Result**

**1) First Test**

BARUNASTRA ITS

Test No. 1  
 Tests in Regular seas  
 Wave Height, Hw = 0.050 m  
 Wave Period, Tw = 1.500 s

NOTATION	DIMENSION	MEAN	ST.DEV	Amax+	Amax-
Wave-ref	m	0.000	0.018	0.026	-0.026
SURGE	m	0.000	0.071	0.109	-0.132
SWAY	m	0.000	0.046	0.086	-0.084
HEAVE	m	0.000	0.017	0.024	-0.026
ROLL	deg	0.000	0.404	0.811	-0.748
PITCH	deg	0.000	7.287	11.048	-11.279
YAW	deg	0.000	1.887	4.472	-2.942

Fig. 2. First test results

The data has shown that the ship was tested with regular waves having a height of 5 cm and 1.5 second periods along three minutes. The result of the test indicates that the pitching motion has the highest value at -11.278 degrees which identifies

that the *Center of Gravity* (CG) of the ship is relatively in the behind position of the ship. So that it will have more moment force in the rear position. The data is also processed into graphs which are shown in fig. 3.

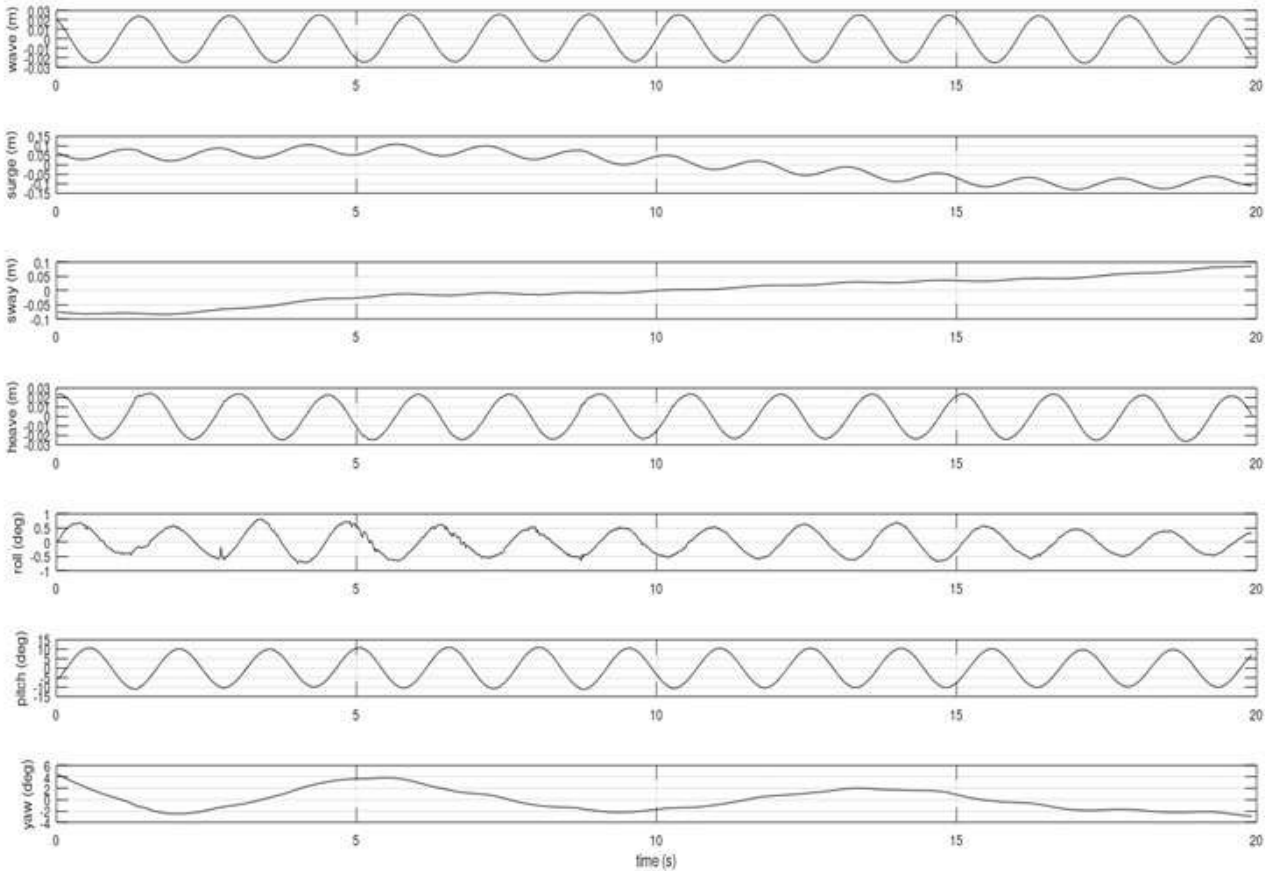


Fig. 3. Six DOF graph pattern

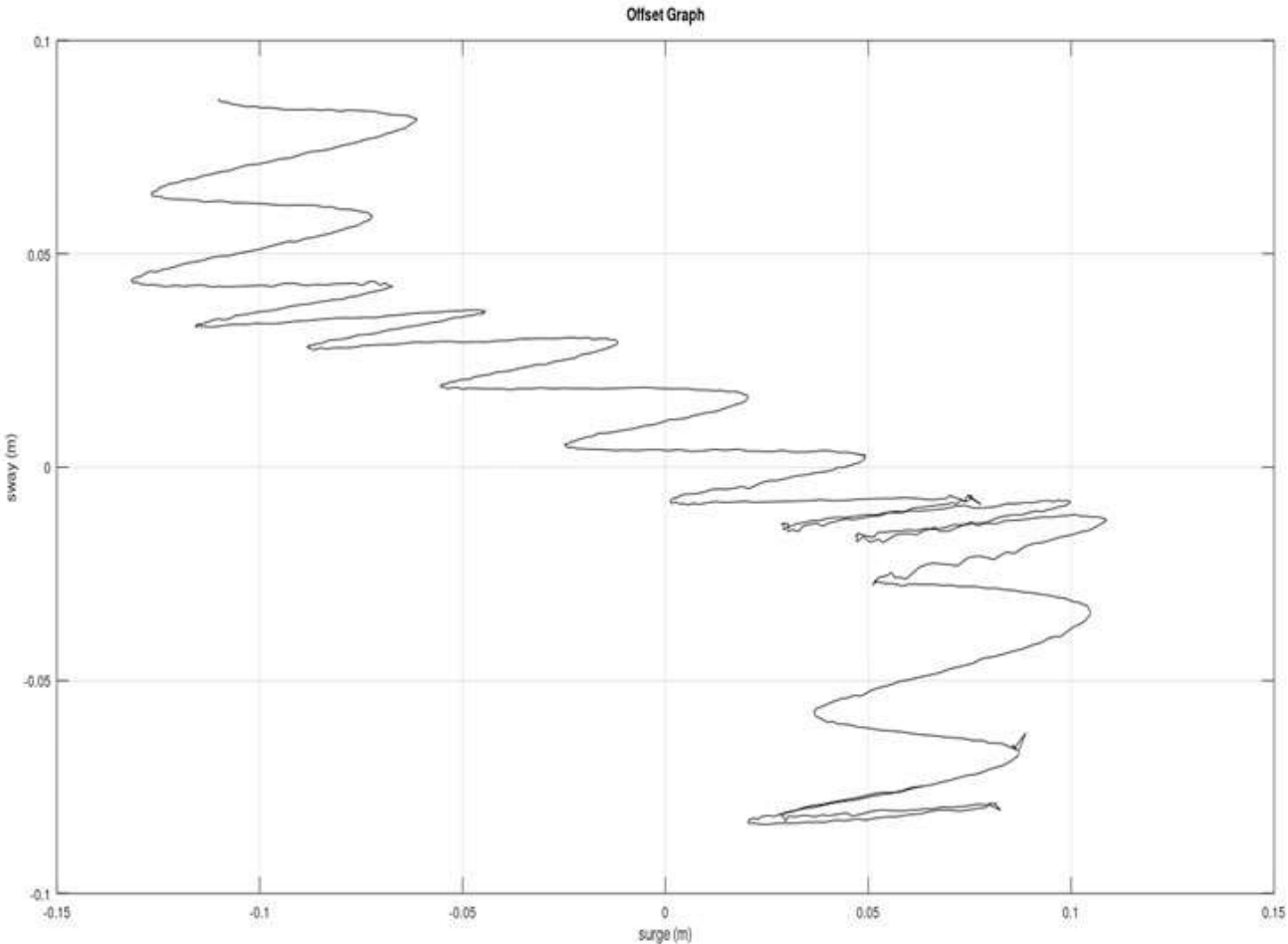


Fig. 4. First result offset graph

From the graph above we can determine the pattern of each motion and the properties of the hull against the waves. The heave, roll, and pitch motion have a sinusoidal pattern relating to the wave reference pattern that indicates a strong correlation with the wave frequency, suggesting these motions are primarily influenced by the wave force. However, the sway and yaw have lower amplitude implying better stabilization in lateral movement and direction control. The offset graph reveals the cyclic oscillatory pattern, and

this indicates the ship experiences forward-backward and lateral movement, despite the *station-keeping* algorithm's attempt to maintain position and orientation.

**2) Second Test**

We conducted the second test with the same properties as first test but the load has been adjusted to reach maximum stabilization by placing the CG in the middle of the ship. The result can be seen in fig. 5.

BARUNASTRA ITS

Test No. 2

Tests in Regular seas

Wave Height,  $H_w$  = 0.050 m

Wave Period,  $T_w$  = 1.500 s

NOTATION	DIMENSION	MEAN	ST.DEV	Amax+	Amax-
Wave-ref	m	0.000	0.018	0.025	-0.025
SURGE	m	0.000	0.033	0.063	-0.066
SWAY	m	0.000	0.029	0.046	-0.038
HEAVE	m	0.000	0.019	0.029	-0.028
ROLL	deg	0.000	0.313	0.590	-0.493
PITCH	deg	0.000	7.259	10.811	-10.975
YAW	deg	0.000	2.092	3.754	-4.000

Fig. 5. Second test result

According to the result, there is some improvement in rotational motion. Motion values are lower than in the first test. Therefore, it can be concluded that the ship has good stability. The dominant motion is still in pitch motion with

maximum amplitude -10.975 degrees. Yaw motion observed has lower amplitude than previous test. Same as the previous, the data would be processed to the graph, here is the graph of the second task.

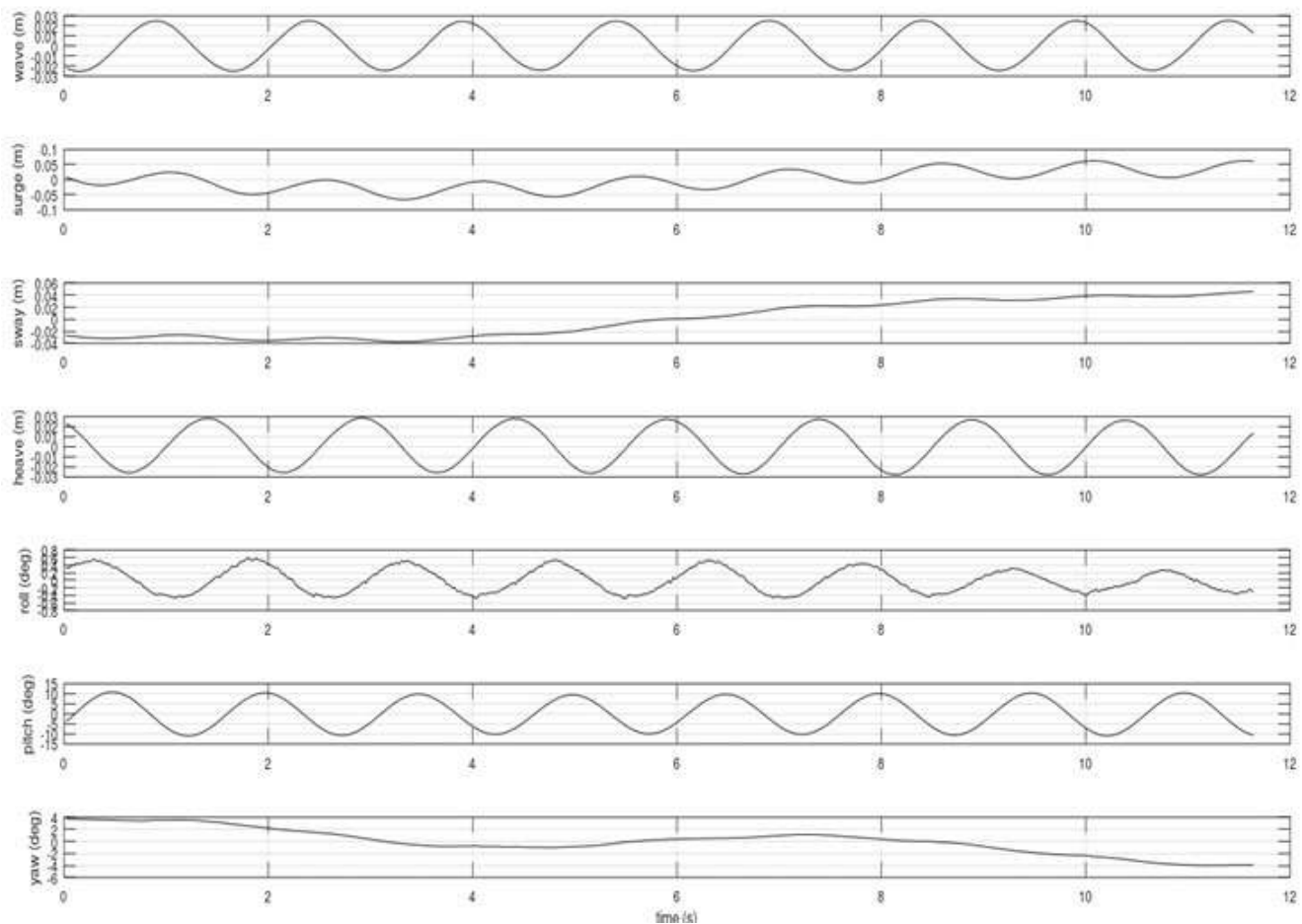


Fig. 6. Six DOF graph pattern

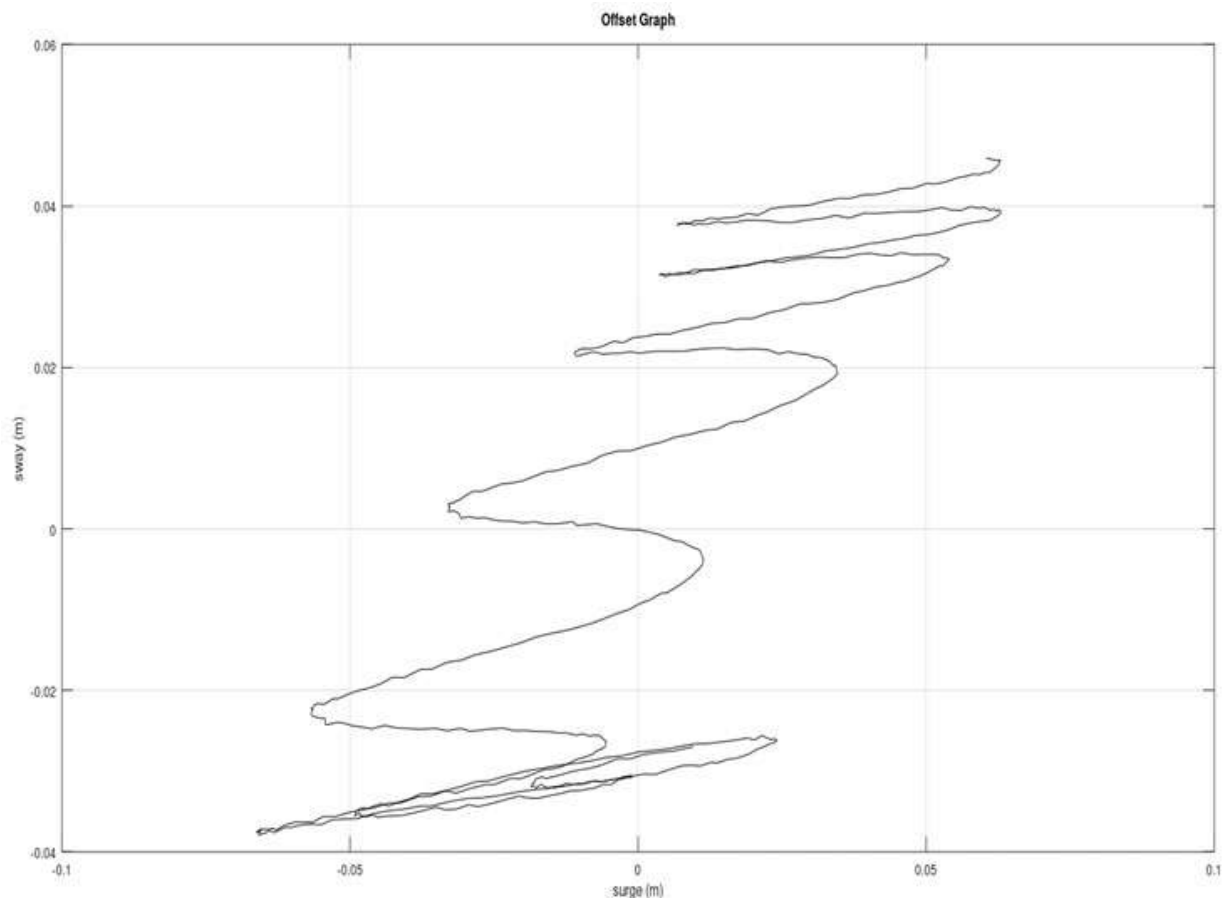


Fig. 7. Second result offset graph

According to the graph, the surge, heave, roll, and pitch have a similar pattern with the wave frequency, and it indicates these motions are influenced with wave force. In contrast, sway and yaw have different patterns with the wave pattern so these motions are more stable in lateral and directional movement. For the sway motion, it has lower maximum amplitude than the first test and for the surge it has lower maximum amplitude as well. The *station keeping* algorithm can handle the motions for this test because the surge and sway

motions are still under the threshold of the algorithm +10 until -10 degree.

After comparing the two analyses, The Ares' performance is good against 5 cm regular waves because the dominant motion only has pitching motion, and the station-keeping algorithm can handle the waves because it is not beyond the threshold. Therefore, the algorithm is sufficient and responsive for running *station-keeping* on speed challenge and rescue delivery tasks.





Fig. 8. Preparation for testing

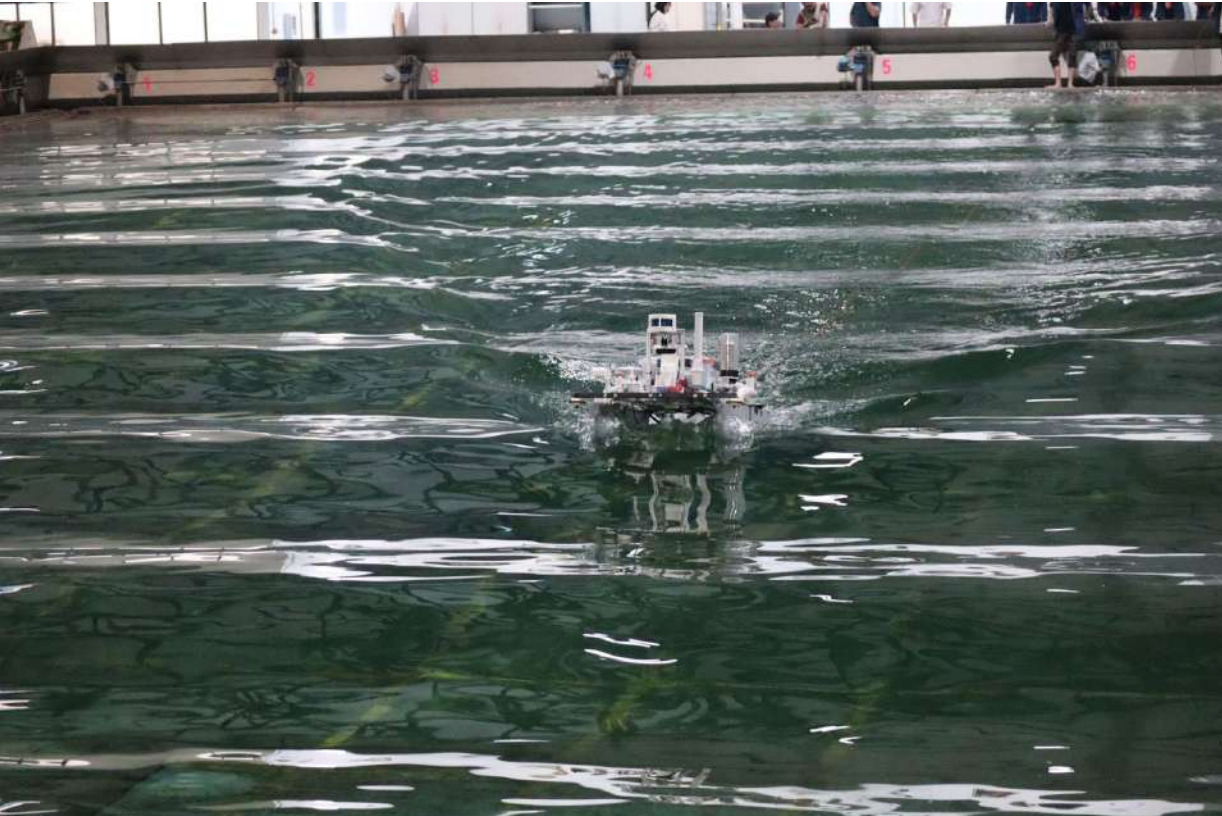


Fig. 9. Seakeeping test

**II. IN-WATER TESTING / TRIAL**

**A. Scope**

In-water testing evaluates the ASV's performance in navigation, holonomic control, and obstacle avoidance using LiDAR and camera-based systems. It also tests mission-specific algorithms such as path-following, speed

challenge, docking, and return to home. Additionally, the testing assesses hardware resilience to water exposure, real-time mapping and localization through LiDAR-IMU fusion, and the reliability of long-distance communication with ground control.

**B. Schedule**

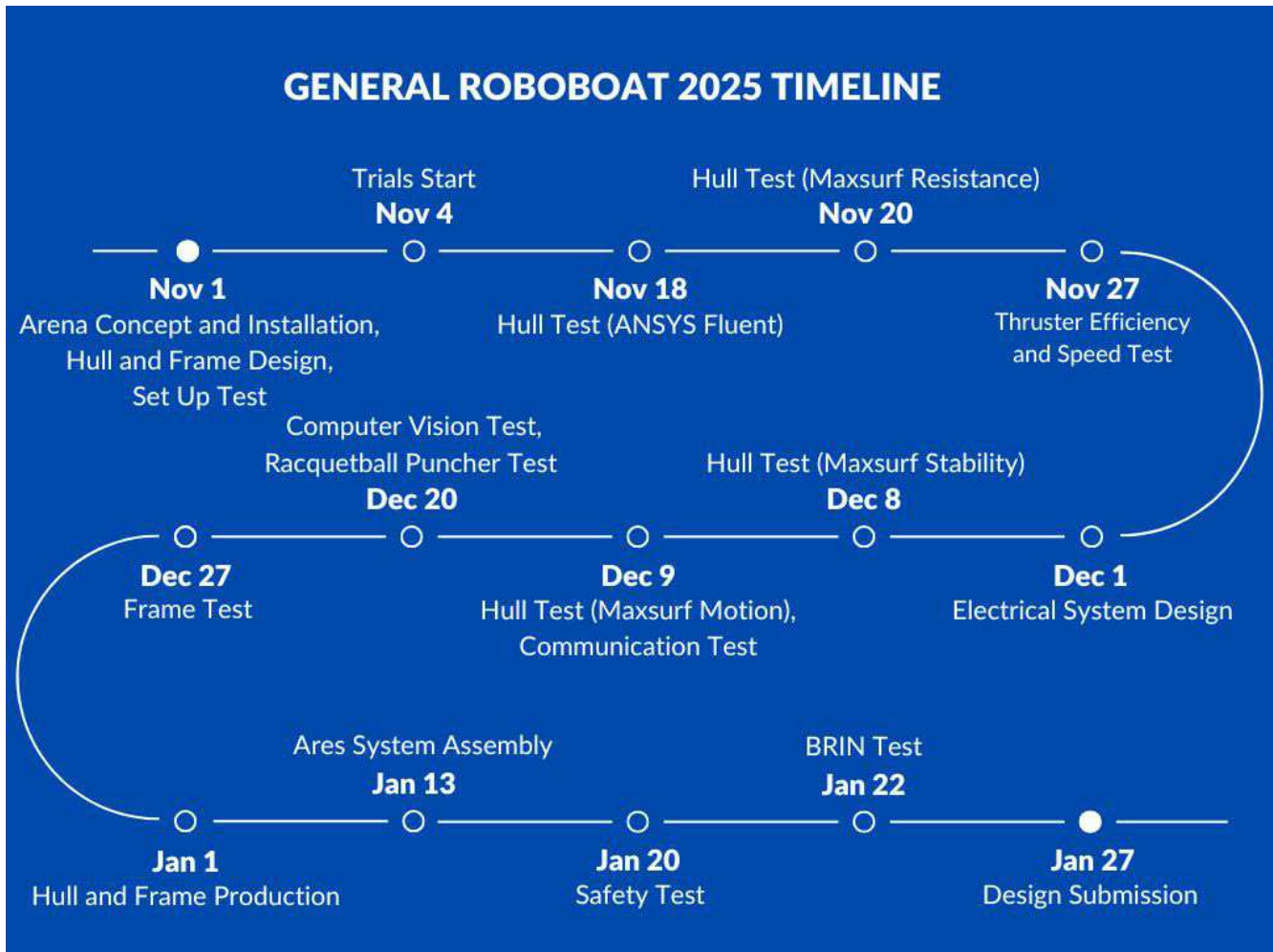


Fig. 10. Barunastra General building and testing timeline

Testing was conducted from November 4th, 2024, to January 26th, 2025, with an average testing time of 8 hours per session and about two to three times per week. Initial tests used the previous ship to refine basic functionality such as path-following, station keeping, and obstacle avoidance. From January 11th, 2025, the new ship was used with a focus on more complex testing on trying to complete each mission. The entire series

of tests ended on January 26th, 2025, with a final evaluation of the ship's ability to complete missions autonomously and ensure that all test targets were achieved properly.

### ***C. Resources and Tools***

Beside Ares and the arena, an important resource for conducting the test is human resources. The main programmer as autonomy controller, and another technical division such as electrical and mechanic must be on site while the test is conducted. Before Ares production had been completed, Theseus and Proteus vessels were used for early in-water testing. Additionally, electricity for powering equipment, charging batteries, and operating testing tools is obtained from nearby security post. A tent is also set up near the testing area to provide a sheltered area and storage for equipment, ensuring smooth operations regardless of weather conditions. Furthermore, the mechanical and electrical tool kits were always brought for on-site maintenance.

### ***D. Environment***

The testing was conducted in the campus lake, a water body spanning approximately 3,835 m<sup>2</sup> with a depth up to 2.5 meters. Open water introduces potential obstacles such as tree branches, roots, wild animals, and debris. Despite fishing being prohibited, some individuals continue to fish in the lake, creating additional risks during testing activities. Additionally, the weather in Surabaya presents challenges, with average daytime temperature reaching 34°C and high UV index, while the rainy season at the year's end further complicates testing conditions.

### ***E. Risk Management***

#### ***1) Environment Control***

Due to the lake's environment the mechanical team regularly cleans foreign objects from the water to prevent thrusters from becoming stuck or damaged. Additionally, campus security monitors the lake to prevent unauthorized activities, such as illegal fishing, that could disrupt testing.

#### ***2) Weather Protocols***

The electrical division installed a fan housing and applied seals to the access ports to ensure the electrical box remains waterproof. To further minimize the risk of water intrusion, the battery housed in the hull is connected to the electrical box through a flexible pipe. Testing was scheduled during favorable weather conditions based on forecasts. In case of unexpected rain, the mechanics constructed a tent near the lake to protect the equipment and provide secure shelter.

#### ***3) Trial's Watchman***

Before each testing session, the technical division must have at least one person ready to undertake on-site division-specific responsibilities to prevent equipment damage, assuring the tools are operated by qualified workers. To maintain continuity and accuracy, the autonomous controller must be performed by the same individual on a constant basis.

- **Electrical:** Before the testing is conducted, all batteries must be fully charged. Another thing to do before the testing is to check all components functionality in the vessel and prepare for backup components at least one of every component used.
- **Mechanic:** The mechanical division uses life jackets when lowering or lifting the vessel to the water, preparing the arena, or rescuing a vessel if something bad happens (sinking, lost communication control, etc.). They are also in charge of maintaining the arena, thrusters, and the vessel's mechanical components.

### F. Result

Through the testing sessions, the team was able to obtain valuable information that was used to continuously improve and develop Ares until it was ready to sail. The detailed testing we conducted as shown in Table I.

TABLE I ON-WATER TRIALS RECORD

Date	Objectives	Constraints	Results	Lessons Learned
4 Nov	<ul style="list-style-type: none"> <li>• Using px4 as main controller</li> <li>• Testing new x-drive thruster configuration</li> <li>• Conducting all tests with remote control</li> </ul>	<ul style="list-style-type: none"> <li>• Lost connection of Radio Controller and Datalink</li> </ul>	<ul style="list-style-type: none"> <li>• The new thruster configuration goes well</li> </ul>	<ul style="list-style-type: none"> <li>• Need to write autonomy program</li> </ul>
7 Nov	<ul style="list-style-type: none"> <li>• Testing docker</li> <li>• Testing old software system (follow the path mission)</li> <li>• Develop and test pure pursuit waypoint</li> </ul>	<ul style="list-style-type: none"> <li>• Ethernet cable loss</li> <li>• GPS antenna cable loss</li> <li>• Error in mission manager system</li> </ul>	<ul style="list-style-type: none"> <li>• Docker runs well</li> <li>• Follow the path mission complete without the obstacle</li> </ul>	<ul style="list-style-type: none"> <li>• Check the hardware before goes into lake</li> <li>• Knowing error of waypoint and mission manager problem</li> </ul>
11 Nov	<ul style="list-style-type: none"> <li>• Gate buoy, follow the path, and return to home arena installation</li> <li>• Collecting dataset from installed arena</li> </ul>	<ul style="list-style-type: none"> <li>• Camera cable was not installed when the vessel has been on the water</li> <li>• Had not taken gate buoy dataset</li> </ul>	<ul style="list-style-type: none"> <li>• Gate buoy, follow the path, and return to home arena had been installed</li> <li>• Successfully run autonomously to follow the path mission</li> <li>• Got to follow the path and return to home dataset</li> </ul>	<ul style="list-style-type: none"> <li>• Check every cable and device before the vessels on the water</li> </ul>
16 Nov	<ul style="list-style-type: none"> <li>• Collect dataset for gate buoy and yellow ball.</li> <li>• Address electrical issues related to batteries.</li> </ul>	<ul style="list-style-type: none"> <li>• Lack of communication within the team about the trial schedule.</li> <li>• All batteries were drained without charging.</li> </ul>	<ul style="list-style-type: none"> <li>• Successfully collected dataset for gate buoy and yellow ball.</li> </ul>	<ul style="list-style-type: none"> <li>• Improve communication within the team regarding trial plans.</li> <li>• Ensure batteries are charged and functional before trials.</li> </ul>

		<ul style="list-style-type: none"> <li>• Personal mistake during dataset collection.</li> <li>• Mosquitoes causing distractions.</li> </ul>		<ul style="list-style-type: none"> <li>• Double-check procedure to avoid mistakes during dataset collection.</li> <li>• Take precautions against mosquitoes during trials.</li> </ul>
20 Nov	<ul style="list-style-type: none"> <li>• Navigation channel mission</li> <li>• Follow the path mission</li> <li>• Return to home mission</li> <li>• Testing object detection using camera</li> </ul>	<ul style="list-style-type: none"> <li>• Broken type-c cable</li> <li>• Broken lipo checker</li> </ul>	<ul style="list-style-type: none"> <li>• Object detection (camera) works well</li> <li>• Navigation channel complete</li> <li>• Follow the path not complete</li> <li>• Return to home not complete</li> </ul>	<ul style="list-style-type: none"> <li>• Knowing the error in follow the path and return to home mission</li> </ul>
24 Nov	<ul style="list-style-type: none"> <li>• Attempting follow the path autonomously</li> </ul>	<ul style="list-style-type: none"> <li>• Camera cable is broken</li> <li>• Camera position is too low</li> <li>• Rain</li> </ul>	<ul style="list-style-type: none"> <li>• Successfully run autonomously for follow the path mission</li> </ul>	<ul style="list-style-type: none"> <li>• Camera position need to be raised</li> </ul>
30 Nov	<ul style="list-style-type: none"> <li>• Perform trials to test ASV functionality under various conditions.</li> <li>• Implement differential control and mapping with LiDAR.</li> <li>• Test X-drive navigation.</li> </ul>	<ul style="list-style-type: none"> <li>• Limited electrical support during trials, leading to delayed testing at noon.</li> <li>• Thrusters frequently entangled with debris despite cleaning efforts.</li> </ul>	<ul style="list-style-type: none"> <li>• Successfully initiated missions without waypoints and completed the "follow the path" mission.</li> <li>• Return-to-home mission was completed but with waypoint issues.</li> </ul>	<ul style="list-style-type: none"> <li>• Ensure better electrical and mechanical preparations for trials.</li> <li>• Develop strategies for minimizing debris interference with thrusters.</li> </ul>
4 Des	<ul style="list-style-type: none"> <li>• Perform differential control for assigned missions.</li> <li>• Visualize point cloud in RViz without data loss.</li> </ul>	<ul style="list-style-type: none"> <li>• Short notice for the trial.</li> <li>• Propeller got dirty with debris.</li> </ul>	<ul style="list-style-type: none"> <li>• Waypoint following became more stable after retuning.</li> <li>• Initial object avoidance performance was observed but requires further testing to confirm effectiveness.</li> </ul>	<ul style="list-style-type: none"> <li>• Notify the team of trial schedules earlier for better preparation.</li> <li>• Regular maintenance is needed to keep</li> </ul>

	<ul style="list-style-type: none"> <li>• Enhance ASV model visualization in RViz.</li> </ul>		<ul style="list-style-type: none"> <li>• Antenna worked optimally without any signal disconnect during the trial.</li> </ul>	<ul style="list-style-type: none"> <li>• propellers clean.</li> </ul>
7 Des	<ul style="list-style-type: none"> <li>• Optimize the accuracy of LiDAR data.</li> <li>• Test X-drive functionality.</li> <li>• Prepare for docking trials.</li> </ul>	<ul style="list-style-type: none"> <li>• Limited mechanical and vehicle support delayed trials to 4 PM.</li> <li>• Thruster mounting broke but was replaced.</li> <li>• Gateboy port failure.</li> </ul>	<ul style="list-style-type: none"> <li>• LiDAR functioned but lacked precision.</li> <li>• The ASV successfully operated autonomously.</li> <li>• Antenna signal monitoring was implemented.</li> </ul>	<ul style="list-style-type: none"> <li>• Improve mechanical readiness and logistics to avoid delays.</li> <li>• Handle equipment carefully to prevent damage.</li> <li>• Prioritize efficiency during trials.</li> </ul>
11 Des	<ul style="list-style-type: none"> <li>• Implement SLAM functionality.</li> <li>• Integrate Nav2 for enhanced navigation.</li> </ul>	<ul style="list-style-type: none"> <li>• Point cloud visualization in Rviz on the local system remains non-functional.</li> </ul>	<ul style="list-style-type: none"> <li>• Achieved holonomic control of the ASV.</li> </ul>	<ul style="list-style-type: none"> <li>• Investigate and resolve Rviz point cloud issues.</li> <li>• Adjust thruster values for consistency.</li> </ul>
15 Des	<ul style="list-style-type: none"> <li>• Perform docking missions.</li> <li>• Fix odometry issues.</li> <li>• Test Nav2 functionality.</li> </ul>	<ul style="list-style-type: none"> <li>• Poor GPS signal reception.</li> <li>• Odometry drift.</li> <li>• Severe front trim despite adding ballast at the rear.</li> </ul>	<ul style="list-style-type: none"> <li>• Successfully performed SLAM mapping.</li> <li>• LiDAR system operated without issues.</li> </ul>	<ul style="list-style-type: none"> <li>• Explore alternative GPS antenna placements to improve signal reception.</li> <li>• Reassess weight distribution for better trim.</li> </ul>
19 Des	<ul style="list-style-type: none"> <li>• Implement docking algorithm for initial conditions.</li> <li>• Plan to follow waypoint in holonomic mode.</li> <li>• Perform LiDAR mapping.</li> </ul>	<ul style="list-style-type: none"> <li>• Rain affecting operations.</li> <li>• GPS signal loss, resolved by changing the antenna.</li> <li>• Detection failure at close range, leading to dataset collection.</li> <li>• Trim issue requiring additional ballast at the rear.</li> <li>• Voltage drop on two 4S batteries.</li> </ul>	<ul style="list-style-type: none"> <li>• Successfully implemented docking algorithm for the initial conditions.</li> </ul>	<ul style="list-style-type: none"> <li>• Account for weather conditions (like rain) affecting sensor performance.</li> <li>• Ensure proper ballast to maintain even keel.</li> <li>• Consider battery performance and voltage</li> </ul>

				<ul style="list-style-type: none"> <li>monitoring during operation.</li> <li>Collect datasets to improve detection in close range.</li> </ul>
22 Des	<ul style="list-style-type: none"> <li>Perform dock searching missions.</li> <li>Implement station-keeping functionality.</li> </ul>	<ul style="list-style-type: none"> <li>Thruster battery needs separation.</li> <li>Mount broke during transport.</li> <li>Hull covered in algae.</li> <li>DDS connection failure.</li> </ul>	<ul style="list-style-type: none"> <li>Successfully followed waypoints using holonomic mode.</li> <li>Completed docking entry and exit missions.</li> <li>Achieved mapping and odometry with LiDAR.</li> <li>Implemented obstacle avoidance using LiDAR.</li> </ul>	<ul style="list-style-type: none"> <li>Ensure robust mounting for transport.</li> <li>Regularly clean the hull to maintain performance.</li> <li>Improve DDS connection reliability.</li> </ul>
3 Jan	<ul style="list-style-type: none"> <li>Implement GPS and DLIO fusion.</li> <li>Develop holonomic waypoint navigation.</li> <li>Perform dock searching missions.</li> </ul>	<ul style="list-style-type: none"> <li>Position and orientation of the ASV on the Rviz map are not real-time, causing heading calculation issues.</li> <li>Discrepancy between compass and map heading values.</li> <li>Left servo damaged; right servo malfunctioned but replaced with spares.</li> <li>Bow thrusters tangled with debris; right bow thruster required disassembly for cleaning.</li> </ul>	<ul style="list-style-type: none"> <li>Conducted DLIO testing with compass orientation (still unsuccessful).</li> <li>Tested traffic light recognition.</li> </ul>	<ul style="list-style-type: none"> <li>Address Rviz real-time position update issues.</li> <li>Improve debris protection for bow thrusters.</li> <li>Enhance compass-to-map heading alignment.</li> </ul>
6 Jan	<ul style="list-style-type: none"> <li>Successfully complete docking mission.</li> <li>Test docking navigation around the docking station.</li> </ul>	<ul style="list-style-type: none"> <li>Poor connection between ground station and ASV over long distances (from the middle to the edge of the lake).</li> <li>Lack of mechanical support during the trial.</li> </ul>	<ul style="list-style-type: none"> <li>Successfully completed the speed challenge mission.</li> <li>Tested performance using NUC (observed FPS drop to 20, compared to Jetson's 120 FPS).</li> </ul>	<ul style="list-style-type: none"> <li>Improve long-range communication reliability.</li> <li>Ensure mechanical support availability during critical trials.</li> </ul>

---

				<ul style="list-style-type: none"> <li>• Optimize FPS performance for consistent system behavior.</li> </ul>
9 Jan	<ul style="list-style-type: none"> <li>• Conduct water-shooting mission.</li> <li>• Test docking functionality with the T500 thruster.</li> </ul>	<ul style="list-style-type: none"> <li>• Low NUC FPS (capped at around 10 FPS).</li> <li>• Left hull took on water.</li> <li>• Arena damaged by recent storm.</li> <li>• One servo exhibited erratic movement.</li> </ul>	<ul style="list-style-type: none"> <li>• Successfully tested with the T500 thruster.</li> <li>• Completed docking tests.</li> </ul>	<ul style="list-style-type: none"> <li>• Optimize FPS performance for better system responsiveness.</li> <li>• Regularly check for water leakage.</li> <li>• Prepare backup equipment in case of arena damage or servo malfunction.</li> </ul>
13 Jan	<ul style="list-style-type: none"> <li>• Stabilize waypoint following.</li> <li>• Improve obstacle avoidance.</li> <li>• Enhance return-to-home functionality with vision.</li> <li>• Ensure stable thruster and servo operation.</li> </ul>	<ul style="list-style-type: none"> <li>• Oscillation in waypoint following (fixed with tuning).</li> <li>• Occasional collisions, requiring obstacle avoidance gain adjustment.</li> <li>• Return-to-home with vision not functional, switched to holonomic mode (further testing needed).</li> <li>• Rear thruster sometimes revs without movement (loose cable).</li> <li>• Front thruster thrust varies.</li> <li>• Servo movement intermittent due to frequent exposure to water.</li> <li>• Forgot to place battery checker.</li> <li>• Camera obstructed by sprayer when tilted.</li> </ul>	<ul style="list-style-type: none"> <li>• Waypoint following stabilized.</li> <li>• Object avoidance improved (needs further testing).</li> <li>• Antenna performed reliably without disconnects.</li> </ul>	<ul style="list-style-type: none"> <li>• Regularly check for loose cables and ensure waterproofing components exposed to water.</li> <li>• Ensure proper battery monitoring before trials.</li> <li>• Revisit vision-based return-to-home for improvement.</li> <li>• Consider camera positioning adjustments to avoid obstructions.</li> </ul>

---



17 Jan	<ul style="list-style-type: none"> <li>• Improve camera angle and lidar filter functionality.</li> </ul>	<ul style="list-style-type: none"> <li>• Rainy weather during the trial.</li> <li>• Left thruster intermittently operational.</li> <li>• Front thruster direction reversed.</li> <li>• Initial servo malfunction.</li> </ul>	<ul style="list-style-type: none"> <li>• Increased camera angle for better visibility.</li> <li>• Added lidar filter directed upwards.</li> </ul>	<ul style="list-style-type: none"> <li>• Account for weather conditions in trials.</li> <li>• Ensure thorough checking of thrusters and servos before tests.</li> <li>• Regular maintenance and calibration to avoid equipment malfunctions.</li> </ul>
21 Jan	<ul style="list-style-type: none"> <li>• Test station keeping at 5, 10, 15 cm regular waves.</li> <li>• Test straight-line movement in 5, 10, 15 cm regular waves and 10, 16 cm irregular waves.</li> </ul>	<ul style="list-style-type: none"> <li>• Regular wave period of 1.5s causing excessive vessel oscillation.</li> <li>• Hull opening allowing water ingress.</li> <li>• Damaged servo due to water intrusion.</li> </ul>	<ul style="list-style-type: none"> <li>• Vessel remained stable when moving against waves.</li> <li>• Successfully completed station keeping in various wave conditions.</li> </ul>	<ul style="list-style-type: none"> <li>• Ensure hull openings are sealed to prevent water ingress.</li> <li>• Regular maintenance of servos and components to avoid damage from water exposure.</li> <li>• Test under a range of wave periods and conditions for better stability.</li> </ul>
23 Jan	<ul style="list-style-type: none"> <li>• Fixing more reliable waypoints</li> <li>• Set up the ship from remote efficiently</li> <li>• Running on missions</li> </ul>	<ul style="list-style-type: none"> <li>• Debugging the waypoint algorithm and PID controller</li> </ul>	<ul style="list-style-type: none"> <li>• The terminal can now be accessed remotely, and if the display freezes, it can be restarted from the shore without disconnecting the dongle.</li> <li>• The waypoint algorithm works correctly, and the ship now moves smoothly with the waypoint PID controller.</li> </ul>	<ul style="list-style-type: none"> <li>• Remote access and the ability to reset frozen screens without physical intervention significantly improve the system's usability and reliability.</li> <li>• Fine-tuning waypoint navigation with PID control</li> </ul>

---

			<ul style="list-style-type: none"> <li>• Speed challenge was completed in record time (~33 seconds)</li> </ul>	<p>greatly improves ship performance and speed in a controlled environment. However, real-world mission constraints (like obstacles) can affect the validity of performance metrics.</p>
26 Jan	<ul style="list-style-type: none"> <li>• Optimize localization and mapping with LiDAR</li> </ul>	<ul style="list-style-type: none"> <li>• Lidar has a threshold that requires a minimum of 64 points for DLIO to function properly, but under certain conditions the lidar can only reach 58-62 points.</li> <li>• Lidar scan frequency must be optimized based on the lidar's performance, as scanning at 5Hz while moving quickly causes mapping confusion, and at 20Hz the lidar struggles due to age."</li> </ul>	<ul style="list-style-type: none"> <li>• Lidar threshold was reduced to 32 points to prevent errors due to low point numbers.</li> <li>• Lidar scan frequency was optimized to 15Hz, balancing performance with lidar capability.</li> </ul>	<ul style="list-style-type: none"> <li>• A lidar system requires a minimum number of points for reliable data collection; adjustments to the threshold can prevent errors in data collection.</li> <li>• Optimizing scan frequency based on movement speed and the condition of the lidar hardware is crucial for accurate mapping.</li> </ul>

---

From on-water testing which had been carried out, Ares made significant improvements. We monitors the progress every time by using our own

scoresheets referring to RoboBoat 2025 Autonomy Challenges Scoring Guidelines shown in fig. 10.

metadata		weight measurement			thrust measurement			navigation (shots)		gates following			docking			speed challenge			hall delivery			water delivery			return to home			time diff									
date	start	try	score	weight (lbs)	score	thrust (lbs)	score	success?	score	gates	hit	miss	report?	score	empty bot?	correct bot?	score	water light?	gates start?	blue bot?	gates finish?	time (s)	score	attempt count	hits	score	success?	score	score	vol	diff						
Expected			5448.8	77.2	63.7	44	51.8	YES	290	10	YES	0	YES	400	YES	YES	400	YES	YES	YES	2	YES	25	375	100	0	150	1	0	500	141	1325	2425	18	1.25		
60	9:00	1	0.0	68.5	81.5	30.26	55.8	YES	200	10	YES	0	NO	500	YES	YES	400	YES	YES	YES	1	YES	250	375	100	0	0	0	0	1	3267.5	5437					
61	9:45	1	0.0	68.5	81.5	30.26	55.8	YES	200	10	YES	0	NO	500	YES	YES	400	YES	YES	YES	0	YES	250	0	100	0	0	0	0	1	437.3	5437					
66		1	3812.8	68.5	81.5	30.26	55.8	YES	200	10	YES	0	NO	500	YES	YES	400	YES	YES	YES	2	YES	250	180	100	0	0	144	0	388	4	3.1	3832.8	5437			
66	10:01	1	0.0	68.5	81.5	30.26	55.8	YES	200	10	YES	1	NO	475	YES	YES	400	YES	YES	YES	2	YES	250	375	100	0	0	1	1	2	100	1400	1400	0	1	3337.5	5437
67	10:48	1	0.0	68.5	81.5	30.26	55.8	YES	200	10	YES	1	NO	425	YES	YES	400	YES	YES	YES	0	YES	250	480	100	0	0	0	0	1	1362.5	5437					
68		1	0.0	68.5	81.5	30.26	55.8	YES	200	9	NO	0	NO	375	YES	YES	400	YES	YES	YES	0	YES	250	300	100	0	0	0	1	1812.5	5437						
69	04:59	0	0.0	68.5	81.5	30.26	55.8	YES	200	10	YES	0	NO	400	YES	YES	400	YES	YES	YES	0	YES	250	300	100	0	0	0	1	2	200	0	0	1	1847.5	5437	
70		1	0.0	68.5	81.5	30.26	55.8	YES	200	10	YES	1	NO	475	YES	YES	400	YES	YES	YES	0	YES	250	0	100	0	0	0	1	0	1	0	0	1	811.3	5437	
71	24:22	0	3438.6	68.5	81.5	30.26	55.8	YES	200	10	YES	0	NO	650	YES	YES	400	YES	YES	YES	1	YES	250	325	100	0	0	144	0	388	2	1.25	3428.6	5437			
72	24:44	1	0.0	68.5	81.5	30.26	55.8	YES	200	10	YES	0	NO	400	YES	YES	400	YES	YES	YES	0	YES	250	480	100	0	0	0	1	1	1	1000	1000	0	1	833.5	5437
73	15:08	1	0.0	68.5	81.5	30.26	55.8	YES	200	9	NO	0	NO	375	YES	YES	400	YES	YES	YES	1	YES	250	325	100	0	0	0	1	1	1	1450	1400	0	1	3837.3	5437
74		1	0.0	68.5	81.5	30.26	55.8	YES	200	10	YES	0	NO	450	YES	YES	400	YES	YES	YES	2	YES	250	300	100	0	0	1	1	1	200	0	0	1	1847.5	5437	
75	15:29	1	0.0	68.5	81.5	30.26	55.8	YES	200	9	NO	0	NO	375	YES	YES	400	YES	YES	YES	2	YES	250	325	100	0	0	0	1	1	1	100	0	0	1	1867.5	5437
76		1	0.0	68.5	81.5	30.26	55.8	YES	200	9	NO	0	NO	375	YES	YES	400	YES	YES	YES	0	YES	250	0	100	0	0	0	1	0	0	0	0	1	537.4	5437	
77	18:44	2	0.0	68.5	81.5	30.26	55.8	YES	0	0	NO	0	NO	0	YES	YES	400	YES	YES	YES	0	YES	250	0	100	0	0	0	1	1	1	0	0	1	457.6	5437	
78	16:08	1	0.0	68.5	81.5	30.26	55.8	YES	0	0	NO	0	NO	0	YES	YES	400	YES	YES	YES	0	YES	250	0	100	0	0	0	1	0	0	0	0	1	337.3	5437	
79		1	0.0	68.5	81.5	30.26	55.8	YES	200	10	YES	1	NO	425	YES	YES	400	YES	YES	YES	0	YES	250	0	100	0	0	0	1	0	1	0	0	1	562.1	5437	
80	14:48	2	3217.3	68.5	81.5	30.26	55.8	YES	200	9	NO	1	NO	325	YES	YES	400	YES	YES	YES	1	YES	250	375	100	0	0	144	0	388	2	1.25	3187.5	5437			
81	17:08	1	3437.3	68.5	81.5	30.26	55.8	YES	200	9	NO	0	NO	375	YES	YES	400	YES	YES	YES	1	YES	250	325	100	0	0	144	0	388	2	1.25	3429.3	5437			

Fig. 11. Live scoring mission attempts

From around three months of testing until design documentation submission, Ares has been ready to complete all missions in RoboBoat 2025 using the strategy and approach that has been conducted.

We also plan to continue our on-water testing until the competition day. Therefore, we can enhance all system overall to be ready for Autonomy Challenge RoboBoat 2025.



Fig. 12. On-water testing



Fig. 13. On-site maintenance



Fig. 14. Rescuing the ship

# Appendix I: Sponsors and Supporting Personnel

Alifa Hikmawati, Tabitha Natasya Cyntia Dewi, Rumaisha Afrina, Muhammad Fathoni Al Fadh, Rico Dwi Firmansyah, Fergrini Lefranzy Pattinasarany, Rifa Humaira Putri, Nathan Pascalauren Koroy, Terrania Rafva Nareswari, Zahrina Nur Amalina Syamsudin, Sheany Angela Diaz Wijaya

We would like to express our gratitude to Institut Teknologi Sepuluh Nopember for its support in terms of financial, procurement, etc. We also thank the Directorate of Student Affairs, Mr. Nur Syahroni, Mr. Nur Hasan, Mrs. Maya Sari, Mrs. Mila, Mrs. Nurul and Mrs. Septi, for helping to organise the team's departure needs, such as letters of recommendation and pre-funding support. We

highly appreciate the Campus Facilities and Infrastructure Unit (SARPRAS), Mrs. Yayuk Pamikatsih, Mrs. Any Werdhiastutie, Mr. Alfian and also Campus Security Unit (SKK) as well for facilitating the trial location, also ensuring the security of the trial location so that the trial activities ran smoothly

Special thanks to the sponsors of Barunastra ITS Team that have listed below:

<b>Cruise Sponsor</b>	PT Jaya Konstruksi Manggala Pratama - for cash.
	IKOMA ITS (ITS Student Parents Association) - for cash.
<b>Barge Sponsor</b>	PT Perusahaan Listrik Negara - for cash.
<b>Ferry Sponsor</b>	PT Seascope Surveys Indonesia - for cash.
	PT Len Rekaprima Semesta - for cash.
	PT Meratus Swadaya Maritim - for cash.
<b>Yacht Sponsor</b>	PT Petrokimia Gresik - for cash.
	PT Infrastruktur Telekomunikasi Indonesia - for cash.
<b>Other Sponsors</b>	National Research and Innovation Agency (BRIN) - for provisioning the wave pool at the Hydrodynamics Research Laboratory for Ares' hull stability and station keeping tests.
	Husky-CNOOC Madura Limited - for cash.
	Print & print - for discounted pricing on printing materials.
	PT Pelindo Marine Service - for cash.
	PT PLN Indonesia Power - for cash.
	PT Asian Bearindo Jaya - for discounted pricing on mechanical components.

Additionally, we express our gratitude to Mrs. Junita Dwianingdijah, Mr. Suro, and Mrs. Dieta for their presence and support of the Barunastra ITS team via the ITS Student Parents Association (IKOMA). Apart from that, thanks to our alumni, Mr. Muchmirul Yusa Setiaji and Mr. Anas Mufid, for their individual financial support.

Honour and gratitude are also given as well to Mr. M. Nasir, Mr. M. Ali Mudlofar, Mr. Baharudin Ali, Mr. Affan Hidayat, Mr. Chandra Permana, Mr. Agung Rahmat, Mr. Zainul Haqiqi, Mr. Hudrih, Mrs. Isma Choiriyah, Mr. Kholip, Mr. Rohaman Akbar, Mr. Rizqi A. Ardiansyah, Mr. Noer Abdillah S. N. Ninoi, Mrs. Dina S. Fatimah, and Mrs. Nimas Aisah Mumtaz who are part of

Indonesian Research and Innovation Agency (BRIN) which had helped us in providing the Laboratory for Hydrodynamic Technology in Surabaya for our trial. We also appreciate ITS TV for providing the LCD projector, Gimbal Stabilizer DJI RS 3, and Clip-On microphone (Senheisser) for our video profile shoot. We would also like to thank Manufaktur Robot Industri (MRI), for assisting in mechanical manufacturing and providing the equipment needed by the team. Our sincere gratitude goes to Mr. Henry for his invaluable assistance in facilitating our team operations during the offline competition in the USA directly.

The team also would like to acknowledge Robotika ITS for supporting our team to succeed and maintain its existence. We would especially like to thank the team's advisors, Dr. Rudy Dikairono, S.T., M.T., M.SC., Muhtadin, S. T., M. T., and Lukman Hakim, S. T., M. T. for training and advising our members. The team would also like to thank the alumni, Andreas Raja Goklas Sitorus, Achmad Zidan Akbar, Dion Andreas Solang, Edgar Kazakti Widyas Putra, Ricky Azhar Ramadhan, Fariz Rayyan Januar, Maria Valentia, Akbar Ghifari, Fransiskus Xaverius Clive Kosasih, I Gusti Ayu Anggita Prameswari, I Wayan Agus Darmawan, and Sandi Christanto for their outstanding advice

Lastly, Barunastra would like to appreciate all team members who have strived all efforts and sacrifices to achieve this stage of competition. All detailed team members with their job descriptions are detailed below:

**Taib Izzat Samawi**  
General Manager





